Co-option of truncated envelope proteins derived from endogenous retroviruses in mammals

(哺乳類における内在性レトロウイルス由来欠損型エンベロープタンパク質の共進化)

Joint Graduate School of Veterinary Medicine

Yamaguchi University

Didik Pramono

September 2024

DECLARATION

September 2024, Yamaguchi University, Japan.

I, **Didik Pramono**, declare that I have carried out the work reported in this dissertation. Any reference to the work of others has been acknowledged as cited in this dissertation.

ACKNOWLEDGMENT

I would like to express my deep gratitude to my supervisor, Prof. Kazuo Nishigaki, PhD, who fully supported me and provided me with the opportunity to study with him during my PhD course. I am incredibly grateful for his guidance, wisdom, and patience. I learn from his interesting ideas, logical scientific thinking, and integrity every day while doing the research. I hope to take those lessons with me going forward to be a good scientist.

I would like to express my deep gratitude to associate Prof. Ariko Miyake, PhD, for her support in teaching me wet laboratory techniques, especially when this is my first time coming to this laboratory. With her support, I could run the experiments smoothly during my PhD course. I also learned a lot from her about how to prepare and organize the experiments as thoroughly as possible.

I am deeply indebted to Prof. Tohru Kimura, PhD, for the first time welcoming me, supporting me to enter the university, and promoting the scholarship for my PhD course. I also would like to express my sincere appreciation when he introduced me to Prof. Kazuo Nishigaki, PhD, for the first time coming to this university. I learn so much from him, including his kindness, patience, and integrity as a scientist. I always best wish for his retirement and hope for his health and happiness.

I would also like to express my thanks to Dr. Junna Kawasaki for her advice, support, and fruitful discussion, especially on the bioinformatics subject. I will always remember her kindness in guiding me and your support when I face bioinformatic trouble.

I would like to acknowledge all present and past members of Nishigaki sensei's laboratory for their friendship and their generous support. Especially for Dr. Minh Ngo Ha, for his kindness, support, and discussion whenever I face difficulties during the research.

I am sincerely grateful to Japan's Ministry of Education, Culture, Sports, Science, and Technology (Monbukagakusho) for providing me with a scholarship throughout my studies in Japan.

I would also like to recognize my parents, in-laws, and all of my family and friends for their generosity and support.

In the end, I would like to express my gratitude to my wife, Indah Jamiatun Hasanah, and my son, Lingga Nayihan Pramono, for their support, encouragement, and understanding during this PhD course.

TABLE OF CONTENTS

GENERAL ABSTRACT

Retroviruses are RNA viruses that infect a broad range of vertebrate hosts, including mammals. Retroviruses are uniquely capable of utilizing reverse transcriptases to convert their RNA genome into DNA, which can then be integrated into the host genome. Retroviruses in the family *Retroviridae* are classified into two categories: exogenous retroviruses (exRVs) and endogenous retroviruses (ERVs). A significant proportion of ancient retroviral sequences, designated ERVs, are known to infect germ cells, integrate into the host genome, and are vertically transmitted to the offspring. This process contributes significantly to the generation of ERVs in the mammalian genome via repeated germline reinfection. ERVs are inactivated through methylation and accumulation of mutations, including those involving nucleotide substitutions, deletions, and insertions. Viral gene changes may alter the function of the encoded proteins. The proviral genome is comprised of three major genes: *gag, pol*, and *env*. The *env* genes encode the surface (SU) and transmembrane (TM) subunits that facilitate targeting and entry into specific cell types for infection. Defective env-ERV is an Env protein with a signal peptide and SU subunit but contains a premature stop codon and a lack or partial deletion of the TM subunit. Moreover, env-ERVs may be crucial for physiological functions in the host, including maintenance of homeostasis, placentation, innate immunity regulation, and restriction of infection. This study examines the molecular interactions between viruses and hosts, focusing on events in the evolution of viruses and env-ERV functions.

In Chapter One, I investigate the truncated Env protein, FeLIX, which functions as a restriction factor for mammalian retrovirus infection. The feline leukemia virus (FeLV) is a *Gammaretrovirus* endemic to domestic cats worldwide. FeLV is associated with the development of malignant hematopoietic disorders in cats, including lymphoma and immunodeficiency. FeLV is classified into several subgroups (A, B, C, D, E, and T) based on

the viral receptor interference or receptor usage. The transmission of FeLV-B does not occur among domestic cats, and *in vivo* experimental infections are resistant to FeLV-B. It has been suggested that the presence of enFeLV is associated with this phenomenon. The absence of enFeLV in Florida panthers infected with FeLV-B highlights an association between enFeLV and FeLV-B. However, the molecular mechanisms underlying the restriction of FeLV-B infection in domestic cats remain unclear. The soluble Env protein derived from ERVs functions as a cofactor that assists in FeLV-T infection. However, we show here that soluble Env protein exhibits antiviral activity and provides resistance to mammalian retroviral infection through competitive receptor binding. This finding may explain why FeLV-B transmission is not observed in domestic cats.

In Chapter Two, I characterize the ERV-derived placenta-specific soluble protein, EnvV-Fca, from domestic cats. While investigating the expression of ERV *env* genes in domestic cats, we discovered that EnvV-Fca is closely related to EnvV2-Hum. EnvV-Fca was specifically detected in the placental trophoblast syncytiotrophobic layer and expressed as a secreted protein in cultured cells. Genetic analyses have indicated that the EnvV2 genes are widely present in vertebrates and are under purifying selection among carnivores, suggesting a potential benefit to the host. Moreover, these findings suggest that birds, bats, and rodents carrying EnvV2 play significant roles as intermediate vectors in the spread or cross-transmission of viruses among species.

In Chapter Three, I focus on the evolution of endogenous koala retrovirus, which may function as a restriction factor for koala retrovirus subtype-A (KoRV-A). KoRV is currently transitioning from an exRV to an ERV; therefore, we elucidated the co-evolutionary processes of retroviruses. By searching public databases, we identified endogenized-KoRV truncated envelope (*env*)

genes that were expressed. Of these, five truncated *env* genes were selected and constructed as expression vectors to determine their viral inhibitory effects. We found that some KoRV-truncated Env proteins inhibit KoRV-A infection. In addition, a frameshift mutation in the truncated *env* gene affected the level of inhibition. This study shows that the evolutionary process of ERVs is consistent with the ongoing endogenization of retroviruses. Our findings demonstrated that the evolutionary arms race between viruses and koalas emerged as a viral resistance factor. Furthermore, we investigated the receptor usage of KoRV-A, KoRV-related retroviruses, and FeLV-B. I observed that koala Pit1 (koPit1), but not koPit2, is permissive to KoRV-A, WMV, and FeLV-B infection. GALV and HPG use koPit1 and koPit2 as receptors. Our findings suggest that interspecies transmission of KoRV-related retroviruses may occur via the Pit1 receptor.

In conclusion, this study provides evidence for the characterization and functions of defective env-ERVs as antiviral agents against mammalian retroviruses. Furthermore, this study contributes to the fundamental understanding that soluble Env proteins restrict retroviruses from diverse host species, implying that their functions may support host immunity and antiviral defenses by controlling retroviral spread. Furthermore, this study provides an evolutionary scenario for host-pathogen interactions.

GENERAL INTRODUCTION

According to the latest release by the International Committee on the Taxonomy of Viruses (ICTV), classification includes only exogenous retroviruses (exRVs) (1). The family *Retroviridae* is divided into two subfamilies: *Orthoretrovirinae* and *Spumaretrovirinae*. The *Orthoretrovirinae* subfamily comprises six genera (*Alpharetrovirus, Betaretrovirus, Gammaretrovirus, Deltaretrovirus, Epsilonretrovirus*, and *Lentivirus*), and the *Spumaretrovirinae* subfamily (also known as foamy viruses) comprises five genera (*Bovispumavirus*, *Equispumavirus*, *Felispumavirus*, *Prosimiispumavirus*, and *Simiispumavirus*) (1). Retroviruses are classified into two types: simple and complex retroviruses, based on the composition of their genetic material (2, 3). *Gammaretroviruses* are an example of simple retroviruses, while delta retrovirus is an example of a complex retrovirus (2). Simple retroviruses encode three polyproteins, Gag, Pol, and Env, which are flanked by two long terminal repeats (LTRs). In contrast, complex retroviruses encode accessory proteins in addition to polyproteins (2). These accessory proteins are distinct from those involved in regulating gene expression such as those encoded by tat, rev, tax, and rex (4). However, some accessory proteins are not required for replication. The Gag protein controls the synthesis of internal virion proteins that form the matrix (MA), p12, capsid (CA), and nucleocapsid (NC); Pol contains information on the reverse transcriptase and integrase enzymes; and Env encodes the surface and transmembrane components of the viral envelope protein (4). Additionally, all retroviruses have a smaller coding domain called Pro, which encodes a virion protease. Retroviruses, which belong to the family *Retroviridae*, are enveloped viruses with a diameter of approximately 100 nm and an icosahedral shape. Their RNA genomes are approximately 7–10 kb in length (4). The resulting double-stranded DNA is integrated into the chromosome to form a provirus. During replication, the RNA genome is converted into a DNA intermediate through reverse transcription, which occurs inside the nucleocapsids during entry. Notably, the

integration of viral DNA into chromosomes is an obligatory step in the viral life cycle. During assembly, viral genomic RNA is packaged into nucleocapsids and serves as mRNA for Gag and Pol polyproteins (4).

Feline leukemia virus (FeLV), an example of *Gammaretrovirus* endemic to domestic cats worldwide, has been identified as the infectious agent responsible for feline leukemia and lymphoma (5). In cats, FeLV induces malignant hematopoietic disorders, including lymphoma, myelodysplastic syndrome, acute myeloid leukemia, aplastic anemia, and immunodeficiency (6, 7). FeLVs can be categorized into several subgroups based on the viral receptor interference and host range. FeLV subgroups and their FeLV-A, -B, -C, -D, -E, and -T receptors have been identified (8-18). FeLV infections have been reported in domestic cats worldwide, including Europe, the United States, South America, Japan, Australia, and New Zealand (19-24). FeLV-B arises from recombination in the envelope (env) region between FeLV-A and endogenous FeLV (enFeLV) present in the feline genome (19, 25, 26). FeLV-B uses phosphate transporter 1 (Pit1) and Pit2 as entry receptors (10, 27). FeLV-A is the primary virus that is transmitted horizontally among domestic cats. Although horizontal transmission of FeLV-B rarely occurs, it may rarely be transmitted by coinfection with FeLV-A (26). FeLV-B occurs in 33–68% of cats infected with FeLV-A, presumably by independent recombination events that occur *de novo* after infection of domestic cats with FeLV-A (5, 10, 26). Given that *in vivo* experimental infections have shown resistance to FeLV-B, domestic cats are also resistant to FeLV-B infection; however, the underlying mechanisms remain unknown.

In addition to FeLV-B, various other viruses such as koala retrovirus (KoRV)-related viruses use phosphate transporters as viral receptors and can spread to hosts; interspecies transmission can also occur (28-30). KoRV is present in koala populations in both the exogenous and

endogenous viral form (31). It can be transmitted vertically (from parent to offspring) and horizontally (from one animal to another) (32-34). Forms of horizontal transmission are poorly defined but presumably require close contact (34). Eleven KoRV subtypes (A–K) have been isolated and classified based on sequence variations in the receptor-binding domain of the *env* gene, specifically in the hypervariable region (35). KoRV is a major infectious agent affecting the health of koala populations in both natural and captive environments (36, 37). It has also been associated with neoplastic diseases, including lymphoma and leukemia, resulting in high mortality rates (37-39). Evidence of its immunosuppressive potential has been observed *in vitro* but is limited *in vivo* (40). The full-length genome sequence of KoRV contains *gag*, *pol*, and *env* genes flanking two LTRs with a length of 8.4 kb (33, 41). KoRV is a replication-competent, single-stranded, positive-sense RNA virus belonging to the genus *Gammaretrovirus* (41). The KoRV provirus has been reported to circulate in 100% of the koala populations in northern Australia, whereas koala populations in southern Australia are only partially infected. Some rare populations are free of KoRVs (35, 42). This phenomenon suggests that KoRV is still in the process of endogenous integration into the host and requires further investigation.

Endogenous retroviruses (ERVs) are remnants of an ancient retroviral infection that are vertically transmitted to the offspring and comprise approximately 4–10% of the human, mouse, and cat genomes (43-45). This process generates a substantial proportion of ERVs in the mammalian genome through repeated germline reinfections (46). The invasion of germ cells causes endogenization via vertical transmission of the provirus to the offspring (47). ERVs are inactivated by methylation and accumulation of mutations including nucleotide substitutions, deletions, and insertions (47, 48). These events may be related to viral integration time. Therefore, most ERVs exist as non-functional DNA. However, it is important to note that some ERVs retain their infectivity and ability to replicate (49, 50). In addition, both pathogenic and

emerging viruses are generated through gene mutations or recombination. Various diseases associated with ERV have been reported in mice and humans (51, 52). In addition, changes in viral genes can affect the functions of the encoded proteins (53). The proviral genome comprises of three major polyprotein-encoding genes: *gag*, *pol*, and *env* (54). The *env* genes encode surface (SU) and transmembrane (TM) subunits that facilitate targeting and entry into specific cell types for infection (55). Defective env-ERV refers to an Env protein that has a signal peptide and SU subunit but contains a premature stop codon and lacks or has a partial deletion of the TM subunit. Defective env-ERV may be crucial for physiological functions in the host, such as maintaining homeostasis and placentation, and acting as a restricting factor in the immunological response to exRV infection (8, 56-59). Previous research recognized the critical role played by the env-ERV, which reportedly exhibits restrictive activity against retroviruses in mice (Fv4, Rmcf, and Rmcf2), sheep (enjS56A1), cats (Refrex-1), and humans (Suppressyn) (8, 58-61). The Env-ERV genes exhibit antiviral activity because of their ability to disrupt the entry of exRVs into host cells. The retroviral envelope binds to host cell surface receptors, and env-ERV proteins compete with these proteins to block viral entry and replication (8, 58, 59).

The objective of this study was to characterize and investigate the potential function of defective env-ERVs as restrictive factors for mammalian retroviruses.

SCOPE OF THIS DISSERTATION

Chapter one:

To demonstrate the truncated Env derived from enFeLV, FeLIX protein, is a restriction factor for mammalian retrovirus infection

Chapter two:

To demonstrate the characterization of the endogenous retrovirus-derived placenta-specific soluble protein EnvV-Fca from domestic cats

Chapter three:

To demonstrate the evolution of antiviral machinery of truncated Env of koala retrovirus during endogenization

1. CHAPTER ONE:

FeLIX is a restriction factor for mammalian retrovirus infection.

This work has been published as follows:

Pramono D, Takeuchi D, Katsuki M, AbuEed L, Abdillah D, Kimura T, Kawasaki J, Miyake A, Nishigaki K.2024. FeLIX is a restriction factor for mammalian retrovirus infection. *Journal of Virology*. https://doi.org/10.1128/jvi.01771-23

1.1. ABSTRACT

Endogenous retroviruses (ERVs) are remnants of ancestral viral infections. Feline leukemia virus (FeLV) is an exogenous and endogenous retrovirus in domestic cats. It is classified into several subgroups (A, B, C, D, E, and T) based on viral receptor interference properties or receptor usage. ERV-derived molecules benefit animals, conferring resistance to infectious diseases. However, the soluble protein encoded by the defective envelope (env) gene of endogenous FeLV (enFeLV) functions as a co-factor in FeLV subgroup T infections. Therefore, whether the gene emerged to facilitate viral infection is unclear. Based on the properties of ERV-derived molecules, we hypothesized that the defective env genes possess antiviral activity that would be advantageous to the host because FeLV subgroup B (FeLV-B), a recombinant virus derived from enFeLV env, is restricted to viral transmission among domestic cats. When soluble truncated Env proteins from enFeLV were tested for their inhibitory effects against enFeLV and FeLV-B, they inhibited viral infection. Notably, this antiviral machinery was extended to infection with the Gibbon ape leukemia virus, Koala retrovirus-A, and Hervey pteropid gammaretrovirus. Although these viruses used feline phosphate transporter1 (fePit1) or fePit1 and phosphate transporter2 (fePit2) as receptors, the inhibitory mechanism involved competitive receptor binding in a fePit1-dependent manner. The shift of receptor usage might have occurred to avoid the inhibitory effect. Overall, these findings highlight the possible emergence of soluble truncated Env proteins from enFeLV as a restriction factor against retroviral infection and will help in developing host immunity and antiviral defense by controlling retroviral spread.

1.2. INTRODUCTION

Retroviruses are RNA viruses that infect a wide range of vertebrate hosts, including mammals (4). Retroviruses are unique because they use reverse transcriptase to convert their RNA genome into DNA, which can then be integrated into the host genome. Enormous amounts of ancient retroviral sequences known as endogenous retroviruses (ERVs) infect germ cells, integrate into the host genome, and are vertically transmitted to offspring (43-45). Some ERV Envelope (Env) proteins may have a potent evolutionary significance in the immunological response by acting as restriction factors against exogenous retroviruses (8, 59). Existing research recognized the critical role played by the env gene derived from ERVs (env-ERV), which reportedly exhibits restrictive activity against retroviruses in mice (Fv4, Rmcf, and Rmcf2), sheep (enjS56A1), cats (Refrex-1), and humans (Suppressyn) (8, 58-61). The antiviral activity of env-ERV genes is likely owing to their ability to interfere with the entry of exogenous retroviruses into host cells (8, 58, 59, 62, 63). The retroviral envelope binds to receptors on the host cell surface and mediates cell entry. Env-ERV proteins compete with exogenous retroviral Env proteins for binding to these receptors, thereby blocking viral entry and replication (8, 58).

Feline leukemia virus (FeLV), a Gammaretrovirus endemic to domestic cats worldwide, was identified as the infectious agent responsible for feline leukemia and lymphoma in the early 1960s (5). FeLV induces malignant hematopoietic disorders, including lymphoma, myelodysplastic syndrome, acute myeloid leukemia, aplastic anemia, and immunodeficiency in cats (6, 7). FeLVs can be categorized into several subgroups based on viral receptor interference and host range. FeLV subgroups and their FeLV-A, -B, -C, -D, -E, and -T receptors have been identified (8-10, 12-18). FeLV-B arises through recombination in the env region between FeLV-A and the endogenous FeLV (enFeLV) present in the feline genome (19, 25, 26). FeLV-A is the primary virus transmitted horizontally among domestic cats. Although horizontal

transmission of FeLV-B mostly does not occur, it may rarely be transmitted by coinfection with FeLV-A (27). Given that in vivo experimental infections have shown resistance to FeLV-B (64), domestic cats are resistant to FeLV-B infection; however, the underlying mechanism is unknown. FeLV-B uses phosphate transporter 1 (Pit1) and phosphate transporter 2 (Pit2) as entry receptors (10, 27). FeLV-B occurs in 33–68% of cats infected with FeLV-A, presumably by independent recombination events that occur de novo after infection of domestic cats with FeLV-A (5, 10, 26). In addition to FeLV-B, various other viruses such as koala retrovirus (KoRV), Gibbon ape leukemia virus (GaLV), Hervey pteropid gammaretrovirus (HPG), 4070A amphotropic murine leukemia virus (4070A MuLV), 10A1 MuLV, and woolly monkey virus use phosphate transporters as viral receptors and can spread to hosts; interspecies transmission can also occur (1).

FeLV-T is a variant of FeLV with a mutation in the PHQ motif of Env (11, 65). FeLV-T utilizes Pit-1 as a receptor but lacks inherent cell fusion ability (66) and requires an assisting molecule, namely FeLIX, for viral infection (11). FeLIX is a soluble, truncated Env protein derived from enFeLV, which is released from cells and is present in the culture supernatant of feline cells (11) and serum from domestic cats (67). FeLV-T is not known to exist as a replication-competent virus, but its replication is supported by helper viruses such as FeLV-A. FeLV-T is rarely found in natural cases (19, 25, 68). Of note, experimental inoculation of a recombinant replication-competent FeLV-T showed severe immunodeficiency in domestic cats (69).

FeLV-B transmission does not occur among domestic cats, supporting that in vivo experimental infection shows resistance to FeLV-B infection (64). The presence of enFeLV has been suggested to be associated with this phenomenon, and FeLV-B infection in Florida panthers lacking enFeLV highlighted the association between enFeLV and FeLV-B (70). The presence of ERV is known to confer resistance to exogenous retroviral infection (8, 58, 59, 70, 71). In particular, the recently identified soluble truncated Env proteins confer resistance to viral

infection of FeLV-D or RD-114 (8, 59); however, the molecular mechanism by which FeLV-B infection is restricted in domestic cats remains unexplained. FeLIX was a co-factor for FeLV-T infection (11) before the possibility of antiviral activity of FeLIX was investigated. The idea that FeLIX has evolutionarily emerged to facilitate viral infection seems unlikely because it has a detrimental function in domestic cats. Therefore, this study aimed to explore the antiviral activities of FeLIX and enFeLV-derived truncated Env.

1.3. MATERIALS AND METHODS

1.3.1. Samples

Samples from domestic cats (58) and European wildcats (72) were described previously. Briefly, an SPF cat, a 2-month-old female, was obtained from the Nippon Institute for Biological Science and euthanized, and an autopsy was performed. The study on European wildcats in Navarra, Spain, was conducted with the support of local authorities. Samples were collected from carcasses between 2000 and 2007 and stored frozen at -18 °C. Tissue samples were collected and sent to the Department of Animal Pathology, Faculty of Veterinary Medicine, University of Zaragoza for necropsy. Animal tissues were stored at -80 °C until DNA or RNA was extracted for further investigations.

1.3.2. Cell lines

The cells were cultured in DMEM (FUJIFILM Wako Pure Chemical Corporation, Osaka, Japan) supplemented with 10% fetal calf serum (FCS) and 1× penicillin-streptomycin. The cells were incubated in a CO_2 incubator at 37 °C. In this study, we used the following cell lines: HEK293T (human embryonic kidney transformed with SV40 large T antigen) (73), MDTF (*Mus dunni* fibroblast tail) (74), CHO (75) AH927 (feline fibroblast cells) (76), CRFK (Crandell-Rees feline kidney) (77), 3201 (feline lymphoma cells) (78), GPLac (an *env*-negative

packaging cell line containing the MuLV gag-pol gene and a beta-galactosidase (LacZ)-coding pMXs retroviral vector) (49), and 293Lac cells containing a LacZ-coding pMXs retroviral vector (79). MDTF cells expressing feline phosphate transporter protein 1 (MDTF-fePit1), MDTF cells expressing feline phosphate transporter protein 2 (MDTF-fePit2), CHO cells expressing feline phosphate transporter protein 1 (CHO-fePit1), and CHO cells expressing feline phosphate transporter protein 2 (CHO-fePit2) were established and cultured in the same medium under the aforementioned conditions.

1.3.3. Establishment of cell lines expressing feline Pit1 and Pit2

Feline Pit1 and Pit2 plasmids were described in a previous report (10). PLAT-A (amphotropic MuLV)-packaging cells were transfected with expression vectors (pMSCVneo-fePit1, pMSCVneo-fePit2, or pMSCVneo empty vector) using the TransIT®-293 reagent (Takara, Kusatsu, Japan). Two days later, the supernatants were collected, filtered through a 0.22 μm filter, and then used to infect MDTF cells in the presence of polybrene (10 μg/mL). PLAT-GP (an env-negative)-packaging cells were co-transfected with an MuLV 10A1 env gene-expression vector, along with the pMSCVneo-fePit1, pMSCVneo-fePit2, or pMSCVneo empty vector, using the TransIT®-293 reagent (Takara). Two days later, the supernatants were collected, filtered through a 0.22 μm filter, and used to infect CHO cells in the presence of polybrene (10 μg/mL). The cells were cultured in a medium containing 600 μg/mL neomycin (G418) for 2 weeks. These cells were termed MDTF-fePit1, MDTF-fePit2, MDTF-empty, CHO-fePit1, CHO-fePit2, and CHO-empty for further analyses.

1.3.4. PCR

KOD-ONE Blue (Toyobo, Osaka, Japan), KOD FX Neo, KOD plus Neo, and GoTaq (Promega, Madison, WI, USA) polymerases were used according to the manufacturer's instructions.

1.3.5. PCR product cloning

PCR products were cloned directly into the pCR4Blunt-TOPO (Invitrogen, Carlsbad, CA, USA) or pUC118 vector (Mighty Cloning Kit; Takara). The intact env gene was inserted into the pFUΔss expression vector (49). Sequencing was performed using a contracted service (Fasmac Corporation, Atsugi, Kanagawa, Japan).

1.3.6. Cloning of enFeLV proviruses and construction of Env expression vector

The construction of a genomic library using cat DNA has been reported previously (49). Briefly, splenic DNA from a single cat (ON-T) suffering from lymphoma due to FeLV infection was digested with EcoRI and ligated to Lambda DASH II/EcoRI vectors (Agilent Technologies, Santa Clara, CA, USA). DNA libraries were screened using a DIG-labeled enFeLV LTR probe generated using PCR with primers Fe-36S and Fe-60R in feline normal chromosomal DNA. The PCR DIG Probe Syndissertation kit for probe syndissertation and the CSPD luminescent detection kit for visualization of the bound probe were used according to the manufacturer's instructions (Roche Molecular Biochemicals, Mannheim, Germany). The flanking genomic sequences of the enFeLV proviruses were determined from positive phages, and full-length enFeLV proviruses were amplified from normal cat DNA or ON-T chromosomal DNA using specific primers (Table 1.1). The amplicons were cloned into pCR4 blunt-TOPO (Invitrogen, Carlsbad, CA, USA) and sequenced (Fasmac Corporation).

Env expression vectors of enFeLV-clone1, clone2, and clone3 were constructed through PCR amplified using the prime pair Fe-560S and Fe-550R based on the enFeLV proviruses in TOPO vector and were cloned into pFUΔss between the BamHI and EcoRI restriction sites (Table 1.1). enFeLV-AGTT derived from enFeLV-clone3 was constructed using site-directed mutagenesis with the primer pair Fe-661S and Fe-642R. Env expression vectors were constructed using KOD-ONE Blue (Toyobo, Osaka, Japan) following the manufacturer's

protocol. The resulting Env expression plasmids were confirmed through sequencing (Fasmac Corporation).

1.3.7. Construction of truncated Env expression vectors

The expression vector pFUΔss was used to construct the expression plasmids. The genes were PCR-amplified from each plasmid using specific primers with enzyme sites, and the PCR products were digested with each restriction enzyme and cloned into the pFUΔss expression plasmid. The Env expression plasmid for pFUΔss FeLIX-D249 was constructed via site-directed mutagenesis using the primer pair SDM-FeLIX1 and SDM-FeLIX2 based on the pFUΔss FeLIX-D249 expression plasmid (58). Truncated Env enFeLV-clone4 (referred to as Trunc-C4) was constructed based on enFeLV-clone4 provirus with primer pairs enFeLVc4-F1 and Fe-686R; and FeLV-B/GA RBD (FeB-RBD) with RBD-F1 and Fe-716R and then cloned into the pFUΔss between the BamHI and EcoRI restriction sites (Table 1.1). The resulting mutants and Env expression plasmids were confirmed using sequencing (Fasmac Corporation).

1.3.8. Construction of chimeric replication-competent virus

Replication-competent FeLV-A/61E carrying the enFeLV-AGTT env gene was constructed by replacing the env gene. Briefly, the env gene of enFeLV-AGTT was PCR-amplified using primers Fe-721S and Fe-748R. The amplicon and FeLV-A/61E provirus digested with SnaB1 and Sph1 (Takara) were ligated using In-Fusion HD Cloning Kits according to the manufacturer's protocol (Takara). The resulting chimeras, termed 61E/AGTT, were confirmed using sequencing (Fasmac Corporation). 293Lac cells were transfected with 61E/AGTT using the TransIT®-293 reagent. The culture supernatant was confirmed to infect AH927 and CRFK cells at high titers using LacZ staining. To prepare replication-competent viruses, 293Lac cells transfected with FeLV-A/61E, FeLV-B/Gardner–Arnstein (GA), or 61E/AGTT were cultured,

and the supernatants were used as the virus stock. The supernatant from HEK293T cells persistently infected with FeLV-B/ON-T (49) was used to infect AH927 cells carrying LacZ (AH927Lac cells). The cell supernatant was used as the viral stock. Notably, the supernatant of AH927Lac cells infected with FeLV-B ON-T cells contained FeLV-B and replication-defective FeLV-D, with a low viral titer.

1.3.9. Construction of Env mutants

Env mutants from enFeLV-clone1 were compared with enFeLV-clone2, enFeLV-clone3, and enFeLV-AGTT to identify amino acid candidates for Env mutants. Mutants derived from enFeLV-clone 1 were constructed using site-directed mutagenesis with the plasmids enFeLV-clone1, E345G, and N394K. The primer pairs used for site-directed mutagenesis were as follows: Fe-577S and Fe-569R for enFeLV-clone1 and E345G and Fe-578S and Fe-570R for N394K. Env mutants derived from FeLV-B/GA, FeLV-B/FO36-5B, and FeLV-B/ON-T were constructed via site-directed mutagenesis using the following plasmids (primer pairs): FeLV-B/GA Q73R (Fe-761S and Fe-788R), FeLV-B/FO36-5B K66D (Fe-782S and Fe-807R), and FeLV-B/ON-T R73Q (Fe-792S and Fe-812R). The mutants were constructed using KOD-ONE Blue (Toyobo) following the manufacturer's protocol. The resulting mutants were confirmed using sequencing.

1.3.10. Env-pseudotyped virus preparation

The preparation of Env-pseudotyped viruses carrying LacZ as a marker has been described previously (49). Briefly, GPLac cells were seeded at a concentration of approximately 1×10^6 cells in a six-well plate 1 day prior to transfection. The Env expression plasmids used for viral preparation were as follows: pFUΔss FeLV-B/GA (FeLV-B Gardner–Arnstein Env), pFUΔss FeLV-B/MZ40-5B Env, FeLV-B/KG20-5B Env, FeLV-B/FO36-5B Env (19), FeLV-B/ON-T

Env, FeLV-B mutants (FeLV-B/Q73R Env, FeLV-B/ FO36-5B K66D Env, FeLV-B/ON-T R73Q Env), FeLV-A/clone33 Env (80), pFUΔss FeLV-C/Sarma (81), pFUΔss FeLV-E/TG35-2 (82), pFUΔss FeLV-T/KC18-6 (19), enFeLV-clone1 E345G Env, enFeLV-clone2 Env, enFeLV-clone3 Env, enFeLV-AGTT, GaLV Env, KoRV Env (opt-KoRV-A2), and HPG Env (opt-HPG). The mammalian retrovirus env genes (opt-KoRV-A2 env and opt-HPG env) were synthesized (Eurofins Genomics, Tokyo, Japan). The KoRV Env and HPG Env genes were myc-tagged at the C-terminus and inserted into the pFUΔss vector. MuLV 10A1 Env and MuLV 4070A Env were purchased commercially (Novus Biologicals). GaLV Env was PCR-amplified from PG13 cells (83) and cloned to the pFUΔss vector. The culture supernatants were collected 48 h after transfection (TransIT-293 transfection reagent), filtered through a 0.22 μm filter or centrifuged at 15,400 × g for 2 min at 4 °C, and stored at -80 °C as virus stock for further experiments.

1.3.11. Infection assay

Target cells (approximately 3×10^5 cells/well) were seeded in 24-well plates 1 day prior to infection. The target cells were infected with each 250 μL of Env-pseudotyped virus in the presence of 10 μg/mL polybrene (Nacalai Tesque, Kyoto, Japan) for 2 h. After the addition of fresh medium, the cells were cultured for 2 days post-infection. After 48 h of incubation, the cell supernatants were removed, and the cells were fixed with 250 μL of 2% glutaraldehyde for 15 min at room temperature (20–25 °C) and stained with 5-bromo-4-chloro-3-indolyl-β-D-galactopyranoside (X-Gal); blue-stained nuclei, as visualized under a microscope, were counted. Viral titers are presented as infectious units (IU) per milliliter with standard deviations.

1.3.12. Viral interference assay

The viral interference assay was performed as described previously (10, 11). AH927 cells infected with the replication-competent viruses, FeLV-B/GA and FeLV-B/ON-T, and were

cultured as AH927/FeLV-B/GA and AH927/FeLV-B/ON-T cells for the interference assay. AH927/FeLV-B/ON-T cells contained replication-defective FeLV-D. Target cells were infected with 250 μL of Env-pseudotyped virus for 2 days in the presence of 10 μg/mL polybrene (Nacalai Tesque). Two days post-infection, the cells were stained with X-Gal staining solution, the number of blue-stained nuclei were counted, and single-cycle infectivity was measured and visualized under a microscope. Viral titers are presented as IU per milliliter with standard deviations.

1.3.13. Viral inhibition assay in the presence of truncated Env proteins

HEK293T cells were seeded at a concentration of approximately 1×10^6 cells in a six-well plate 1 day prior to transfection with truncated Env expression plasmids. The supernatants of HEK293T cells transfected with pFUΔss FeLIX-N249, pFUΔss FeLIX-D249, pFUΔss FeLV-B/GA RBD (hereafter termed as FeB-RBD), pFUΔss Env clone4 (Trunc-C4), and pFUΔss empty vector (negative control) for approximately 48 h were the source of truncated Env proteins. The infection assay was conducted as described previously. In 24-well plates, target cells were treated with 250 μL of cell supernatant (source of truncated Env protein) for 2 h. Subsequently, 250 μL of Env-pseudotyped viruses or replication-competent viruses were inoculated into the target cells with 10 μg/mL polybrene for 2 h, after which 250 μL of fresh medium was added. Two days post-infection, the cells were stained with X-Gal. Single-cycle infectivity was determined by counting blue-stained nuclei under a microscope. International unit (IU) per milliliter and standard deviations were used to represent the viral titers.

1.3.14. Viral infection assay in the presence of supernatants of cell cultures

A viral infection assay was performed in the presence of cell supernatants from 3201 cells to investigate the inhibitory effects of cell supernatants on viral infection. The culture supernatant

of cells cultured for 2 days at a concentration of approximately 3×10^6 cells was collected and kept at -80 °C after it was filtered through a 0.22 μm filter. The viral interference assay was essentially followed by an infection assay in 24-well plates. First, 250 μL of cell supernatant was incubated for 2 h. Next, 250 μL of Env-pseudotyped viruses were inoculated into AH927 cells in the presence of 10 μg/mL polybrene (Nacalai Tesque). The supernatants of 3201 cells were depleted using anti-FeLV gp70 SU (gp70; NCI, Frederick, MD, USA). The supernatant was treated for 4 h at 4 °C with goat anti-FeLV gp70 antibody or normal goat serum as a control (Wako Pure Chemical Industries, Ltd., Osaka, Japan), conjugated with protein G-agarose (Santa Cruz Biotechnology), and centrifuged at 15,400 × g for 2 min at 4 °C.

1.3.15. Detection of fePit1 and fePit2 expression levels via RT-qPCR

Total RNA was extracted from the tissues of a specific pathogen-free cat (SPF) described in our previous study (58), as well as from the feline cell lines AH927 (feline embryonic fibroblast cells), CRFK (feline kidney cells), Fet-J (PBMCs), MCC (feline large granular lymphoma cells) (84), 3201 (feline T-cell lymphoma cells), and MS4 (feline B-cell lymphoma cells) (85) using the RNAiso Plus kit (Takara, Tokyo, Japan), in accordance with the manufacturer's instructions. Thereafter, cDNA was synthesized using the PrimeScript II first-strand cDNA syndissertation kit (Takara) according to the manufacturer's instructions. Prior to reverse transcription, the RNA samples were treated with recombinant DNase I (TaKaRa). The cDNA was amplified using SYBR Premix Ex Taq II (Tli RNase H Plus; Takara) in the CFX96 Touch real-time PCR detection system (Bio-Rad, Hercules, CA, USA). Feline Pit1 was amplified using the primers Fe-844S and Fe-874R. Feline Pit2 was amplified using the primers Fe-845S and Fe-875R, and the internal control feline peptidyl prolyl isomerase A (PPIA) was amplified using the primers Fe-227S and Fe-204R. Thermal cycling was performed according to the manufacturer's instructions.

1.3.16. Detection of FeLIX expression level via qRT-PCR

Briefly, the same cDNA samples were used for the detection of FeLIX, including those from the tissues of a specific pathogen-free cat (SPF) and the feline cell lines AH927, CRFK, Fet-J, MCC, MS4, and 3201. The cDNA was amplified using Premix Ex Taq (Probe qPCR; Takara) in the CFX96 Touch real-time PCR detection system (Bio-Rad). FeLIX was amplified using primers FeLIX-F and FeLIX-R, and the amplification was detected using the probe FeLIX-P (containing 6-carboxy-fluorescein; FAM). The internal control feline PPIA was amplified using primers Fe-227S and Fe-204R via SYBR Premix Ex Taq II (Tli RNaseH Plus; Takara). Thermal cycling was performed according to the manufacturer's instructions.

1.3.17. Immunoprecipitation and immunoblotting

Plasmids were introduced into HEK293T or GPLac cells in six-well plates using the TransIT®-293 reagent (Takara). Two days after transfection, cell pellets were collected by washing with phosphate-buffered saline three times. Cells were resuspended in lysis buffer (20 mM Tris-HCl [pH 7.5], 150 mM NaCl, 10% glycerol, 1% Triton X-100, 2 mM EDTA, 1 mM Na_3VO_4, and 1 μg/mL each of aprotinin and leupeptin) to prepare cell lysates, which were then incubated for 20 min on ice. Top-speed centrifugation (15,400 × g) for 20 min at 4 °C was used to remove the insoluble components, and a protein assay kit (Bio-Rad Laboratories, Carlsbad, CA, USA) was used to calculate the protein concentrations.

Cell supernatants were filtered through a 0.22 μm filter and were incubated overnight at 4 °C with the desired antibody. The purified protein (cell lysate and supernatant) was mixed with sample buffer solution (Nacalai Tesque) and then heated at 95–100 °C for 5 min. Sodium dodecyl sulfate-polyacrylamide gel electrophoresis was conducted using 4–20% gels (Invitrogen, Carlsbad, CA, USA) at 100 V for 2 h, and the sample was then transferred to nitrocellulose filters for western blotting with the following primary antibodies used in the

assays: anti-Myc monoclonal antibody conjugated with horseradish peroxidase (FUJIFILM Wako Pure Chemical Corporation; dilution 1:1,000), goat polyclonal anti-FeLV gp70 SU (NCI; dilution 1:15,000), and mouse anti-FeLV TM protein (p15E; antibody PF6J2A; Custom Monoclonals International, CA, USA; dilution 1:5,000). The secondary antibodies were horseradish peroxidase (HRP)-conjugated anti-mouse IgG (Cell Signaling Technology, Danvers, MA, USA; dilution 1:3,000) or HRP-conjugated donkey anti-goat IgG (Santa Cruz Biotechnology; 1:10,000). The substrate was LumiGLO® Reagent (20×) and 20X peroxide (Cell Signaling Technology). For imaging, the blots were developed using Amersham ImageQuant 800 (Cytiva, Shinjuku, Tokyo, Japan).

1.3.18. Phylogenetic and sequence analyses

To identify enFeLV-related sequences in domestic cats (*Felis catus*), the env gene sequence of enFeLV-AGTT was first BLAST-ed against all domestic cat genomes available in the National Center for Biotechnology Information (NCBI, GCA_018350175.1, GCA_016509815.2, GCA_000181335.6, GCA_000003115.1, and GCA_013340865.1). Next, 10 kbp upstream and downstream genomic regions for enFeLV-like viral env genes were downloaded under the condition that only proviruses containing an env gene were analyzed. Sequences were compared using SEAVIEW (86), BioEdit (87), and Genetyx software (Genetyx Corporation, Tokyo, Japan). All enFeLV-related viruses are listed in Table 1.2. A phylogenetic tree was constructed using the sequences listed in Table 1.2. The MEGA11 software package was used for the phylogenetic analysis (52). Alignment was performed using MUSCLE (88). A phylogenetic tree was constructed using the maximum likelihood (ML) method, with robustness evaluated by bootstrapping (1,000 times). The substitution models were selected based on the lowest BIC score (HKY + G) for the LTR (52, 89).

1.3.19. Estimation of the integration timings of FeLV truncated Env and full-length Env

The NCBI RefSeq genomic database was scanned for enFeLV-related viral env genes by BLAST-ing. The enFeLV provirus sequences were extracted. The estimated integration timing based on the substitution rate of 5' LTR and 3' LTR sequences was calculated (Table 1.3). The mean divergence rate of noncoding regions in the domestic cat genome (1.2 × 10-8 substitutions/site/year) was used because the mutation rate of LTRs in enFeLVs is unknown (90). The 5' LTR and 3' LTR sequences of each enFeLV were multiple-aligned, and the genetic distance (D) was calculated using the Kimura two-parameter model (91) in MEGA11 software (52).

1.3.20. Statistical analysis

Data are represented as the mean with standard deviation (SD) in all bar diagrams. The results of assays were considered statistically significant if p-values were <0.05 according to Student's t-test.

1.3.21. Ethical approval

Animal studies were conducted in accordance with the guidelines for the care and use of laboratory animals provided by the Ministry of Education, Culture, Sports, Science, and Technology, Japan. All the experiments were approved by the Genetic Modification Safety Committee of Yamaguchi University.

1.3.22. Data availability

All data in this study are included in the main text, figures, and supplementary information. The sequences described in this paper have been deposited in the DDBJ/EMBL/GenBank under the accession numbers LC196053–LC196055 and LC198317-LC198319.

1.4. RESULTS

1.4.1. Genetic diversity of enFeLV in domestic cats

Much remains unknown regarding the interaction between FeLV-B and enFeLV, and complete analyses of enFeLV in domestic cats have not been conducted. Therefore, in this study, we used two strategies to identify enFeLV sequences in domestic cats. The first approach involved searching for publicly available whole-genome sequence data from domestic cats. We downloaded all available domestic cat sequence data using the env gene of enFeLV-AGTT as a reference because our objective was to determine the Env function of enFeLV. Our second approach involved genomic library screening and PCR using locus-specific primers (Table 1.1). Sequence analysis revealed six proviruses carrying the env gene, namely, enFeLV-clone1, -clone2, -clone3, -clone4, -clone5, and -clone6; three of these proviruses (enFeLV-clone1, enFeLV-clone2, and enFeLV-clone3) had intact open reading frames (ORFs) for env (Figure 1.1), whereas the other three (enFeLV-clone4, enFeLV-clone5, and enFeLV-clone6) had defective env genes. Sequence analysis of the database identified that enFeLV-clone5, referred to as CFE16 (92) and FeLIX (11), carried a truncated *env* gene. The truncated enFeLV-clone4 Env was termed Trunc-C4. EnFeLV-clone6 had an ORF as the defective *env* gene. The obtained proviruses data (Table 1.1) were comprehensively analyzed via the phylogenetic tree using 5′ and 3′ long terminal repeat (LTR) sequences, where enFeLV grouped differently from exogenous FeLV (exFeLV) (Figure 1.2A). Examination of the chromosomal location of enFeLV in the cat genome revealed that it was widely present on almost all chromosomes, with chromosome B4 having the highest copy number; however, no enFeLV was found on chromosomes C1, C2, D2, E1, E2, E3, and F2 (Figure 1.2B).

The 5′ and 3′ LTR sequences of each enFeLV had high sequence identity or were identical to each other. The integration time of each enFeLV locus was estimated by comparing the nucleotide mismatch between the 5′ and 3′ LTRs (Table 1.2). EnFeLVs carrying env were

estimated to have been endogenized less than 1 million years ago (Figure 1.2C). Notably, enFeLV-clone5 (CFE-16 and FeLIX) and enFeLV-clone4 were endogenized less than 700 and 200 thousand years ago, respectively (Table 1.2).

Next, we divided the enFeLV Env structures into four groups (Figures 1.1 and 1.2D). The first group, intact full-length Env, had approximately 666 amino acids with a signal peptide (SP), surface unit (SU) containing variable region A (VRA) and variable region B (VRB), receptor-binding domain (RBD), and transmembrane (TM) region. The second group, defective Env-like Trunc-C4 (length > 300 aa), had SP and VRA and VRB in Env SU but lacked the TM region. The third group, FeLIX (CFE16, enFeLV-clone 4; length = 273 aa), had only SP and VRA and VRB in Env SU, and the fourth group, Env, had a length of 140–273 aa and lacked the VRA, VRB, or TM region. Taken together, the structural diversity of Env was generated less than 1 million years ago (Mya) (Figure 1.1).

1.4.2. Infectivity of enFeLV Env-pseudotyped virus

To determine whether the intact env genes of enFeLVs form infectious viral particles using MLV Gag-Pol and MuLV retroviral vectors carrying LacZ as a marker, GPLac cells were transfected with the *env* gene to produce the enFeLV Env-pseudotyped virus. The results showed that enFeLV-clone2, enFeLV-clone3, and enFeLV-AGTT infected AH927 and CRFK cells as the target cells (Figure 1.3A). They showed high viral titers comparable with those observed in FeLV-B infection (Figure 1.3A). In contrast, enFeLV-clone1 did not cause infection. The expression of enFeLV-clone1 Env, as demonstrated via western blot analysis, showed incomplete cleavage between SU (gp70) and TM (p15e; Figure 1.3C). Amino acids involved in infectivity were determined by comparing the amino acid sequences of enFeLV-clone1 and enFeLV Env (clone2 and clone3). The enFeLV-clone1 mutants E345G (substitution of glutamic acid with glycine at position 345) and N394K (substitution of asparagine with lysine at position

394) were tested for infection with their Env-pseudotyped viruses. The enFeLV-clone1 E345G showed infectivity (Figure 1.3B), and the SU-TM region was cleaved by Env (Figure 1.3C). In contrast, the other mutant (N394K) did not infect target cells (Figure 1.3B) and was not cleaved by Env (Figure 1.3C). This confirmed that the amino acid change from G (glycine) to E (glutamic acid) at position 345 caused cleavage failure of the Env protein, resulting in the loss of viral infectivity. These results suggest that enFeLV Env can generate infectious particles that may pose a threat to domestic cats.

1.4.3. Identification of an entry receptor for enFeLV

FeLV-B is generated through recombination in the env region between FeLV-A and enFeLV (19, 25, 26). We hypothesized that enFeLV uses the same receptor as FeLV-B, termed feline Pit1 (fePit1) and feline Pit2 (fePit2). fePit1 and fePit2 are members of the family of solute carrier proteins SLC20A1 and SLCA20A2, structurally identical sodium-dependent phosphate transporters. *Mus dunni* tail fibroblast (MDTF) cells that were resistant to enFeLV infection (Figure 1.3D), MDTF cells expressing fePit1 (MDTF-fePit1), and MDTF cells expressing fePit2 (MDTF-fePit2) were tested for infection with enFeLV Env-pseudotyped viruses prior to analysis 2 days later.

The results showed that MDTF-fePit1 cells were permissive to enFeLV Env-pseudotyped virus infection of clone1 E345G, clone2, clone3, and AGTT, whereas MDTF-fePit2 cells were not infected with any of the enFeLV Env-pseudotyped viruses (Figure 1.3D). Interestingly, both enFeLV-clone1, estimated to have integrated approximately 220 thousand years ago, and clone2, a recent addition, utilized the same receptor (Table 1.3).

Next, we evaluated the receptor usage of the five FeLV-B strains, showing the structural diversity of *env* genes by recombination analysis (19) (Figure 1.4). MDTF-fePit1 cells were permissible for infection with all FeLV-B Env-pseudotyped viruses (GA, MZ40-5B, KG20-5B,

FO36-5B, and ON-T), whereas only two FeLV-B Env-pseudotyped viruses (FO36-5B and ON-T) could infect MDTF-fePit2 cells (Figure 1.3E). Based on the amino acid sequence of FeLV-B env, lysine at amino acid position 66 and arginine at position 73 in env VRA may be associated with a shift in receptor use. Therefore, FeLV-B/FO36-5B K66D (lysine to aspartic acid) and FeLV-B/ON-T R73Q (arginine to glutamine) mutants were tested for receptor usage. FeLV-B/FO36-5B K66D and FeLV-B/ON-T R73Q infected MDTF-fePit1 cells but not MDTF-fePit2 cells. Furthermore, FeLV-B/GA Q73R (glutamine to arginine) infected both MDTF-fePit1 and MDTF-fePit2 cells, whereas FeLV-B/GA only infected MDTF-fePit1 cells (Figure 1.3E). These results indicate that lysine at position 66 and arginine and glutamine at position 73 affect the receptor usage of FeLV-B infection. We conducted an interference assay with FeLV-B/GA (fePit1) and FeLV-B/ON-T (fePit1 and fePit2) in AH927 cells. The pseudotyped viruses of FeLV-B/GA did not infect the AH927 cells infected with FeLV-B/ON-T. Conversely, FeLV-B/ON-T did not infect the AH927 cells infected with FeLV-B/GA (Figure 1.3F). These results suggest that blocking the fePit1-mediated infection pathway is sufficient to prevent FeLV-B infection. In other words, the major pathway for FeLV-B infection may involve fePit1.

1.4.4. Expression of fePit1 and fePit2 in feline tissues and cell lines

Proteins of 681 and 653 amino acids were predicted to be encoded by fePit1 and fePit2, respectively (10, 93). Approximately 88% of the amino acids in fePit1 and fePit2 are identical. qRT-PCR showed the expression of fePit1 and fePit2 mRNA; the cerebellum, large intestine, ovaries, and spleen exhibited the highest levels of fePit1 expression. The cerebellum, kidneys, uterus, and liver exhibited the highest fePit2 expression (Figure 1.5A). The fePit1 and fePit2 genes were detected in all feline cell lines, including AH927 (feline fibroblast cells), CRFK (kidney cells), Fet-J (peripheral blood mononuclear cells [PBMCs]), MCC (large granular lymphoma cells), MS4 (B-cell lymphoma cells), and 3201 (T-cell lymphoma cells; Figure

1.5B). Hematopoietic cell lines tended to express Pit1 and Pit2; however, they are expressed at lower levels in AH927 and CRFK cells. These findings indicate that fePit1 and fePit2 are broadly expressed in feline tissues and cell lines.

1.4.5. Truncated Envs from enFeLV

FeLIX (CFE16, enFeLV-clone5) and Trunc-C4 had similar structures, with lengths of 273 aa and 369 aa, respectively (Figure 1.6A). We examined whether truncated env genes expanded across domestic cats in Japan. Proviruses encoding FeLIX on chromosomes B1 (Chr B1) and B4 were detected using PCR in genomic DNAs from blood in domestic cats (Figure 1.6B). In addition to examining the loci, a single-nucleotide polymorphism (SNP) in the genes encoding FeLIX was identified as either aspartic acid (D) or asparagine (N) at amino acid position 249 on chromosome B1. Asparagine (N) was found at amino acid position 249 in B4. These cells were termed FeLIX-N249 and FeLIX-D249, respectively. Notably, an SNP of FeLIX was located within the FeLV-A-neutralizing epitope “MGPNL” at amino acid positions 246–250 in FeLV-A/61E Env. Furthermore, the neutralizing epitope was not conserved in FeLIX-N249 (MGPNP) and FeLIX-D249 (MGPDP) and contained a substitution of proline (Figure 1.7). Trunc-C4 was detected in 12 of 22 cats, suggesting that Trunc-C4 is not conserved in domestic cats (Figure 1.8). We determined whether FeLIX and Trunc-C4 are evolutionarily conserved in felids. We detected FeLIX-D249 on chromosome B1 and FeLIX-N249 on chromosome B4 in all European wild cats (nine cats); however, Trunc-C4 was not detected. As the 5′ LTR and 3′ LTR of Trunc-C4 showed a high genetic distance between them, this provirus could be generated by recombination; therefore, the integration time calculated by LTRs may not support that estimated based on animal segregation (Figure 1.2A). These results suggest that FeLIX emerged as a common ancestor of domestic cats and European wild cats.

Next, we quantified FeLIX expression in normal feline tissues (specific-pathogen-free [SPF] cats) and cell lines using qRT-PCR. FeLIX was broadly expressed in tissues, with the highest levels identified in immune system tissues (spleen, bone marrow, and lymph nodes) and PBMCs. FeLIX was detected in 3201, MS4, and MCC cells but not in AH927 and Fet-J cells. FeLIX was barely detectable in CRFK cells, with an extremely low relative expression level of 0.003 (Figure 1.6C and 1.6D). Sequence analysis showed that both FeLIX-N249 and FeLIX-D249 were expressed in 3201 cells, whereas only FeLIX-N249 was expressed in all other cells as well as in tissues from the spleen, bone marrow, mandibular lymph node, and lungs from one cat (Figure 1.6E).

We could not determine the expression of Trunc-C4 in domestic cats because of the high sequence similarity with the enFeLV sequences. Next, we determined the expression of FeLIX and Trunc-C4 as soluble proteins. The supernatants of HEK293T cells transfected with FeLIX-N249, FeLIX-D249, and Trunc-C4 expression plasmids were immunoprecipitated using an anti-FeLV gp70 antibody, and western blot analysis was conducted using the same antibody (Figure 1.6F and 1.6G). We confirmed the presence of FeLIX in the supernatants of 3201 cells, consistent with previous reports (11, 67). However, a faint band was observed in the supernatant of AH927 cells (Figure 1.6H); this likely represented a non-specific band, as the AH927 cells did not express FeLIX-N249 or FeLIX-D249 (Figure 1.6E). Overall, the results showed that these proteins were present in the cell supernatants, suggesting that FeLIX-N249, FeLIX-D249, or Trunc-C4 is secreted from cells as soluble proteins.

1.4.6. Truncated Env proteins derived from enFeLV confer resistance to enFeLV and FeLV-B infection

FeLIX acts as a co-factor for FeLV-T infection (11). However, truncated ERV Env proteins exhibit antiviral functions (58, 59). Therefore, we investigated whether truncated Env proteins

from enFeLVs showed antiviral activity, which benefits the host. HEK293T cells were transfected with each expression plasmid, and the supernatants were collected as sources of FeLIX-N249, FeLIX-D249, and Trunc-C4 proteins. The RBD from FeLV-B/GA, termed FeB-RBD, was used in this study because it showed an inhibitory effect against the FeLV-B/GA strain (94). Next, FeLIX-N249, FeLIX-D249, Trunc-C4, and FeB-RBD were assessed for their inhibitory effects on enFeLV Env-pseudotyped viruses (clone1 E345G, clone2, clone3, and AGTT) and FeLV-B (GA, MZ40-5B, KG20-5B, FO36-5B, and ON-T) in AH927 and CRFK cells. The target cells were treated with the truncated Env proteins for 2 h. Subsequently, pseudotyped viruses were infected into target cells for infection analysis 2 days later. FeLIX, Trunc-C4, and FeB-RBD significantly ($p < 0.01$) inhibited infection with all four enFeLV Env-pseudotyped viruses and all five FeLV-B Env-pseudotyped viruses (Figures 1.9A, 1.9B, 1.10A, 1.10B, and 1.11). Notably, different inhibitory effects on enFeLV-clone2 and clone3 were observed between FeLIX-N249 and FeLIX-D249 when HEK293T cells were used as the target cells for the assay (Figure 1.12). To determine the specificity of the inhibitory effects of FeLIX, Trunc-C4, and FeB-RBD, the inhibition assay was extended to FeLV-A, FeLV-C, and FeLV-E Env-pseudotyped viruses. The results showed that they had no inhibitory effects on FeLV-A, FeLV-C, or FeLV-E infection (Figure 1.9B). Furthermore, infection of AH927 and CRFK cells by enFeLV-AGTT, FeLV-B/ON-T, and FeLV-B/GA Env-pseudotyped viruses was inhibited in a dose-dependent manner (Figures 1.9C and 1.10C). The inhibitory effect of FeLIX on replicative viral infections was tested. A chimeric replication-competent virus carrying enFeLV-AGTT env (61E/AGTT) was constructed from FeLV-A/61E. We evaluated FeLIX against the replication-competent infectious viruses FeLV-B/ON-T, FeLV-B/GA, 61E/AGTT, and FeLV-A/61E. Interestingly, FeLIX showed a complete inhibitory effect on replication-competent infectious viruses (Figure 1.9D and 1.10D). However, this effect was not observed

in FeLV-A 61E infections. Collectively, FeLIX blocked the infection and replication of FeLV-B and enFeLV.

1.4.7. Feline Pit1-dependent inhibitory effect of FeLIX

We attempted to elucidate the mechanism underlying the inhibitory effect of FeLIX on FeLV-B and enFeLV infection in MDTF-fePit1 and MDTF-fePit2 cells. FeLIX inhibited both retroviral infections in MDTF-fePit1 cells (Figure 1.9E and 1.9F). However, FeLV-B/FO36-5B, FeLV-B/ON-T, and FeLV-B/GA Q73R mutants, which showed shifted receptor usage, were not inhibited by FeLIX in MDTF-fePit2 cells (Figure 1.9G). FeLV-B/ON-T R73Q, FeLV-B/GA Q73R, and FO36-5B K66D, which showed shifted receptor usage, were inhibited by FeLIX in AH927, CRFK, and MDTF-fePit1 cells (Figures 1.9B, 1.10B, and 1.9F). Inhibition by FeB-RBD was fePit1-dependent but not fePit2-dependent, resulting in an effect similar to that of FeLIX. These results suggest that FeLIX inhibits viral infection via fePit1 but not fePit2.

1.4.8. Inhibitory effects of FeLIX from the supernatant of 3201 cells against FeLV-B and enFeLV infection

FeLIX was present in the supernatants of 3201 cells, as previously reported (11, 67), and qRT-PCR and western blot analyses confirmed the expression of FeLIX in 3201 cells (Figure 1.6D and 1.6H). We tested the supernatant of 3201 cells for pseudotyped FeLV-B and enFeLV in AH927 cells as target cells. The supernatant of 3201 cells showed significantly inhibited infection with FeLV-B (GA, MZ40-5B, KG20-5B, and ON-T) and enFeLV (AGTT, clone 1 E345G, and clone2; $p<0.01$; Figure 1.13A). The level of inhibition of FeLV-B GA from the supernatant of 3201 cells tended to be lower than that of other viruses. Infection with FeLV-A, FeLV-C, or FeLV-E was not inhibited in the supernatant of the 3201 cells (Figure 1.13A). Notably, the antiviral effect of the culture supernatant derived from 3201 cells was not

significant when a high viral titer (10^5 units/mL of FeLV-B/GA) was used to examine the antiviral effect (Figure 1.14).

Next, the supernatant of 3201 cells was subjected to FeLIX depletion using an anti-FeLV gp70 antibody (gp70; National Cancer Institute [NCI], Frederick, MD, USA) to evaluate the specificity of FeLIX. The inhibition of FeLV-B (ON-T and MZ40-5B) and enFeLV (clone1 E345G and clone2) infection disappeared; however, treatment with normal goat antisera did not affect the inhibitory effect of the supernatant from 3201 cells (Figure 1.13B). Furthermore, FeLV-T infection was monitored to assess whether this antibody depleted FeLIX in the supernatant of the 3201 cells. First, the supernatants from 3201 cells supported FeLV-T infection, whereas the supernatants from AH927 cells, which did not express FeLIX, did not support FeLV-T infection. FeLV-T infection was lost in the FeLIX depletion experiment using an anti-FeLV gp70 antibody (Figure 1.13C).

1.4.9. Thermal sensitivity of FeLIX

The inhibitory effect of FeLIX following heat treatment was examined; culture supernatants from 3201 cells and HEK293T cells transfected with FeLIX-N249 were treated at 56 °C for 30 min. The results showed that the inhibitory effects of FeLIX-N249 on FeLV-B/ON-T were abolished; however, FeLV-T/KC18-6 infection was still observed (Figure 1.15A). Furthermore, we examined the effects of the heat treatment of FeLIX from the supernatant of 3201 cells on FeLV-B/ON-T and FeLV-T/KC18-6 infection. The results showed a significant reduction in the function of FeLIX as either an inhibitor for FeLV-B/ON-T or a co-factor for FeLV-T/KC18-6 infections (Figure 1.15B; $p<0.05$); however, FeLV-T/KC18-6 infection remained. To further confirm FeLV-T infection, the supernatant of 3201 cells was serially diluted and then treated at 56 °C for 30 min. The viral titer of FeLV-T infection decreased to ten-fold when FeLIX was diluted at a ratio of 1:16 and FeLV-T infection was abolished at a dilution of 1:32. However,

FeLV-T infection remained when FeLIX was diluted at ratios between 1:2 and 1:8 (Figure 1.15C). These results suggest that FeLIX is heat-sensitive, and the antiviral activity and co-factor function of FeLIX were abolished after incubation at 56 °C for 30 min.

1.4.10. Inhibitory effect of FeLIX on non-feline mammalian retroviruses

The entry receptors of several non-feline retroviruses, including GaLV, KoRV-A, HPG, and 4070A MuLV, have been reported (28-30, 37), and their hosts are monkeys, koala, and bats (*Pteropus alecto*) (30, 37, 95). We first assessed whether these viruses could infect feline cells. GaLV, KoRV, HPG, and 4070A MuLV cells were susceptible to AH927 and CRFK cells with high viral titers (Figure 1.16A). Furthermore, GaLV and HPG could infect both MDTF-fePit1 and MDTF-fePit2, whereas KoRV could only infect MDTF-fePit1. As 4070A MuLV could infect MDTF cells (Figure 1.16B), the virus receptor was determined in Chinese hamster ovary (CHO) cells, which are not permissive to 4070A MuLV infection. We found that 4070A MuLV could infect CHO cells expressing fePit2 (CHO-fePit2) but not CHO cells expressing fePit1 (CHO-fePit1; Figure 1.17A). These results suggest that these non-feline retroviruses have the potential to cause infection via the feline phosphate transporter. GaLV and HPG used both fePit1 and fePit2, KoRV used fePit1, and 4070A used fePit2 as their receptors.

Next, we tested the inhibitory effects of FeLIX-N249, FeLIX-D249, and Trunc-C4 on non-feline retroviruses KoRV-A, GaLV, HPG, and 4070A MuLV. The results showed that they exhibited marked inhibitory effects against viral infections in AH927 and CRFK cells. However, 4070A MuLV was not inhibited by FeLIX-N249, FeLIX-D249, or Trunc-C4 in the feline cells (Figure 1.16C, 1.17B, and 1.18). Further experiments showed that infection with these viruses was inhibited by FeLIX in MDTF-fePit1 cells but not in MDTF-fePit2 cells (Figure 1.16D and 1.16E). A dose-dependent inhibitory effect of FeLIX on KoRV infection was observed (Figure 1.16F and 1.17C). The supernatant of 3201 cells significantly ($p<0.01$)

inhibited GaLV, KoRV, and HPG infection in AH927 cells. In particular, the inhibition of KoRV infection by the supernatant of 3201 cells was effective (Figure 1.16G). The inhibitory effect of the supernatant from 3201 cells on GaLV, KoRV, and HPG infection disappeared after the depletion of FeLIX using the antibody, whereas treatment with normal goat antisera did not affect the inhibitory effect of the supernatant of 3201 cells (Figure 1.16H). Overall, these results indicated that FeLIX could also confer resistance against non-feline retroviral infections.

1.5. DISCUSSION

Transmission of FeLV-B among domestic cats does not naturally occur, and resistance to FeLV-B infection has been demonstrated in in vivo infection models (64). This phenomenon has been suggested because of the presence of enFeLV, and the finding of FeLV-B infection in Florida panthers lacking enFeLV highlights the association between enFeLV and FeLV-B (96). Besides, the presence of ERV is known to provide resistance to exogenous retroviral infection (8, 58-60). However, the molecular mechanisms restricting FeLV-B infection in domestic cats have long remained unknown (71). While FeLIX has been identified as a co-factor for FeLV-T infection, it is unlikely that FeLIX emerged evolutionarily to facilitate viral infection because of its detrimental function in domestic cats. We attempted to address these questions that have been elusive to date. Based on previous findings on identifying antiviral effects of defective Env proteins (8, 58, 59), we have proposed plausible explanations for these unresolved issues. In particular, this study highlights that the presence of defective Env is beneficial to the host and that Env, which is scattered throughout the mammalian genome, functions as an antiviral molecule. Notably, the presence of antiviral mechanisms also highlights the possibility of cross-species utilization.

In this study, we determined that FeLIX is a restrictive factor for the feline retroviruses FeLV-B and enFeLV, as well as for the mammalian retroviruses KoRV, GaLV, and HPG. The antiviral

machinery is driven by truncated Env proteins encoded by enFeLVs secreted from feline cells. We determined that the antiviral effect of FeLIX is dependent on fePit1. These results implied that receptor interference was the mechanism underlying FeLIX activity. Therefore, FeLIX may function as a barrier to intraspecies and interspecies transmission of retroviruses. These results suggested that truncated Env might constitute an antiviral system in cats. Although soluble Env exhibits antiviral activity, it retains the ability to promote viral infection by FeLV-T, which is detrimental to the host. Antiviral activity may have emerged in an evolutionary arms race, but the ability to promote viral infection may have been created by the emergence of new exogenous retroviruses. Our findings provide insights into the coevolutionary history of retroviruses and their hosts. In particular, we focused on these retroviruses, which infect in a Pit-dependent manner and spread infections.

FeLIX and Trunc-C4 are truncated Env proteins that have an SP and an N-terminal region of SU, which is a putative RBD, but lack the C-terminal region of SU and TM owing to a premature stop codon. The amino acid sizes of FeLIX and Trunc-C4 are 273 and 369, respectively. We demonstrated that both molecules exhibited antiviral activity; however, their antiviral activity differed, as FeLIX was more effective in inhibiting infection. This highlights the importance of factors other than the structural similarity of the truncated Env. Moreover, FeLIX with a single amino acid substitution between FeLIX-N249 (MGPNP) and FeLIX-D249 (MGPDP) within the FeLV-A neutralization epitope “MGPNL” (97) showed comparable antiviral activities in both AH927 and CRFK feline cells. However, when evaluated in human cells (HEK293T), different activities were observed during enFeLV infection. Amino acid mutations at the neutralization epitope of FeLV-A are present in both FeLIX-N249 and FeLIX-D249, and two enFeLV Env sequences harbored mutations in this epitope. This amino acid mutation may appear to specifically preserve the antiviral effect of FeLIX by neutralizing antibodies. In addition, it has been suggested that viruses with the MGPNL epitope have an in

vivo growth advantage relative to FeLV-A (98). Thus, this amino acid change may have emerged as an adaptive response during molecular coevolution. The truncated Env protein lacking TM is not bound to the cell membrane and is thus efficiently released from the cells (99). Thus, the RBD plays a crucial role in facilitating the initial stage of the interaction between the viral envelope and its receptors, enabling viral entry (94, 99, 100). Earlier reports have shown that the expression of env genes in ERVs can prevent viral infection through receptor interference mechanisms (e.g., Fv-4, Rmcf, Rmcf2, Refrex-1, and Suppressyn) (58-61). FeLIX has a structure similar to that of Refrex-1, as it contains the RBD and is primarily secreted in a soluble form, which can offer protection to cells that express both proteins as well as to cells that do not express them. Furthermore, the investigation of enFeLV-derived FeLIX and its evolution revealed that it used Pit1 as the entry receptor, clearly demonstrating the mechanism underlying the antiviral effect of FeLIX. These findings suggest that truncated Env exerts antiviral effects through competitive receptor binding.

Previous studies showed that the culture supernatant of FeLV-negative, feline 3201 cells contained FeLIX as a co-factor for FeLV-T infection (11). Contrary to its role in supporting viral infection, the present study showed that FeLIX in the culture supernatant of 3201 cells inhibited retroviral infection (enFeLV, FeLV-B, KoRV, GaLV, and HPG). There have been limited reports regarding the effect of FeLIX on FeLV-B infection; however, most of them used FeLIX to investigate the cofactors of FeLV-T infection (11, 67). This is a crucial difference from previous reports. A previous study showed that FeLIX in cat serum acts as a co-factor of FeLV-T infection, whereas FeLV-B only served as a control for infection (67), and lacked a specific means for evaluating the inhibition assay, and a separate study suggested that FeLV-B RBD could inhibit FeLV-B infection (94). Moreover, in our study, feline cells were used for the assay, and the protocol involved incubating the truncated Env proteins prior to retrovirus infection. Additionally, two functions of FeLIX were found to be inactivated by treatment at

56 °C for 30 min under conditions that inactivate complement (Figure 1.15). Heat-inactivation is required to inactivate the complement before conducting experiments (101). Therefore, the antiviral activity of the serum could not be evaluated. Notably, a small amount of FeLIX, i.e., a FeLIX level that is 50-fold lower than that required to block FeLV-B infection, can facilitate FeLV-T infection (Figure 1.15). The biochemical activity required for viral infection differed from that involved in inhibiting viral infection. The antiviral effect of the 3201 cell supernatant was not effective against extremely high-titer viruses (Figure 1.14). Our study also revealed that the antiviral effect varied among FeLV-B strains, with the FeLV-B/GA strain being the least susceptible to the supernatant of 3201 cells. These factors may explain why the antiviral effect of FeLIX has not been addressed.

This study revealed that enFeLV used only fePit1, instead of fePit2, as an entry receptor by analyzing the amino acid mutation of enFeLV Env and receptor usage. We found that FeLV-B typically used fePit1 as a receptor; however, some FeLV-B strains could use both fePit1 and fePit2. Our findings reveal that, unlike observations from previous studies (10), FeLV-B/GA infection primarily occurred through fePit1 but not Pit1 and Pit2. Furthermore, a mutant amino acid change at position 73 (arginine) was responsible for enhanced binding to the Pit2 receptor, consistent with the results of a previous study (10). In addition, the presence of lysine at position 66 can affect receptor usage by facilitating FeLV-B expansion to Pit2. Gene sequences showing lysine and arginine at positions 66 and 73, respectively, in FeLV-B Env were not found in any enFeLV clones or in the database, suggesting that these amino acid sequences were not derived from the enFeLV env gene sequence but may have been acquired by genetic mutation. These findings suggest that receptor shifts have occurred to escape host selection pressure, such as the presence of FeLIX, enFeLV, or the host immunity response. Similarly, FeLV-B showing Env structure diversity may have occurred through host selection pressure, as FeLV-B is a recombinant virus that consists of FeLV-A and an enFeLV *env* gene (26).

This seems to be consistent with the results of other studies that revealed a recombinant virus between FeLV-A and the ERV-DC *env* gene in FeLV-D (49); it also occurred on RD-114 by recombination of ERV-DC and a baboon endogenous virus-related *env* gene (102-105) in response to the selection pressure of the host defense. Selection pressure could trigger the generation of viral variants that avoid these barriers; however, in a positive sense, ERV provides a naturally essential antiviral defense and immunity to the host (8, 58-61). As a result, we believe that an ERV, such as that having the truncated Env, plays an essential evolutionary role against retroviral infections. We speculate that enFeLV-truncated Env plays a key role in the selective recombination of FeLV-A and enFeLV to generate FeLV-B in domestic cats. The presence of FeLIX in cats could affect the frequency of FeLV-B transmission and the severity of the disease caused by FeLV-B. In particular, it can affect the risk of transmission from domestic cats to other animals. This is consistent with the results of previous studies suggesting that the noncoding RNA of enFeLV-LTRs also tends to control FeLV replication via an RNA interference mechanism (70). Additionally, another study suggested that FeLV-B Env confers strong resistance against feline SERINC5 that depends on its GlycoGag for developing this resistance (106). These results explain a possible antiviral synergistic phenomenon in cats regarding the role of ERV in protecting against the FeLV infection.

Wildlife retroviral models include KoRV, GaLV, and HPG. KoRV, which has been identified in koalas and causes serious illnesses, appears to endogenize and may contain env-ERV in its genome to protect against viral infections (107). In Australia and Asia, HPG was first isolated from the bat genome (*Pteropus alecto*) (30). *Pteropus alecto* has a large flying range, which increases the possibility of virus transmission throughout the area and may lead to disease outbreaks in various species.

KoRV, GaLV, and HPG have been reported to use Pit1 as receptors (28-30). Our findings demonstrated that FeLIX inhibited related Pit1 tropism in retroviruses such as KoRV, GaLV,

and HPG. This implies that in the limitation function of the same virus entry mechanism, truncated Env can potentially act as a component of natural host immunity, to protect against not only current intraspecies but also interspecies viral infections. However, new retroviral variants may emerge owing to mutations or recombinants that escape host selection pressure. Here, we emphasize that the truncated Env potentially blocks retroviral infection in a wide range of species by targeting a shared viral entrance receptor.

The prevention of viral infection by soluble Env proteins may lead to the consideration of next-generation therapeutic strategies for infectious diseases, including severe acute respiratory syndrome coronavirus 2 (SARS-CoV-2) infections, as soluble angiotensin-converting enzyme 2 (ACE2) decoys are highly effective in blocking infection of all variants of SARS-CoV-2 (108, 109). Finally, although the antiviral effects of FeLIX and defective Env proteins can be demonstrated in vitro, the exact roles of these soluble proteins in vivo remain unclear, which is a limitation of this study.

In conclusion, our findings provided evidence of an antiviral agent against FeLV-B infection in domestic cats that could be extended to non-feline mammalian retroviruses. Furthermore, this study conveyed a fundamental understanding that soluble Env proteins restrict retroviruses from diverse host species through binding interactions with a common entryway receptor and will help to protect against retroviral infection, implying that their functions help improve host immunity and antiviral defense by controlling retroviral spread. This study portrays an evolutionary scenario of host-pathogen interactions and has significant implications for developing treatments for infectious diseases, including vaccine design.

1.6. TABLES, FIGURES, SUPPLEMENTARY DATA IN CHAPTER ONE

Tables

Table 1.1 Sequence of primers used in this study

Primer	Sequence (5'– 3')
enFeLVC4	ACCTGGATCCGCCGCCACCATGGAAGGTCCAACGCACCC
RBD-F1	ACCTGGATCCGCCGCCACCATGGAAAGTCCAACGCACCC
FeLIX-1F	CTGGATCCATGGAAGGTCCAACGCACCCAA
FeLIX-P	TCCCCTCATTCTGGAAAATCACCCTCAGGA
FeLIX-F	CACCCGATATACCCTAGAGATGAG
Fe-36S	AACCGCTTGGTACARTTCATAAGAG
Fe-217S	ATCCGGATCCATGGAAGGTCCAACGCACCCAAAA
Fe-227S	GTCAACCCCATCGTGTTTTT
Fe-265S	AATTGCTGGCGAGGAAGTTATC
Fe-360S	TCACTATGGAGGGGTGATGTTG
Fe-362S	TTCTTGCTGCCTATTGTCTGGA
Fe-361S	CTCAGGTGCCCCTAAAAAGAGA
Fe-431S	GCTTGTGAGATGTGGGTACAGC
Fe-456S	GGTAATGGACATCCAAGGTTCC
Fe-457S	AAGGTAAGGTTTTCCCCCACAT
Fe-560S	GCCGAATTCGCCGCCCACCATGGAAGGTCCAACGCACCCAAAACCCTCT
Fe-710S	GACATCAAACCAAGAACCTCGA
Fe-711S	GGATCCACGCCTCTCATGTA
Fe-720S	GCCCCTGGTTTTATACCGGGTACGTA
Fe-721S	AGCTCAGACGATCCATCGAGATGGAAGGTCCAACGCACCC
Fe-761S	CAGCCTATGAGGAGGTGGCGACAGAGAAACACACCCTTT
Fe-766S	ACCTGGATCCGCCGCCACCATGGTATTGCTGCCTGGGTC
Fe-792S	CAGCCTATGAGGAGGTGGCAACAGAGAAACACACCCTTT
Fe-782S	TCCCAGGGTATGGATGTGATCAGCCTATGAGGAGGTG
Fe-844S	CAATCAGGAAGGGCTTGATC
Fe-845S	GACAGTAGAAACACTAATGG
Fe-861S	CTTGGGATGGACCTAAGTCATGG
Fe-862S	ACCAATCAGGACCCCTCAGA
Fe-60R	GAGTCTTATTTGCATACAGGCTGGT
Fe-204R	CTGCTGTCTTGGGAACTTTGTC
Fe-237R	CGGCCTGCTTATCTGACTCTTC
Fe-397R	CTCAGGCACTTCTAGCTGCTCA
Fe-400R	CCTGACGCAAAAAGAGTCTCAA
Fe-399R	TCAGCAACTCTCTGTTAATCTTTGG
Fe-466R	AAGCACCGGGCTAATTTAGAGA
Fe-448R	AACACATCAAAGCACACCTCGT
Fe-475R	CAGAGGAAGTGGGGAAGAAAGA
Fe-550R	GGCGCTAGCCTAAATGGAATCATACATTTAGCTGG
Fe-554R	CCAGTGCCAAGCTTGCATGCCTGCA
Fe-686R	TGCAGAATTCTCATGTTGTGGGTCGGATAGGCA
Fe-716R	TGCAGAATTCTCACAGATCCTCCTCGGAGATCAGCTTCTGCTCGGCCTGAGGCGGCGTAATGG
Fe-730R	ATGGGCAAGACAGCTTGGTT
Fe-747R	GGGTGCGTTGGACCTTCCATCTCGATGGATCGTCTGAGCT
Fe-748R	ATCATACATTTAATTGGAAATTAGCTGGGGTGATACGGTT
Fe-750R	CGGCCTGCTTATCTGACTCT
Fe-788R	AAAGGGTGTGTTTCTCTGTCGCCACCTCCTCATAGGCTG
Fe-790R	TGCAGAATTCTCAAAGGTTACCTTCGTTCTCTA
Fe-807R	CACCTCCTCATAGGCTGATCACATCCATACCCTGGGA
Fe-812R	AAAGGGTGTGTTTCTCTGTTGCCACCTCCTCATAGGCTG
Fe-874R	CCACACAGCAGAACCAAACAT
Fe-875R	CTCAGGAAGGATGCAATGAG
Fe-891R	TAGCTGGGGTGAGGTATTAC
Fe-892R	GCTTAACCAACGGAGTCCCA
FeLIX-1R	GAAGCGAGAAGCATGGTTACG
SDM-FeLIX1	TCAGGCCATGGGACCAAATCCAGTCCTGCCTGATC
SDM-FeLIX2	GATCAGGCAGGACTGGATTTGGTCCCATGGCCTGA

Table 1.2 Characteristic of enFeLV in domestic cat used in this study

Name	Chromosome: provirus position	Chromosome: *env* position	ORF	Length of amino acids (Env)	Age (Mya)	Accession number	Source
enFeLV-clone1	ChrB4: 83161862..83153192	ChrB4:83168073..83170071	Intact *env*	666	0.2166	LC196053.1	In this study
enFeLV-clone2	ChrB3:77504220..77495524	ChrB3:77510006..77512004	Intact *env*	666	0.1062	LC196054.1	In this study
enFeLV-clone3	ChrA2:158856703..158865693	ChrA2:158862891..158864892	Intact *env*	666	0	LC196055.1	In this study
enFeLV-clone4	ChrB4:63249450..63253973	ChrB4:63247526..63246420	Truncated *env*	369	0.2166	LC198317.1	In this study
enFeLV-clone5	ChrB4:45466253..45466874	ChrB4:45469880..45470699	Truncated *env*	273	0.696	LC198318.1	In this study
enFeLV-clone6	ChrA3:22964466..22967845	ChrA3:22966277..22967249	Truncated *env*	90	0.3294	LC198319.1	In this study
enFeLV-AGTT	ChrA1: 205669512..205679407	ChrA1:205676200..205678198	Intact *env*	666	0	AY364318.1	Isolate
enFeLV-GGAG	ChrA2: 69618599..69628466	ChrA2:69625273..69626377	Truncated *env*	368	0.11	AY364319.1	Isolate
enFeLV-CFE6	ND	ND	Intact *env*	668	0.2334	M25425.1	Isolate
enFeLV-CFE16	ND	ND	Truncated *env*	273	0.4668	M25582.1	Isolate
Fca strain C3	ND	ND	Truncated *env*	450	ND	OP595720.1	Isolate
Fca strain C12	ND	ND	Intact *env*	666	0	OP595706.1	Isolate
Fca strain C16	ND	ND	Truncated *env*	514	0	OP595709.1	Isolate
Fca strain C30	ND	ND	Intact *env*	666	0.5574	OP595707.1	Isolate
Fca strain C31	ND	ND	Truncated *env*	469	ND	OP595714.1	Isolate
Fca strain C33	ND	ND	Truncated *env*	437	ND	OP595716.1	Isolate
Fca strain C34	ND	ND	Intact *env*	666	0	OP595708.1	Isolate
ChrA1:237978323	ChrA1:237978323..237983035	ChrA1:237981730..237982045	Truncated *env*	48	0	CM028198	Cat genome (NCBI)
ChrA2:126590453	ChrA2:126590453..126599114	ChrA2:126596525..126598523	Intact *env*	666	0	AP023153	Cat genome (NCBI)
ChrB1:153791216	ChrB1:153791216..153795411	ChrB1:153791714..153792041	Truncated *env*	48	0	CM031415	Cat genome (NCBI)
ChrB1:204333001	ChrB1:204333001..204356576	ChrB1:204345879..204346698	Truncated *env*	273	0.4644	NC_058371	Cat genome (NCBI)
ChrB2:29977771	ChrB2:29977771..29986443	ChrB2:29983847..29984951	Truncated *env*	368	0	CM031416	Cat genome (NCBI)
ChrB2:3162779	ChrB2:3162779..3171382	ChrB2:3168829..3176877	Intact *env*	666	0	CM031416	Cat genome (NCBI)
ChrB3:137955648	ChrB3:137955648..137964319	ChrB3:137961723..137963721	Intact *env*	666	0	CM028203	Cat genome (NCBI)
ChrB4:1815451	ChrB4:1815451..1824152	ChrB4:1821542..1823540	Intact *env*	666	0	CM031418	Cat genome (NCBI)
ChrB4:83104800	ChrB4:83104800..83113469	ChrB4:83110877..83112875	Intact *env*	666	0.2166	CM031418	Cat genome (NCBI)
ChrB4:45570261	ChrB4:45570261..45574773	ChrB4:45577391..45578210	Truncated *env*	273	0.4632	CM031418	Cat genome (NCBI)
ChrB4:29885536	ChrB4:29885536..29894216	ChrB4:29894159..29894411	Truncated *env*	84	0.3258	CM028204	Cat genome (NCBI)
ChrB4:82927705	ChrB4:82927705..82931318	ChrB4:82929648..82930302	Truncated *env*	218	ND	CM028204	Cat genome (NCBI)
ChrB4:85235849	ChrB4:85235849..85244527	ChrB4:85236446..85238444	Intact *env*	666	0.654	CM001384	Cat genome (NCBI)
ChrB4:47523766	ChrB4:47523766..47528223	ChrB4:47527257..47527386	Truncated *env*	43	0.207	CM001384	Cat genome (NCBI)
ChrB4:47520004	ChrB4:47520004..47524419	ChrB4:47522893..47523331	Truncated *env*	146	0.69	CM001384	Cat genome (NCBI)
ChrD1:109672515	ChrD1:109672515..109679862	ChrD1:109673547..109673604	Truncated *env*	19	ND	CM001387	Cat genome (NCBI)
ChrD1:700129	ChrD1:700129..703822	ChrD1:700870..701017	Truncated *env*	49	ND	CM028207	Cat genome (NCBI)
ChrD3:26685272	ChrD3:26685272..26688966	ChrD3:26687913..26688060	Truncated *env*	49	ND	CM028209	Cat genome (NCBI)
ChrD4:68171	ChrD4:68171..76919	ChrD4:70243..70263	Truncated *env*	20	2.064	CM001390	Cat genome (NCBI)
ChrD4:92824	ChrD4:92824..101492	ChrD4:93422..95420	Intact *env*	666	0	CM028210	Cat genome (NCBI)
ChrF1:11537581	ChrF1:11537581..11543055	ChrF1:11541748..11541865	Truncated *env*	39	6	CM001394	Cat genome (NCBI)
ChrF1:9624604	ChrF1:9624604..9629638	ChrF1:9628585..9628732	Truncated *env*	49	ND	CM028214	Cat genome (NCBI)
ChrX:8830722	ChrX:8830722..8839611	ChrX:8832832..8833393	Truncated *env*	187	3.402	CM001396	Cat genome (NCBI)

ND: not determined due to not complete of sequence or not available

Table 1.3 The estimated of integration timing based on the substitution rate of 5'LTR and 3'LTR sequences

Provirus name	LTR length (bp)		Pairwise Genetic Distance	Calculated integration age (thousand years ago)
	5`LTR	3`LTR		
enFeLV-clone1	556	554	0.00361	216.6
enFeLV-clone2	573	564	0.00177	106.2
enFeLV-clone3	563	565	0	Recently
enFeLV-clone4	554	556	0.00361	0.2166
enFeLV-clone5	516	518	0.0116	696
enFeLV-clone6	516	555	0.00549	329.4
enFeLV-AGTT	568	568	0	Recently
enFeLV-GGAG	554	553	0.00181	108.6
enFeLV-CFE6	514	516	0.00389	233.4
enFeLV-CFE16	515	517	0.00778	466.8
Fca strain C3	Absent	543	ND	ND
Fca strain C12	542	543	0	Recently
Fca strain C16	542	542	0	Recently
Fca strain C30	538	541	0.00929	557.4
Fca strain C31	Absent	541	ND	ND
Fca strain C33	Absent	542	ND	ND
Fca strain C34	538	538	0	Recently
ChrA1:237978323	542	543	0	Recently
ChrA2:126590453	552	551	0	Recently
ChrB1:153791216	542	542	0	Recently
ChrB1:204333001	520	517	0.00774	464.4
ChrB2:29977771	556	557	0	Recently
ChrB2:3162779	517	516	0	Recently
ChrB3:137955648	556	558	0	Recently
ChrB4:1815451	571	572	0	Recently
ChrB4:83104800	556	554	0.00361	216.6
ChrB4:45570261	519	521	0.00772	463.2
ChrB4:29885536	555	568	0.00543	325.8
ChrB4:82927705	Absent	555	ND	ND
ChrB4:85235849	584	554	0.0109	654
ChrB4:47523766	654	292	0.00345	207
ChrB4:47520004	262	515	0.0115	690
ChrD1:109672515	268	289	0.527	ND
ChrD1:700129	268	289	0.525	ND
ChrD3:26685272	268	289	0.527	ND
ChrD4:68171	555	562	0.0344	2064
ChrD4:92824	554	555	0	Recently
ChrF1:11537581	538	520	0.1	6000
ChrF1:9624604	268	289	0.527	ND
ChrX:8830722	615	598	0.0567	3402

ND: not determined due to not complete of LTR sequence

Figures

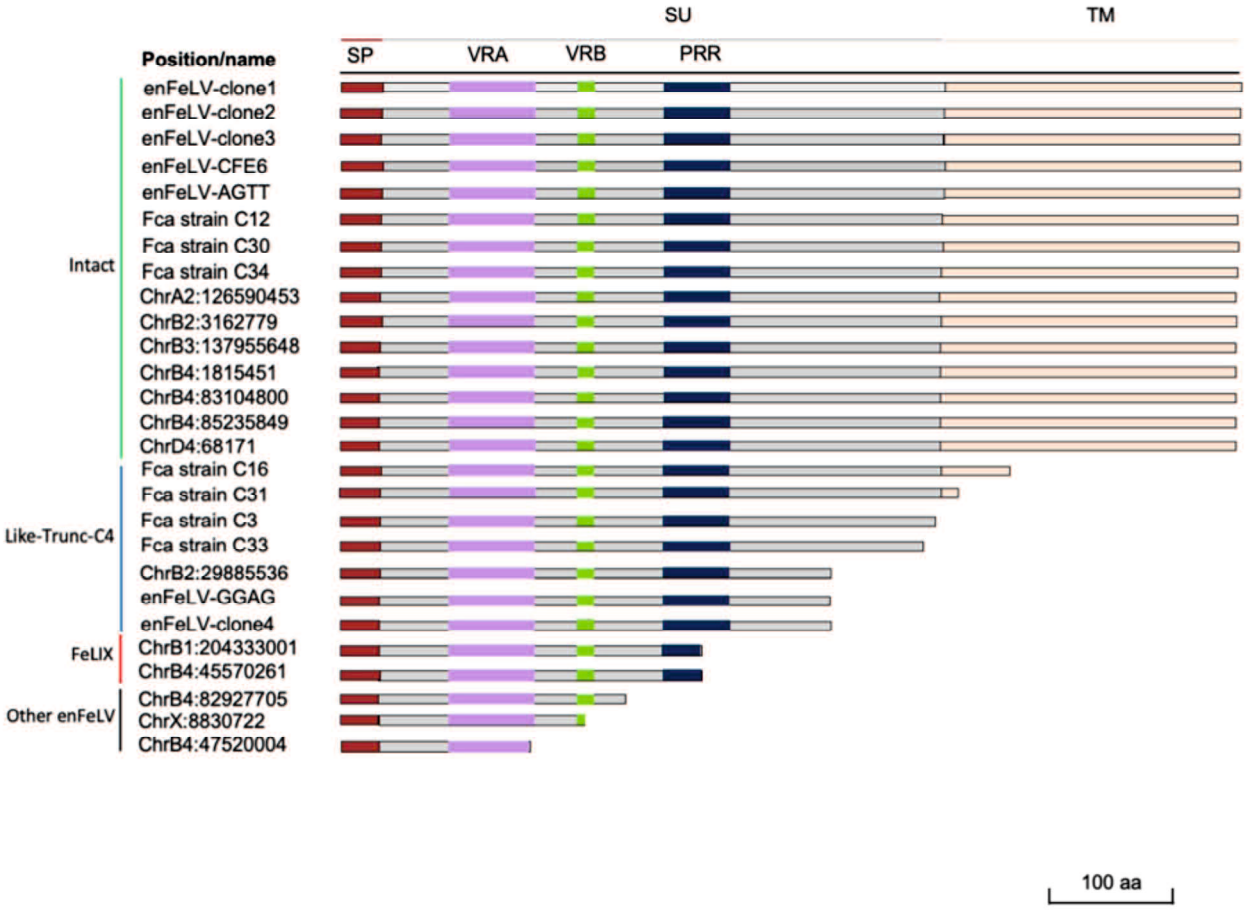

Figure 1.1 EnFeLV Env open reading frames (ORFs) in domestic cats. Publicly available whole-genome sequence data and genomic library screening were utilized to identify enFeLV Env ORFs in the cat genomes.

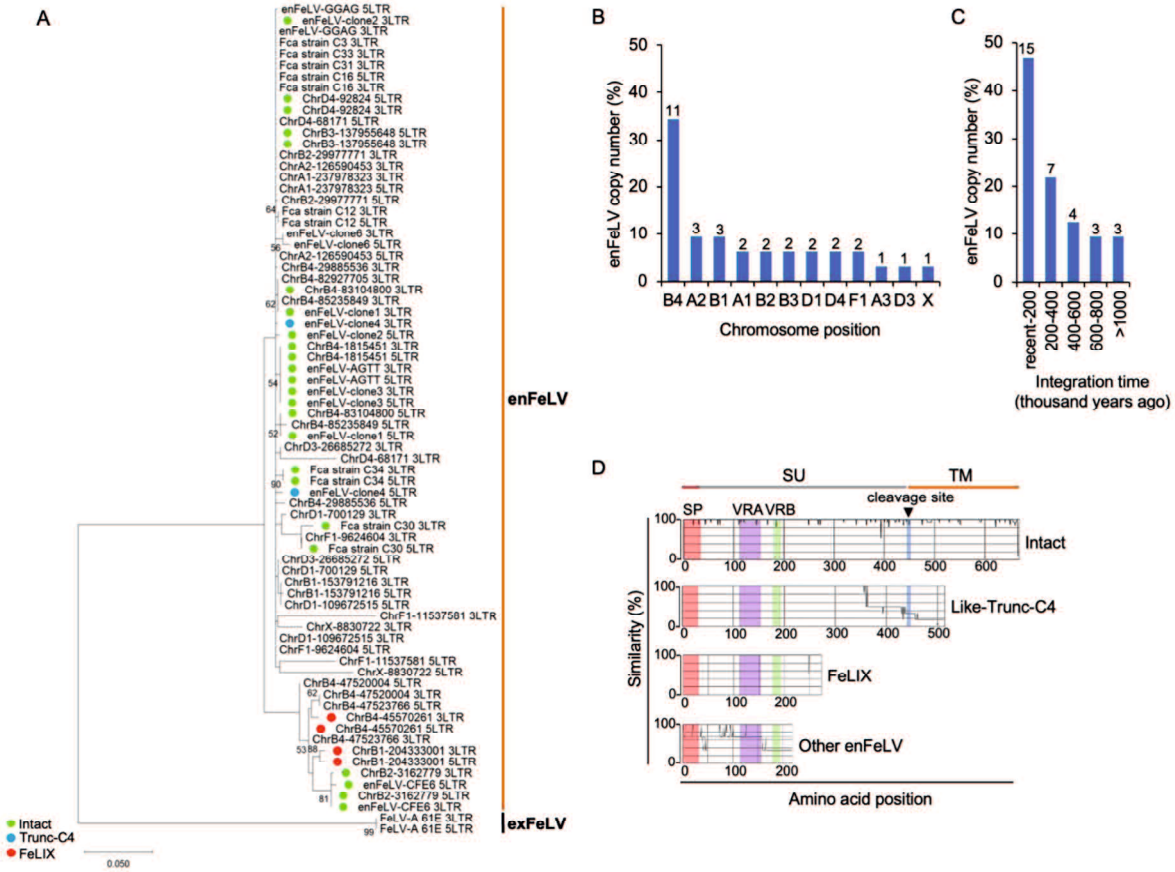

Figure 1.2 Endogenization of enFeLV in domestic cats. (A) Phylogenetic tree of enFeLV carrying the env gene based on LTRs. Intact Env, FeLIX and Trunc-C4 are indicated by green, red and blue circles, respectively. (B) Chromosome position of enFeLV proviral integration in domestic cat genome. The number of viral integrations is indicated in the top bar. (C) Integration time of enFeLV proviruses in domestic cat genome. (D) Structure of enFeLV Env classification (4 groups); Group 1: Intact, intact full-length Env has approximately 666 amino acids (aa); Group 2: Like-Trunc-C4, defective Env like-Trunc-C4 (length > 300 aa), which has signal peptide (SP) and variable region A (VRA) and variable region B (VRB) in Env surface unit (SU) but lacks transmembrane unit (TM) region; Group 3: Like-FeLIX (length < 300 aa), which has only SP and VRA and VRB in Env SU; Group 4; Env has a length between 140 and 273 aa and lacks VRA, VRB, or the TM region.

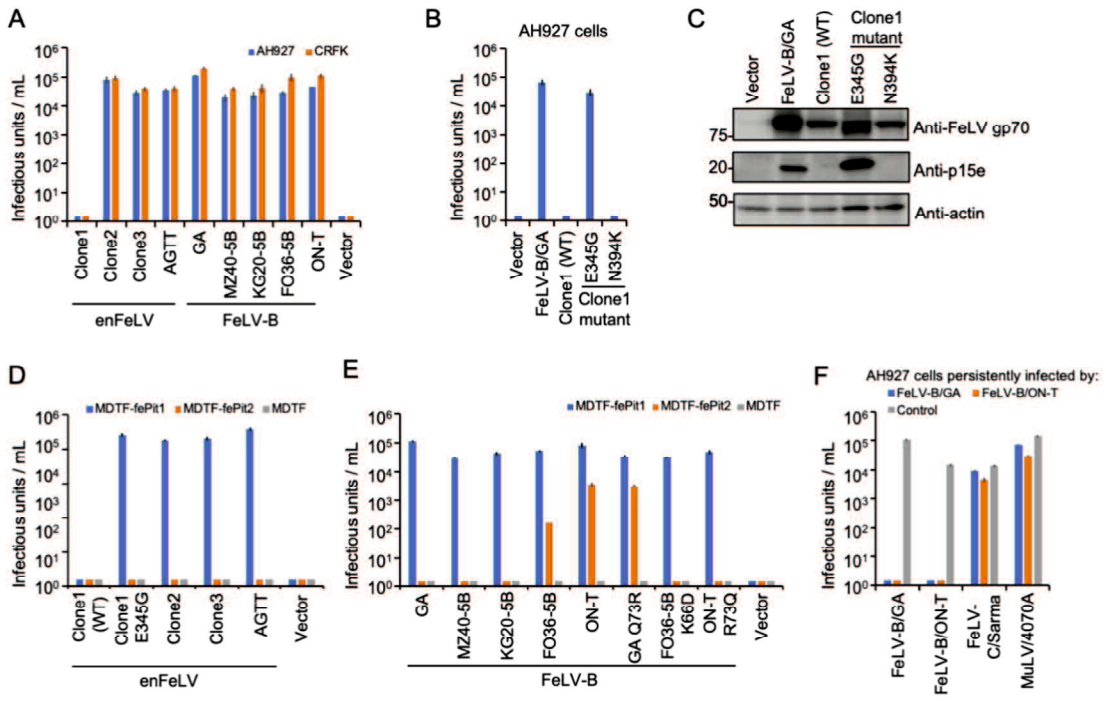

Figure 1.3 Infectivity and receptor usage of enFeLV Env-pseudotyped viruses. (A) Infectivity of enFeLV (clone1, clone2, and clone3) and FeLV-B (GA, MZ40-5B, KG20-5B, FO36-5B, and ON-T) Env-pseudotyped viruses. (B) Infectivity of Env mutants (E345G and N394K) from enFeLV clone1. (C) Western blot analysis of enFeLV Envs proteins in HEK293T cells using anti-FeLV gp70 and anti-FeLV p15e antibodies. Actin was used as a control. (D) Infection assay of enFeLV (clone1/WT, clone1 E345G, clone2, clone3, and AGTT) in MDTF-fePit1, MDTF-fePit2, and MDTF (empty vector) as target cells for receptor usage. (E) Infection assay of FeLV-B (GA, MZ40-5B, KG20-5B, FO36-5B, and ON-T) and FeLV-B mutants (GA Q73R, FO36-5B K66D, and ON-T R73Q) in MDTF-fePit1, MDTF-fePit2, and MDTF (empty vector) as target cells for receptor usage. (F) Interference assay of FeLV-B/GA and FeLV-B/ON-T. AH927 cells pre-infected with either FeLV-B/GA or FeLV-B/ON-T were infected by the Env-pseudotyped viruses. FeLV-C/Sarma and MuLV 4070A were used as controls. Viral titers are indicated on the x-axis. The infectious units (IU) were determined by counting the number of

log10-galactosidase (LacZ)-positive cells per milliliter (mL) of virus indicated on the y-axis. Virus infection titers with standard deviations were averaged from three independent experiments. Mock represents the negative control.

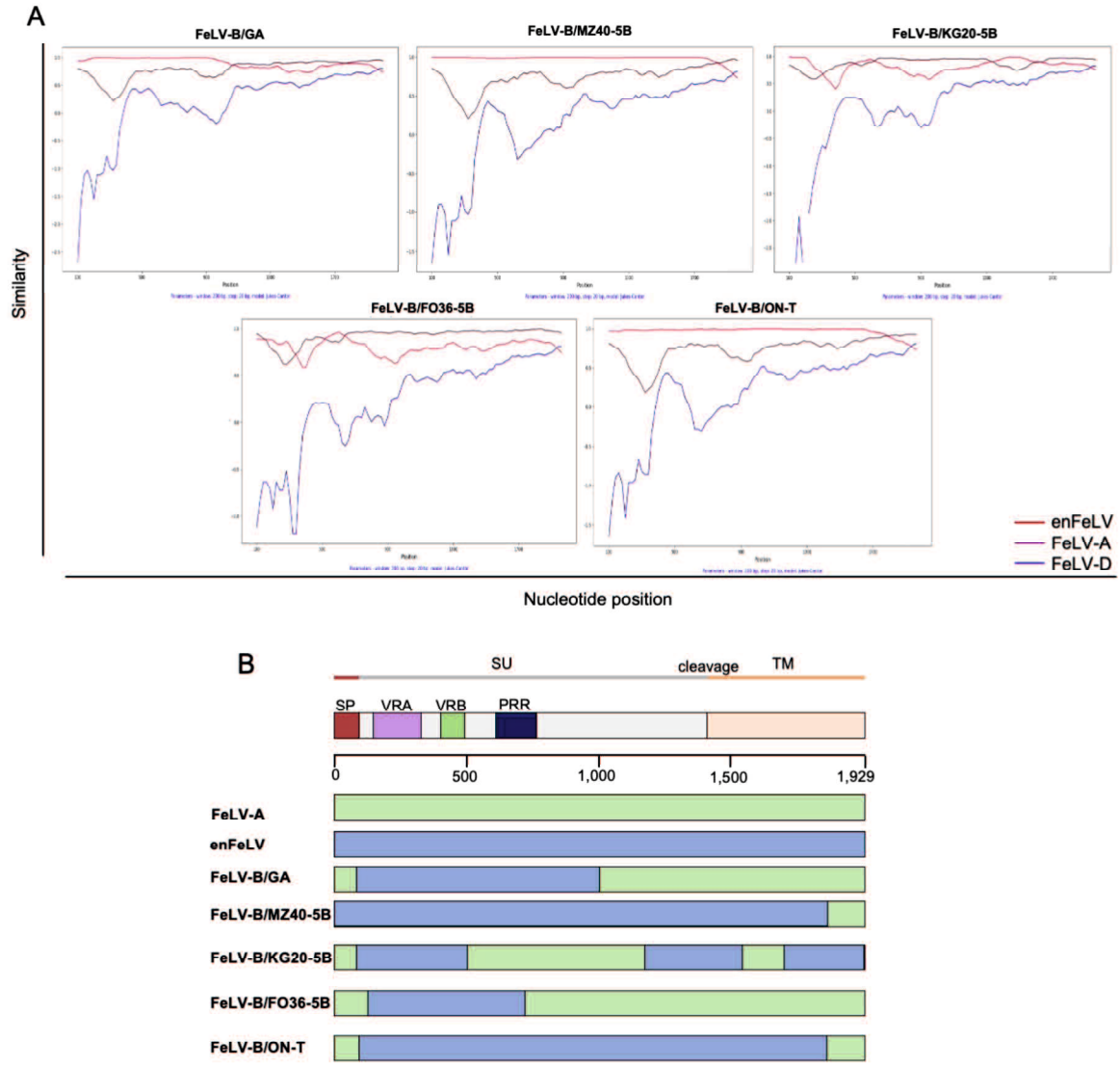

Figure 1.4 Recombination analysis of FeLV-B env genes used in this study. (A) FeLV-B and enFeLV recombinant junctions were identified using similarity plots. Plots indicate similarity between a series of highlighted sequences. Each graph is an analysis of the title sequence and the reference FeLV env sequences (color-coded). The x-axis represents the position of the env sequences, and the y-axis represents the similarity. (B) Structural schematic of the various recombination structures identified using similarity plot analysis. The motifs are abbreviated as SP (signal peptide), VRA (variable region A), VRB (variable region B), PRR (proline-rich region), and C-dom. SU (surface unit) and TM (transmembrane unit). Colors indicate parts of the recombinant protein.

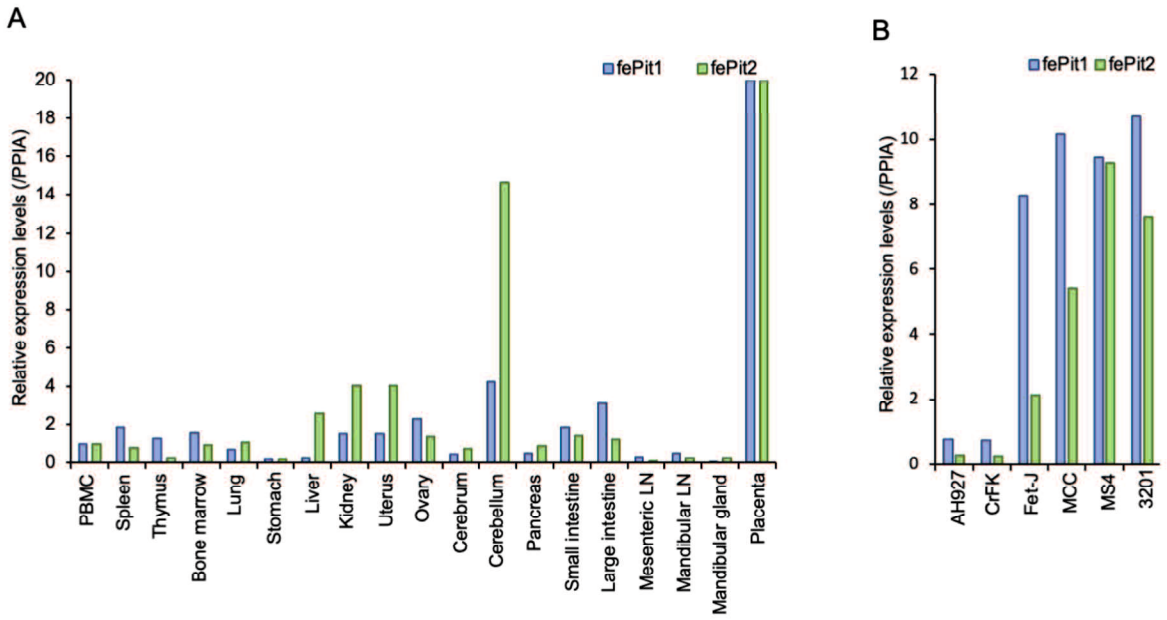

Figure 1.5 FePit1 and fePit2 expression in feline tissues and cell lines. Quantification of fePit1 and fePit2 transcripts via quantitative RT-PCR in feline tissues and cell lines. The x-axis indicates the analyzed samples. The y-axis shows the expression level normalized to that of peptidylprolyl isomerase A (PPIA). LN, Lymph node.

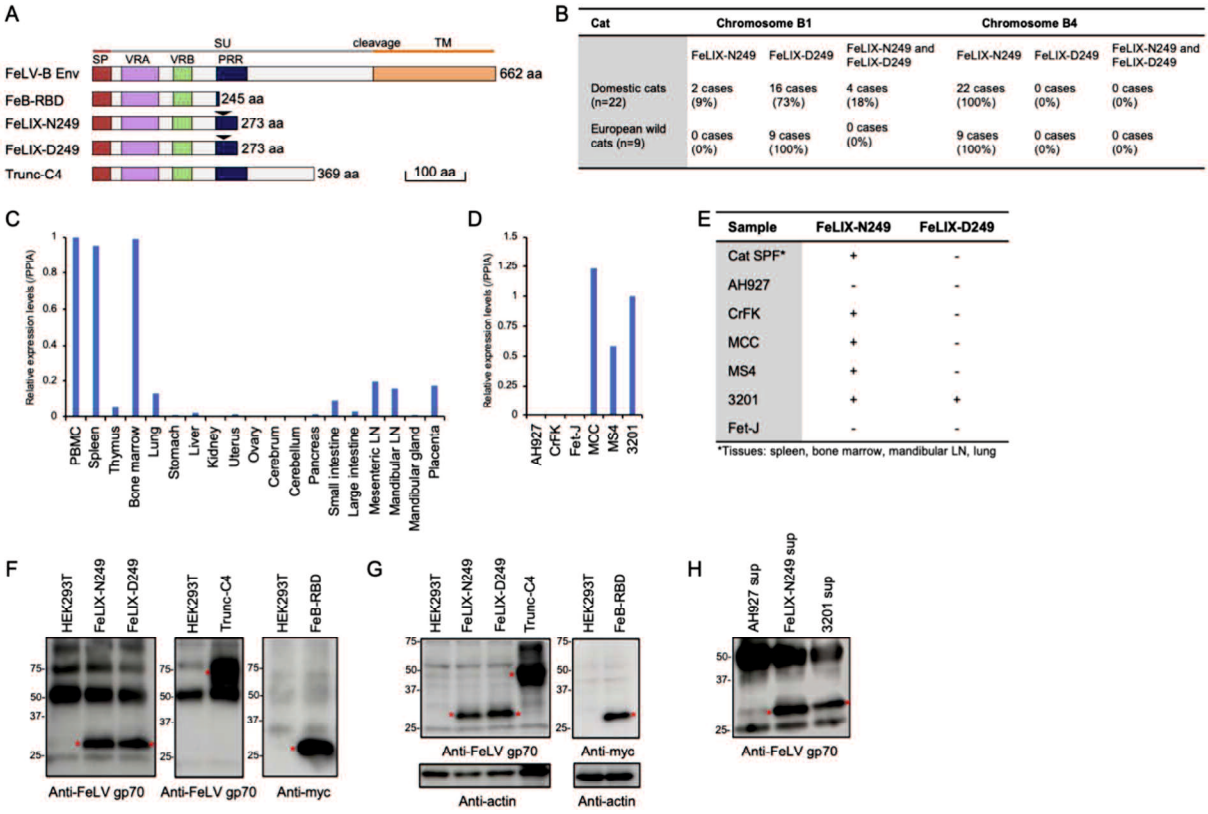

Figure 1.6 Structural schematic and expression of truncated Envs. (A) Schematic representation of the structure of FeLIX-N249 (asparagine at position 249), FeLIX-D249 (aspartic acid at position 249), and Trunc-C4. The receptor-binding domain (RBD) of FeLV-B/GA with myc-tag is also shown. SP, signal peptide; SU, surface unit; TM, transmembrane unit; VRA, variable region A; VRB, variable region B; PRR, proline-rich region. The number of amino acids is indicated on the right side. (B) Detection of proviruses encoding FeLIX in the domestic cat (n = 22) and European wild cat (n = 9) genome. (C, D) FeLIX expression in feline tissues and cell lines. Quantification of feline FeLIX transcripts using quantitative RT-PCR in feline tissues and cell lines. The x-axis indicates the analyzed samples. The y-axis indicates the expression level normalized to the expression of peptidylprolyl isomerase A (PPIA). Normalized expression in PBMCs and 3201 cells is shown as 1 in feline tissues and cell lines, respectively. LN, lymph node. Expression of FeLIX-N249 and D-249 was determined via RT-PCR and sequencing in feline tissues (spleen, bone marrow, mandibular LN,

and lung) and indicated feline cell lines. (F) Detection of FeLIX-N249 and D-249, Trunc-C4, and Fe-B-RBD in cell culture supernatants and (G) in cell lysates from HEK293T cells transfected with indicated plasmids. (H) Detection of FeLIX in the supernatant of indicated cells. Red asterisks indicate truncated Env proteins. FeLIX-N249 and D-249, as well as Trunc-C4, were analyzed via immunoprecipitation (IP) and western blotting (WB) using a goat anti-FeLV gp70 antibody (81S-210-2, NCI), while Fe-B-RBD was assessed with an anti-Myc antibody.

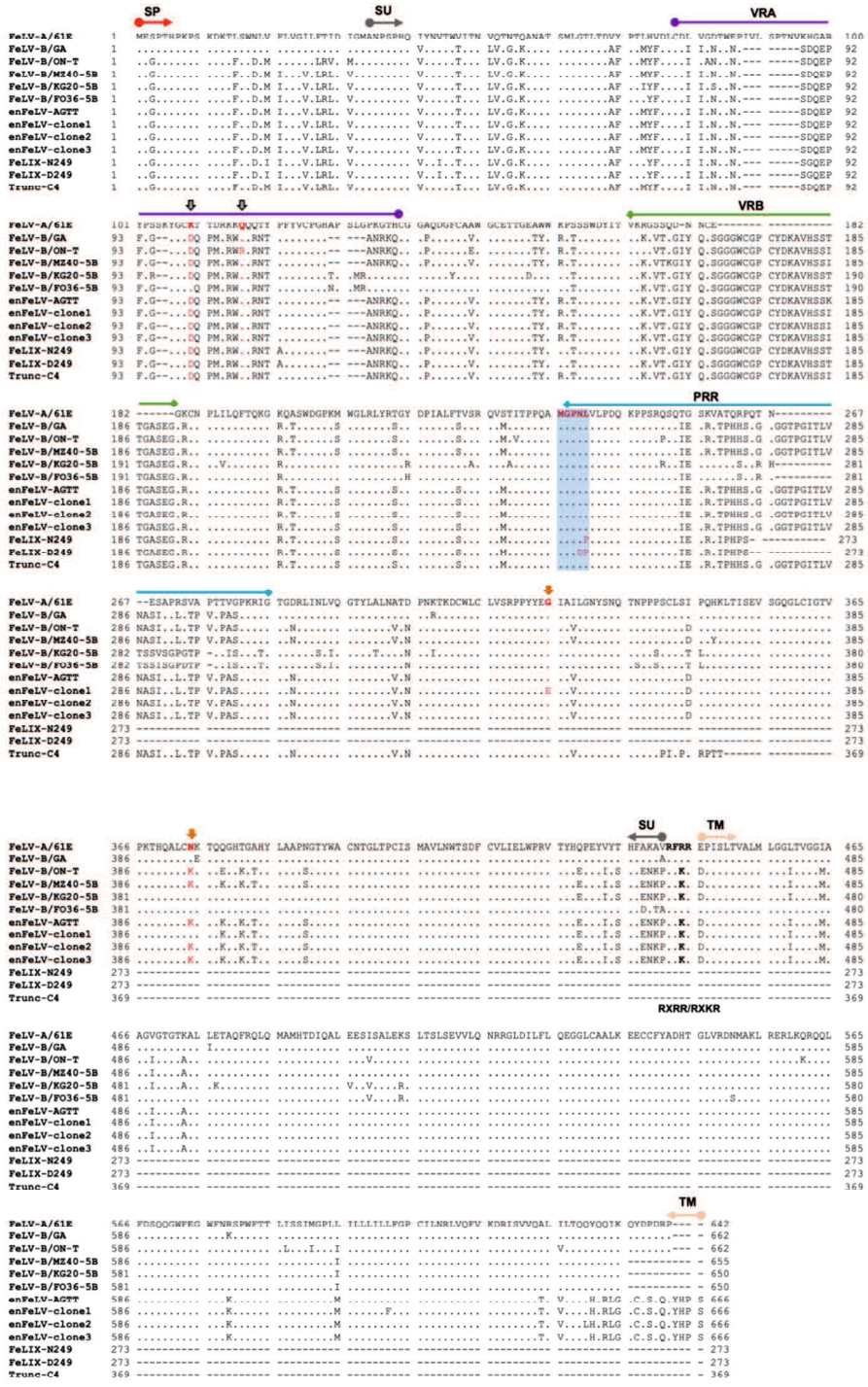

Figure 1.7 Alignment of the amino acid sequences of FeLV-A, FeLV-B strain, enFeLV, and FeLIX, Trunc-C4. The critical amino acids responsible for the receptor shift of FeLV-B, namely lysine (K) at position 66 and glutamine (Q) at position 73, are indicated by black narrow highlighting. Amino acids at positions 345 (glycine, G) and 394 (lysine, K) utilized in

constructing enFeLV mutants are highlighted in orange narrow, while black bold letters denote the cleavage site (RXRR/RXKR). Amino acid 'MGPNL' epitopes are indicated by shading blue. Conserved amino acid residues are marked by dots, gaps in the amino acid sequence by hyphens, and stop codons by asterisks. The abbreviations used are as follows: SU (surface unit), TM (transmembrane unit), VR (variable region), and PRR (proline-rich region).

Cat	Integration of Trunc-C4	
	Positive PCR	Negative PCR
Domestic cats (n=22)	12 cases (55%)	10 cases (45%)
European wild cats (n=9)	0 cases (0%)	9 cases (100%)

Figure 1.8 Detection of Trunc-C4 in domestic cats and European wild cats. The viral integration of Trunc-C4 was determined via PCR in cat genomes (n = 22) and European wild cats (n= 9).

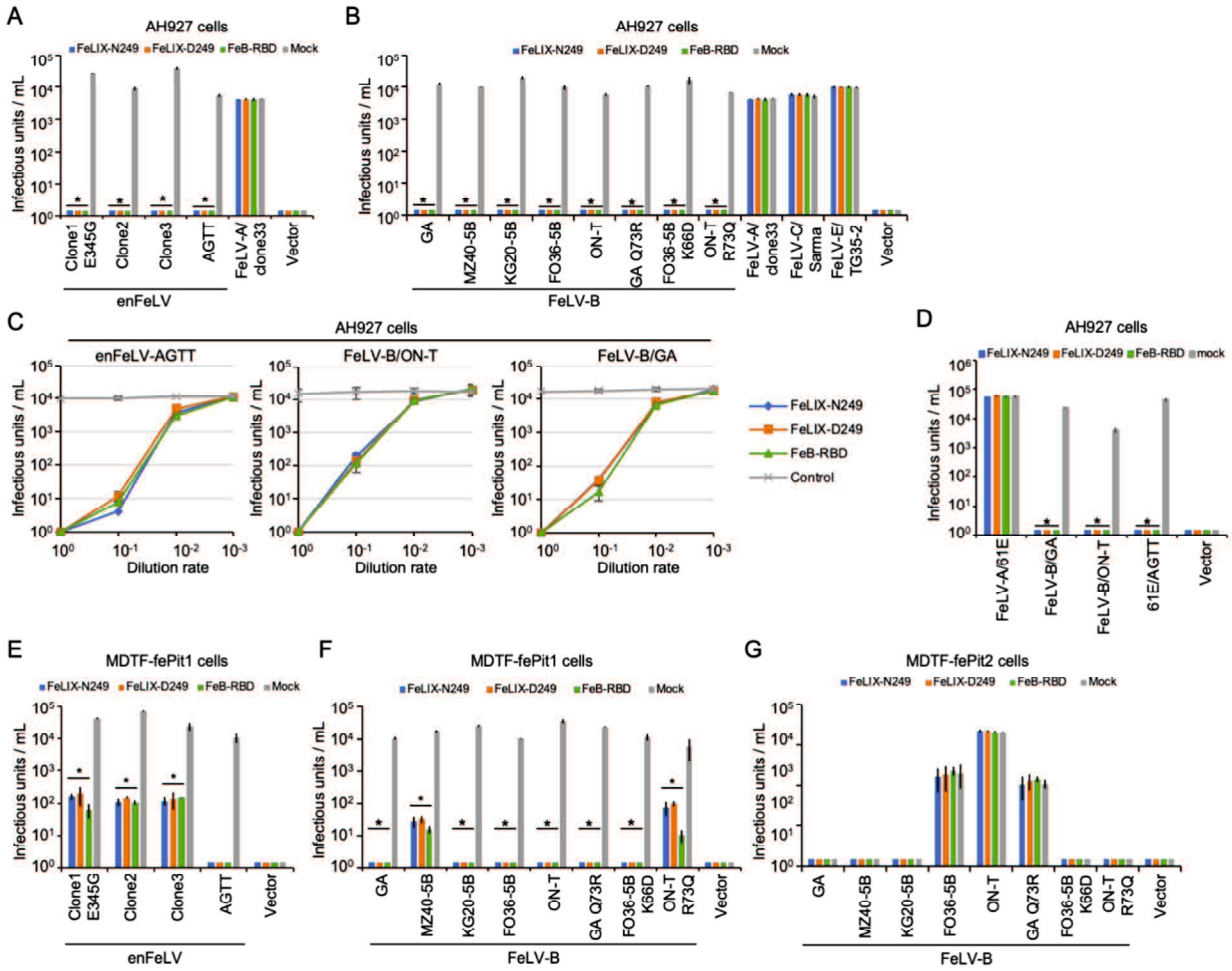

Figure 1.9 Inhibitory effect of the truncated Env proteins derived from enFeLV for enFeLV and FeLV-B infection and restriction mechanism. (A) Inhibition assay using FeLIX-N249 and FeLIX-D249 for evaluating the infection of Env-pseudotyped viruses, enFeLV (Clone 1 E345G, Clone 2, Clone3, and AGTT), (B) FeLV-B (GA, MZ40-5B, KG20-5B, FO36-5B, and ON-T), and FeLV-B mutants (GA Q73R, FO36-5B K66D, and ON-T R73Q) in AH927 cells. (C) Dose-dependent inhibition of FeLIX for Env-pseudotyped viral infection (FeLV-B/ON-T, FeLV-B/GA, and enFeLV-AGTT) in AH927 cells. (D) The replication-competent viruses assessed included FeLV-B/GA, FeLV-B/ON-T, FeLV-A carrying the enFeLV-AGTT env gene, and FeLV-A/61E in AH927 cells. Restriction mechanism in (E, F) MDTF-fePit1 and (G) MDTF-fePit2 cells. FeLV-A/clone33, FeLV-C/Sarma, and FeLV-E/TG35-2 were also used in this assay. FeLIX-N249, FeLIX-D249, FeB-RBD, and the empty vector/mock were sourced from supernatants of HEK293T cells transfected with their respective expression vectors. Each

supernatant was added to the culture for 2 h. Subsequently, cells were infected with the Env-pseudotyped virus. The infectious units (IU) shown on the x-axis were determined by counting the number of log10-galactosidase (LacZ)-positive cells per milliliter (mL) of virus indicated on the y-axis. Virus infection titers with standard deviations represent the means of three independent infection experiments. Comparisons were performed using Student's *t*-test (*$p <$ 0.01).

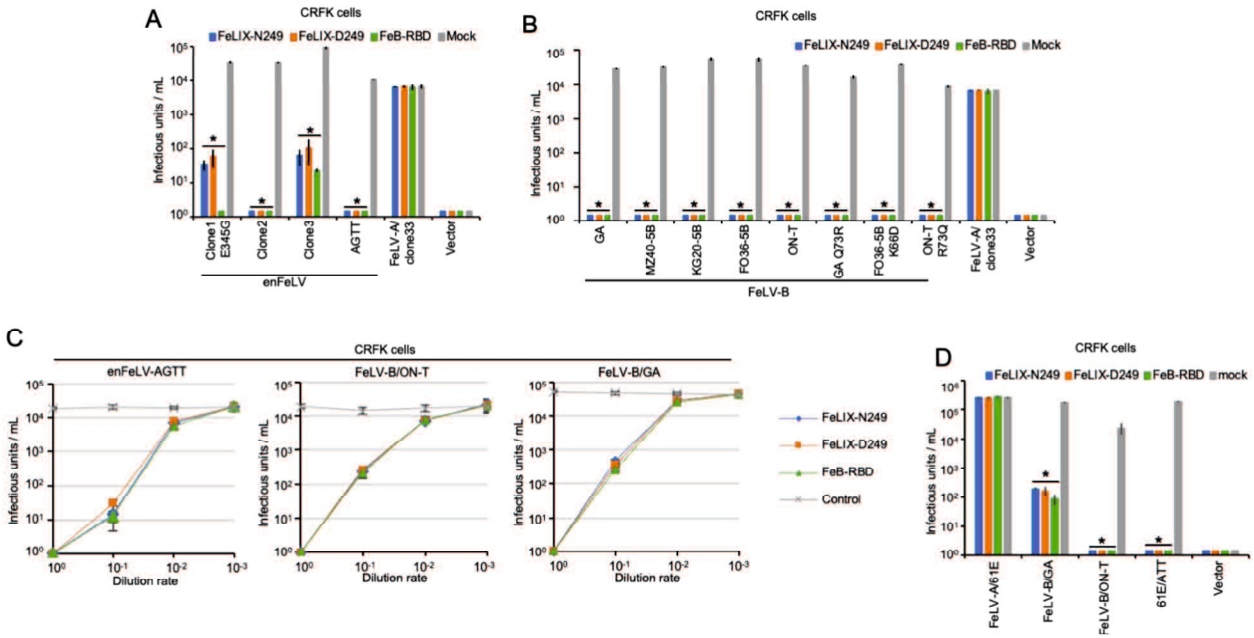

Figure 1.10 Inhibitory effect of the truncated Env proteins derived from enFeLV for enFeLV and FeLV-B infection. (A) Inhibition assay using FeLIX-N249 and FeLIX-D249 for the infection of Env-pseudotyped viruses, enFeLV (Clone 1 E345G, Clone 2, Clone3, and AGTT), (B) FeLV-B (GA, MZ40-5B, KG20-5B, FO36-5B, and ON-T), and FeLV-B mutants (GA Q73R, FO36-5B K66D, and ON-T R73Q) in CRFK cells. (C) Dose-dependent inhibition of FeLIX for Env-pseudotyped viral infection (FeLV-B/ON-T, FeLV-B/GA, and enFeLV-AGTT) in CRFK cells. (D) against replication-competent viruses assessed included FeLV-B/GA, FeLV-B/ON-T, FeLV-A carrying the enFeLV-AGTT env gene, and FeLV-A/61E in CRFK cells. FeLIX-N249, FeLIX-D249, FeB-RBD, and the empty vector/mock were sourced from supernatants of HEK293T cells transfected with their respective expression vectors. Each supernatant was added to the culture for 2 h. Subsequently, cells were infected with the Env-pseudotyped virus. The infectious units (IU) shown on the x-axis were determined by counting the number of log10-galactosidase (LacZ)-positive cells per milliliter (mL) of virus indicated on the y-axis. Virus infection titers with standard deviations represent the means of three independent infection experiments. Comparisons were performed using Student's *t*-test (*$p <$ 0.01).

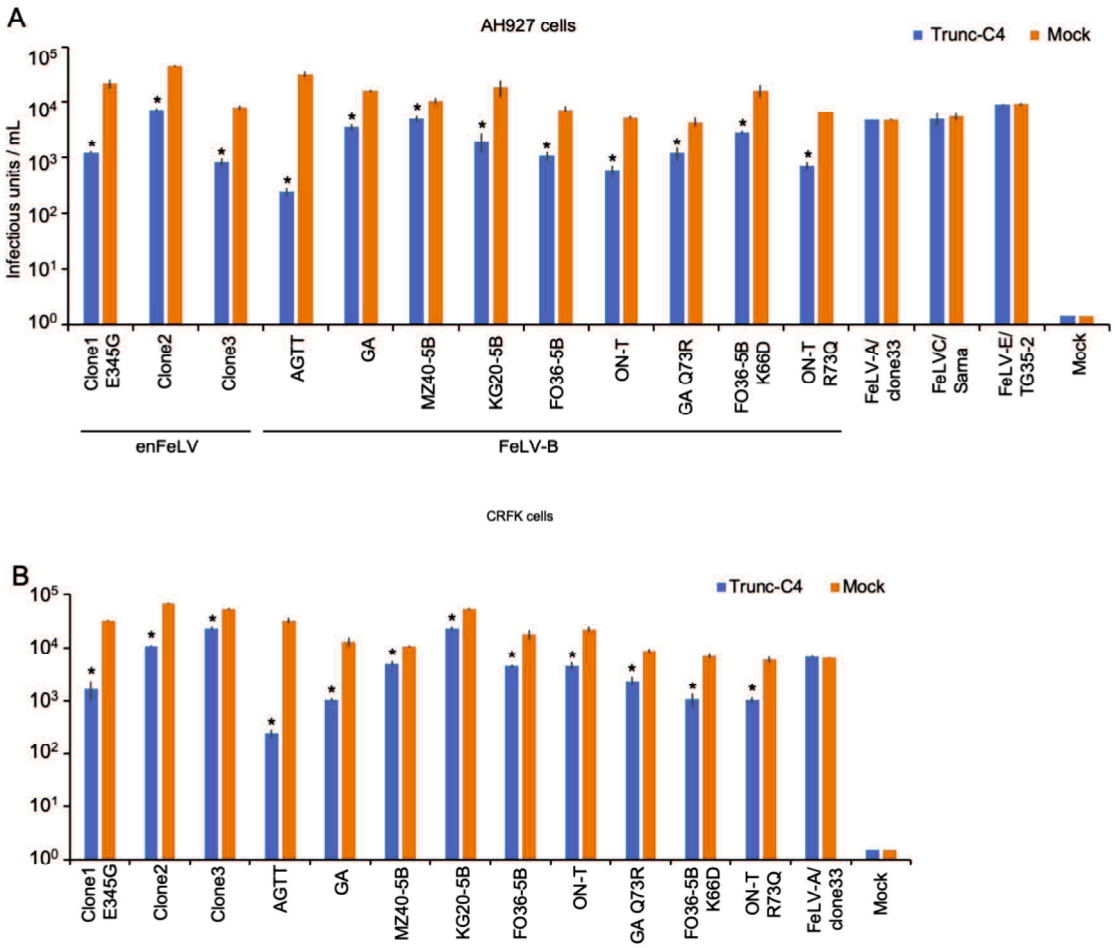

Figure 1.11 Inhibitory effect of Trunc-C4 against Env-pseudotype viruses, enFeLV (Clone 1 E345G, Clone 2, Clone3, and AGTT), FeLV-B (GA, MZ40-5B, KG20-5B, FO36-5B, and ON-T), and FeLV-B mutants (GA Q73R, FO36-5B K66D, and ON-T R73Q) in (A) AH927 cells and (B) CRFK cells. The infectious units (IU) were determined by counting the number of log10-galactosidase (LacZ)-positive cells per milliliter (mL) of the virus. Virus infection titers with standard deviations represented the means of three independent experiments. Mock represents the negative control. Comparisons were performed using Student's *t*-test (*$p < 0.01$).

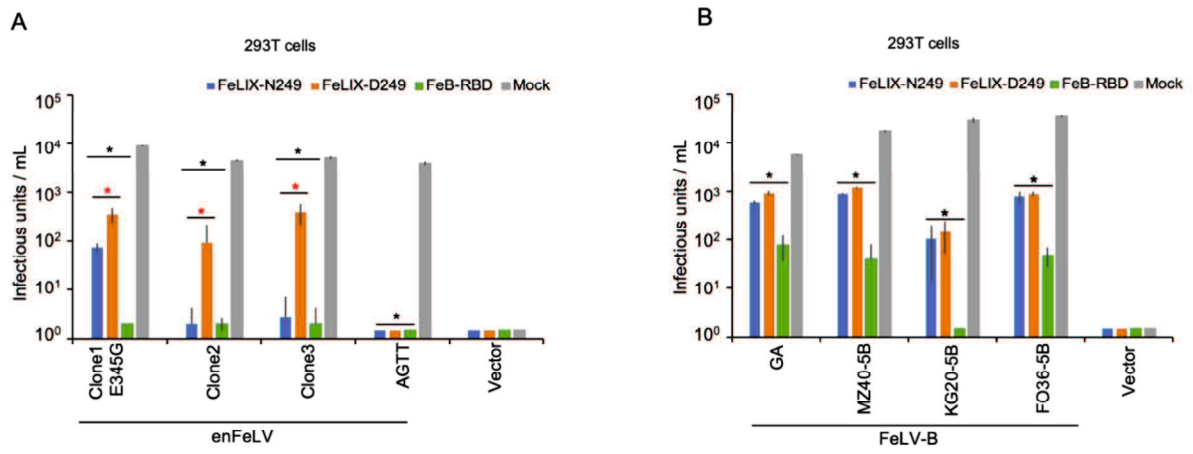

Figure 1.12 Inhibitory effect of FeLIX for enFeLV and FeLV-B Env-pseudotype viruses in HEK293T cells as target cells. (A) Supernatants collected from HEK293T cells transfected with expression vectors encoding FeLIX-N249, FeLIX-D249, and FeB-RBD were subjected to an inhibition assay against enFeLV (Clone 1 E345G, Clone 2, Clone 3, and AGTT). (B) The same supernatants were also evaluated for inhibition against FeLV-B (GA, MZ40-5B, KG20-5B, FO36-5B, and ON-T). As a control, supernatants from HEK293T cells transfected with an empty vector/mock were utilized. In each case, 250 µL of the respective supernatant was added to the cell cultures before infection with Env-pseudotyped virus. Infectious units (IU) were determined by counting the number of log10-galactosidase (LacZ)-positive cells per milliliter (mL) of virus. Virus infection titers with standard deviations represent the average of three independent experiments, with the mock serving as the negative control. Statistical comparisons were performed using Student's t-test (*$p < 0.01$).

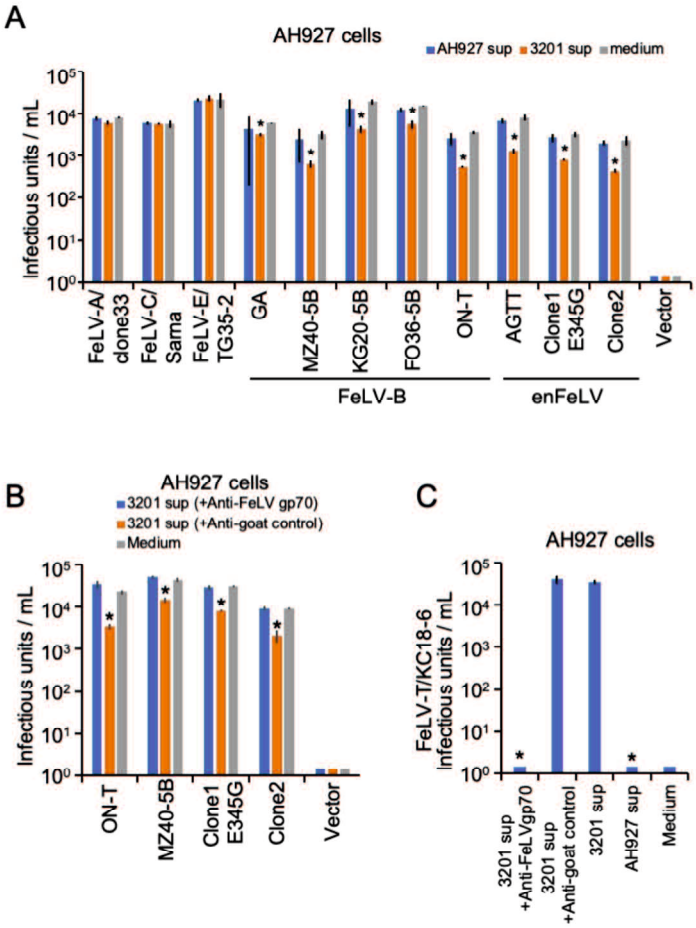

Figure 1.13 Inhibitory effect of FeLIX from the supernatant of 3201 cells on enFeLV and FeLV-B infection. (A) Inhibition assays of Env-pseudotyped enFeLV and FeLV-B viruses were conducted using the culture supernatant from 3201 cells in AH927 cells as target cells. (B) The culture supernatants from the 3201 cells were treated with either goat anti-FeLV gp70 antibody or normal goat serum (control), after which the culture supernatant from which FeLIX was removed was used for the inhibition assays for enFeLV and FeLV-B. (C) The culture supernatant from the 3201 cells and the culture supernatant from which FeLIX was removed were used for the infection assay for FeLV-T. The infectious units (IU) were determined by counting the number of log10-galactosidase (LacZ)-positive cells per milliliter (mL) of virus (x-axis). Virus infection titers with standard deviations represent the means of three

independent experiments. Medium represents the negative control. Comparisons were performed using Student's t-test (*$p < 0.01$).

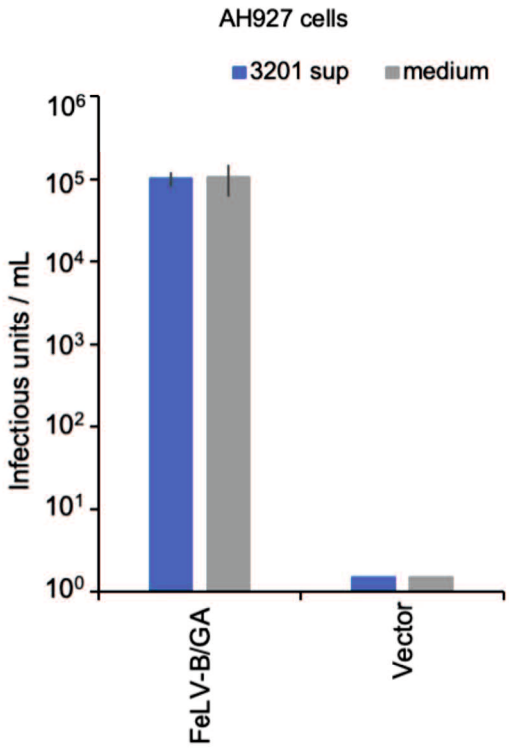

Figure 1.14 Inhibitory effect of FeLIX from the supernatant of 3201 cells with FeLV-B infection in high viral titer. Inhibition assays of FeLV-B/GA in high viral titers were conducted using the culture supernatant from 3201 AH927 cells as target cells. The infectious units (IU) were determined by counting the number of $\log_{10}$-galactosidase (LacZ)-positive cells per milliliter (mL) of the virus (x-axis). Virus infection titers with standard deviations represent the means of three independent experiments. Medium represents the negative control. Comparisons were performed using Student's t-test (*$p < 0.01$).

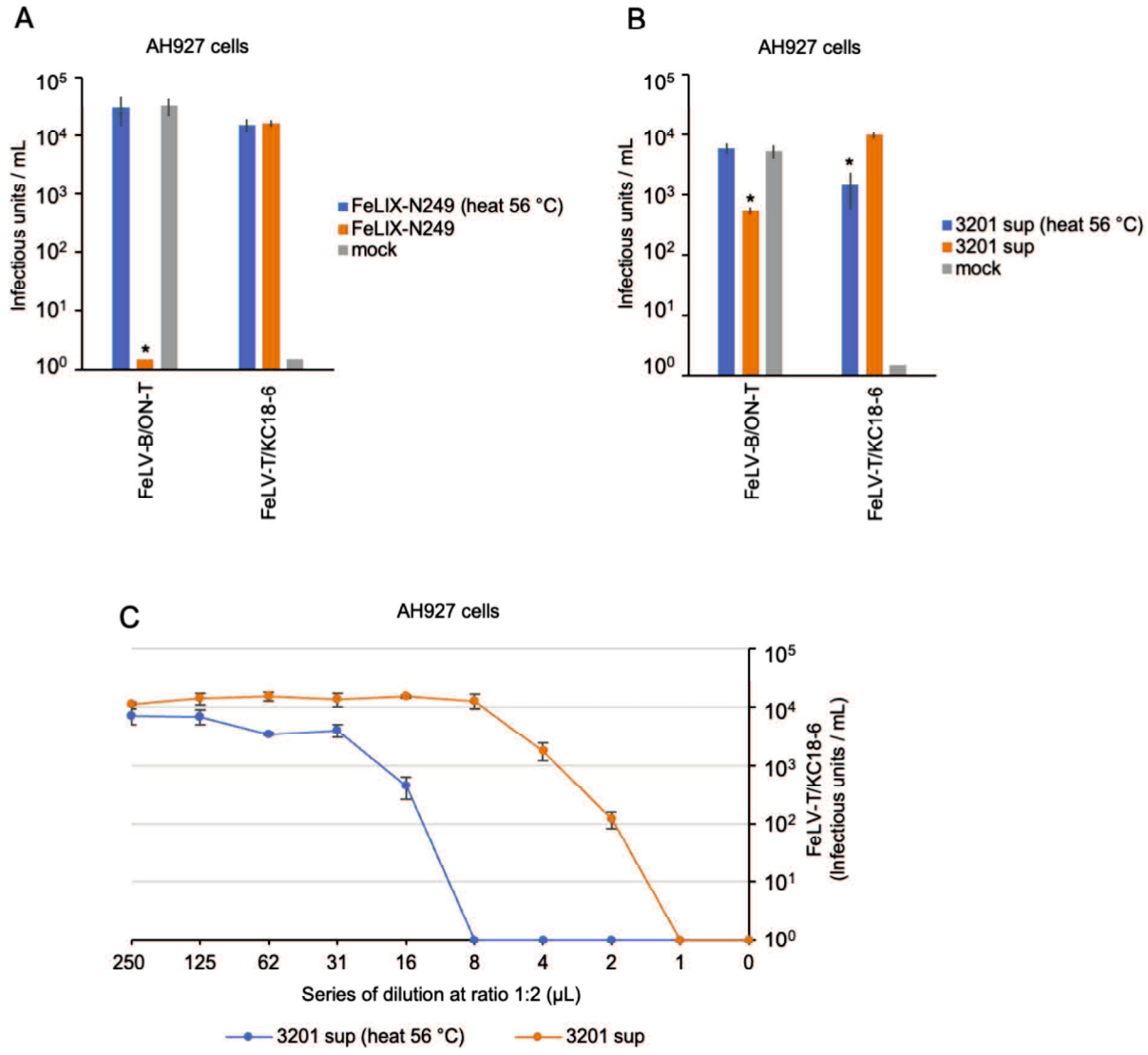

Figure 1.15 Thermal sensitivity of FeLIX. Supernatants obtained from HEK293T cells transfected with expression vectors encoding (A) FeLIX-N249 or from (B) 3201 cells were subjected to heat treatment at 56 °C for 30 min. Subsequently, 250 µL of the treated supernatants from these cells were utilized for inhibition assays against FeLV-B infection in AH927 cells. (C) The supernatants from 3201 cells, diluted in the medium as indicated on the x-axis, were subjected to heat treatment at 56 °C for 30 min, followed by assessment for their effects on FeLV-T infection in AH927 cells. Infectious units (IU) were determined by quantifying the number of $\log_{10}$-galactosidase (LacZ)-positive cells per milliliter (mL) of virus. Viral titers are depicted as the logarithm of infectious units (IU) per milliliter (mL) with

standard deviations, representing the average values derived from three independent experiments. Mock samples served as negative controls.

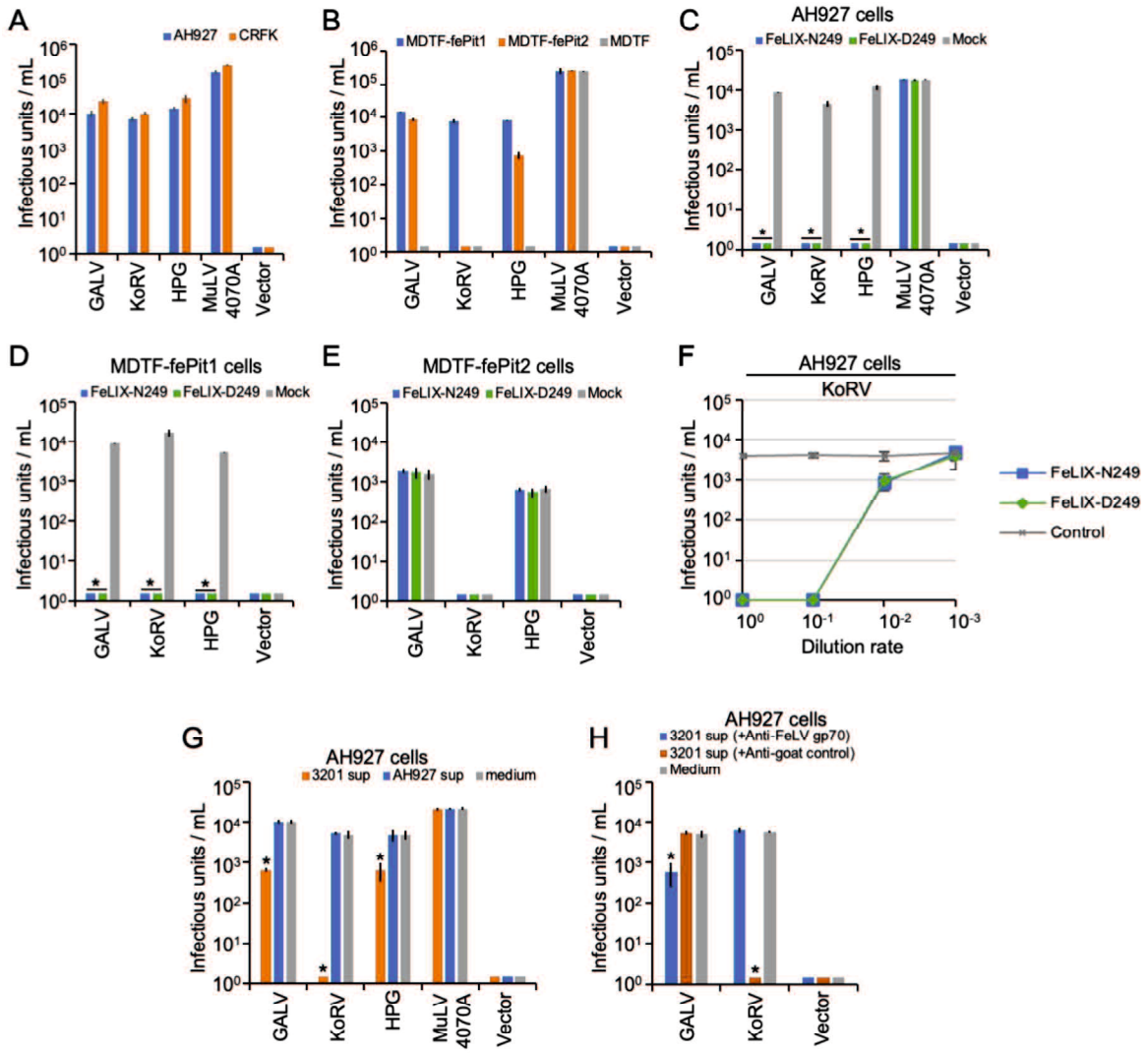

Figure 1.16 Inhibitory effect of FeLIX for non-feline mammalian retrovirus infection. (A) Infection of non-feline mammalian retroviruses (GaLV, KoRV, HPG, and MuLV 4070A) for feline, AH927, and CRFK cells; (B) for receptor usage in MDTF/fePit1, MDTF/fePit2, and MDTF/empty vector. Supernatants from HEK293T cells transfected with expression vectors encoding FeLIX-N249 and FeLIX-D249 were used for inhibition assays against non-feline mammalian retroviruses (GaLV, KoRV, HPG, and MuLV 4070A) in (C) AH927 cells, (D) MDTF-fePit1 cells, and (E) MDTF-fePit2 cells. (F) Dose-dependent inhibition of FeLIX for

KoRV Env-pseudotyped viral infection in AH927 cells. (G) Inhibition assays of Env-pseudotyped virus of KoRV, GaLV, HPG, and 4070A ampho-MuLV were conducted using the culture supernatant from 3201 cells in AH927 cells. (H) The culture supernatants from the 3201 cells were treated with either goat anti-FeLV gp70 antibody or normal goat serum (control). Subsequently, the culture supernatant from which FeLIX was removed was used for the inhibition assays for KoRV, GaLV, and HPG infection. The infectious units (IU) were determined by counting the number of $\log_{10}$-galactosidase (LacZ)-positive cells per milliliter (mL) of the virus. The viral titers are illustrated as the log number of infectious units (IU) per milliliter (mL). Virus infection titers with standard deviations represent the means of three independent experiments. Mock represents the negative control. Comparisons were performed using Student's *t*-test (*$p < 0.01$).

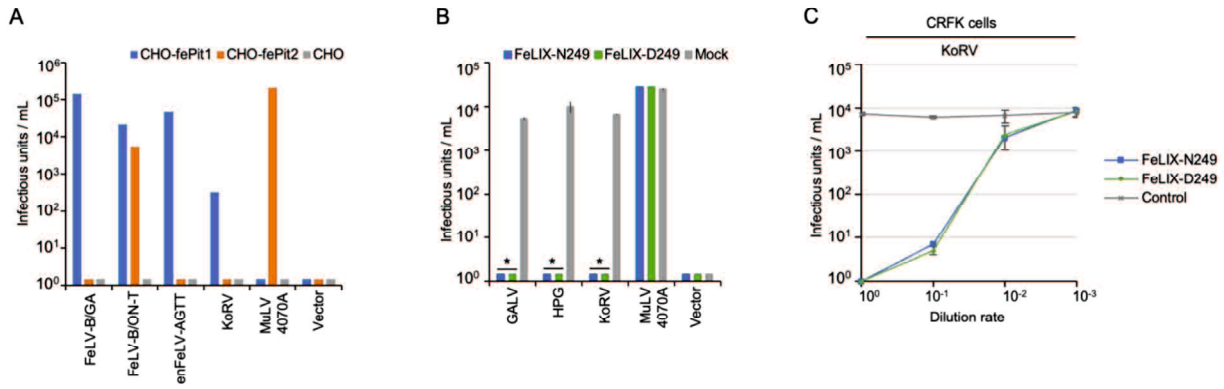

Figure 1.17 Infectivity and receptor usage of MuLV 4070A Env-pseudotyped viruses. Infectivity of MuLV 4070A Env-pseudotyped viruses in Chinese hamster ovary (CHO) cells expressing feline Pit1 (CHO-fePit1) and feline Pit2 (CHO-fePit2). Infection assay of MuLV 4070A, FeLV-B/GA, FeLV-B/ON-T, enFeLV-AGTT, and KoRV in CHO-fePit1, CHO-fePit2, and CHO-empty vector as target cells for receptor usage. The infectious units (IU) were determined by counting the number of $\log_{10}$-galactosidase (LacZ)-positive cells per milliliter (mL) of the virus. The viral titers are illustrated as the log number of infectious units (IU) per milliliter (mL).

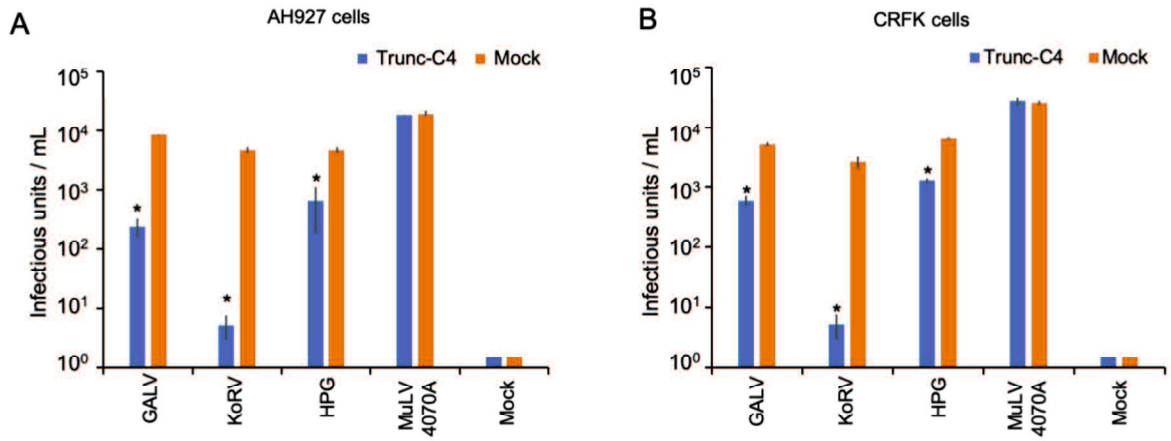

Figure 1.18 Inhibitory effect of Trunc-C4 for non-feline mammalian retroviruses. Inhibition assays were performed using supernatants collected from HEK293T cells transfected with Trunc-C4 expression vectors and empty vectors against non-feline mammalian retroviruses in (A) AH927 and (B) CRFK cells. Infectious units (IU) were quantified by counting the number of $\log_{10}$-galactosidase (LacZ)-positive cells per milliliter (mL) of virus. The virus infection titers, accompanied by standard deviations, represent the average values derived from three independent experiments, with mock samples used as the negative controls.

2. CHAPTER TWO

Characterization of the endogenous retrovirus-derived placenta-specific soluble protein EnvV-Fca from domestic cats.

This work has been published as follows:

Pramono D, Sugimoto K, Kimura T, Miyake A, Nishigaki K. 2024. Characterization of the placenta-specific EnvV-Fca soluble protein derived from an endogenous retrovirus. *FEBS Letter*. https://doi.org/10.1002/1873-3468.14873

2.1. ABSTRACT

Endogenous retroviruses (ERVs) are remnants of ancestral viruses in the host genome. The present study identified the expression of a defective retroviral env gene belonging to the ERV group V member Env (EnvV) in *Felis catus* (EnvV-Fca). EnV-Fca was specifically detected in the placental trophoblast syncytiotrophobic layer and expressed as a secreted protein in cultured cells. Genetic analyses indicated that EnvV2 genes are widely present in vertebrates and are under purifying selection among carnivores, suggesting a potential benefit for the host. This study suggests that birds, bats, and rodents carrying EnvV2 may play significant roles as intermediate vectors in spreading or cross-transmitting viruses among species. Our findings provide valuable insights into the evolution of ERV in vertebrate hosts.

2.2. INTRODUCTION

Endogenous retroviruses (ERVs) are ancient retroviral sequences that infect germ cells and are vertically transmitted to offspring in various vertebrate hosts, including mammals (4, 43-45). This process generates a substantial proportion of ERVs in the mammalian genome via repeated germline reinfection (46). ERVs are inactivated through methylation and the accumulation of mutations, including nucleotide substitutions, deletions, and insertions (47). Changes in viral genes can affect the function of the encoded proteins (53, 110). The proviral genome comprises three major polyproteins: *gag, pol,* and *env* (54). The env genes encode surface (SU) and transmembrane (TM) subunits that facilitate targeting and entry into specific cell types for infection (55). Defective env-ERV refers to an Env protein that has a signal peptide and SU subunit but contains a premature stop codon and lacks or has a partial deletion of the TM subunit. Defective env-ERV may be crucial for physiological functions in the host, such as maintaining homeostasis, placentation, and acting as a restricting factor for infection (8, 56-59). In domestic cats, Refrex-1, derived from the defective env genes of ERV-DC7 and ERV-

DC16, protects against feline leukemia virus subgroup D and ERV-DC genotype I infections (58). In addition to its restrictive function, Refrex-1 maintains cellular homeostasis by regulating copper levels (56) and is fixed in the domestic cat population (58). Suppressyn is found in humans and is specific to the placenta (59, 111). Suppressyn, an env-ERV derived from human endogenous retrovirus-F, regulates Syncytin-1 (the full-length env gene) involved in placentation (57). Suppressyn has an antiviral activity that restricts infection by mammalian type D retroviruses (59). Defective Env-ERV protein expression can restrict viral infection by competing with exogenous Env for entry into host cell receptors during viral entry. This interaction between the defective Env-ERV protein and host receptors can protect host cells from viral Env protein invasion by controlling viral entry (8, 55, 59). These reports highlight the crucial function of defective env-ERV in hosts.

Other ERVs have been identified and expressed in mammals as placenta-specific proteins. Syncytin is a captive retroviral envelope protein involved in human placental function (112). Another placenta-specific protein, group V member ERV Env (EnvV), has been identified. EnvV can be classified into two groups, EnvV1 and EnvV2, which share high similarity (113). EnvV in humans was initially identified, and neither EnvV1 nor EnvV2 exhibited fusion activity. The open reading frame (ORF) of EnvV1 comprises 477 amino acids, whereas the ORF of EnvV2 contains 535 amino acids (114). A single nucleotide insertion causes a truncation event at the C-terminus of genes, resulting in a frameshift (113). EnvV1- and EnvV2-encoded proteins are highly conserved during primate evolution (115). EnvV2 is intact in all analyzed primate species, whereas EnvV1 is preserved only in chimpanzees, gorillas, gibbons, rhesus macaques, baboons, African green monkeys, tamarins, and saki monkeys. In these species, EnvV1 exhibits a full-length ORF with no C-terminal truncation or stop codons. The EnvV2 ORF in primates has been conserved since its integration over 40–45 million years

ago and provides evidence of purifying selection of the EnvV2 gene among primates. Additionally, EnvV2 in macaques (EnvV2-Mac) exhibits fusion activity, but not with EnvV1 (115). Recently, after performing a genetic analysis using publicly available data, Simpson et al. (116) reported that EnvV1 and EnvV2 are highly conserved in two mammalian orders, Artiodactyla and Carnivora, suggesting that cross-species transmission occurred between these two orders at least 60 million years ago.

This study aimed to identify defective env-ERV genes that may be beneficial to the host. RNA-seq analysis was performed using feline ovarian tissue, and the expression of retroviral elements was successfully detected. This element was identified as EnvV Felis catus (EnvV-Fca).

2.3. MATERIALS AND METHODS

2.3.1. Animals and sampling

The domestic cat sample used in this study has been previously described (58). Briefly, the Nippon Institute for Biological Science provided a euthanized 2-month-old female specific-pathogen-free (SPF) cat, and an autopsy was performed. Animal tissues were stored at -80 °C until DNA or RNA was extracted for further investigation. Placental tissue was kindly provided by Dr. Daigo Umehara (Roji Animal Clinic, Fukuoka, Japan).

2.3.2. RNA-seq analysis using ovarian tissue

Total RNA was extracted from the ovaries of the SPF cat as previously described (58). The RNA-seq analysis was performed at the Yamaguchi University Genetic Experiment Facility (Yamaguchi, Japan).

2.3.3. Cell lines

Cells were cultured in Dulbecco's modified Eagle's medium (FUJIFILM Wako Pure Chemical Corporation, Osaka, Japan) supplemented with 10% fetal calf serum and 1× penicillin–streptomycin. The cells were incubated in a CO_2 incubator at 37 °C. The following cell types were used in this study: HEK293T (human embryonic kidney transformed with SV40 large T antigen) (73), 3201 (feline lymphoma cells) (78), 3281 (feline lymphoma cells) (117), FL74 (feline lymphoma cells) (118), FT-1 (feline T-cell leukemia cells) (119), MS4 (feline B-cell lymphoma cells) (85), KO-1 (lymphoma cells) (85), feline mammary adenocarcinoma cells (FMC, FKNp, FON, FRM, and FNNm) (120), CrFK (feline kidney cells) (77), Fcwf-4 (feline macrophage-like cells) (121), G355 (feline fetal brain cells) (122), Fc9 (feline fetal cells), and Fet-J (feline peripheral lymphocytes) (119).

2.3.4. PCR

The KOD-One Polymerase Kit (Toyobo, Osaka, Japan) was used for various cloning processes. Primers were designed based on unique sequences outside and inside each provirus to preserve the target gene. The primers used in this study are listed in Table 2.1.

2.3.5. Construction of expression vectors

The pFUΔss expression vector was used to construct the expression plasmids, as previously described (49). Each gene was PCR amplified from its respective plasmid using specific primers and enzyme sites. The PCR products were digested with their corresponding restriction enzymes and cloned into the pFUΔss expression plasmid. The expression plasmid for EnvV-Fca was constructed from domestic cat tissue cDNA using the primer pairs listed in Table 2.1. The plasmid was then inserted into the pFUΔss vector. The EnvV2-Mac sequence was obtained from the NCBI database and synthesized by Eurofins Genomics (Tokyo, Japan). The EnvV2-

Mac gene was then inserted into the pFUSE-hIgG2-Fc2 vector (InvivoGen, San Diego, CA, USA). A myc tag was added to the C-terminus of EnvV-Fca and EnvV2-Mac. The resulting expression plasmids were confirmed using sequencing (Fasmac Corporation, Atsugi, Japan).

2.3.6. Transfection

HEK293T cells were transfected with expression plasmids using the TransIT-293 transfection reagent (Takara, Shiga, Japan), following the manufacturer's instructions.

2.3.7. Immunoblotting

Plasmids were introduced into HEK293T cells using the TransIT®-293 reagent (Takara) in six-well plates. After two days, the cell pellets were collected by washing them thrice with phosphate-buffered saline (PBS). Cells were mixed with lysis buffer containing 20 mM Tris-HCl (pH 7.5), 150 mM NaCl, 10% glycerol, 1% Triton X-100, 2 mM EDTA, 1 mM Na_3VO_4, and 1 μg/mL of aprotinin and leupeptin to prepare cell lysates. The lysates were then placed on ice for 20 min. Insoluble components were removed through centrifugation at 15,400 × g for 20 min at 4 °C. The protein concentrations were calculated using a protein assay kit (Bio-Rad, Hercules, CA, USA).

The cell supernatants were filtered using a 0.22-μm filter and incubated with the desired antibody overnight at 4 °C. The purified protein, which included the cell lysate and supernatant, was mixed with Sample Buffer Solution (Nacalai Tesque, Kyoto, Japan) and heated at 95–100 °C for 5 min. Sodium dodecyl-sulfate polyacrylamide gel electrophoresis was performed using 4–20% gels (Invitrogen, Carlsbad, CA, USA) at 100 V for 2 h. The gels were then transferred onto nitrocellulose membranes for western blot analysis. Anti-Myc monoclonal antibody conjugated with horseradish peroxidase (FUJIFILM Wako Pure Chemical Corporation; dilution, 1:1000) was used. The substrate used was LumiGLO® Reagent (20×)

and 20× peroxide (Cell Signaling Technology, Danvers, MA, USA). Blots were imaged using Amersham ImageQuant 800 (Cytiva, Shinjuku, Japan).

2.3.8. Detection of EnvV-Fca expression via quantitative RT-PCR

Total RNA was extracted from the tissues of an SPF cat (14) and various feline cell lines using an RNAiso Plus kit (Takara) according to the manufacturer's instructions. cDNA was synthesized using a PrimeScript II first-strand cDNA syndissertation kit (Takara) following the manufacturer's instructions. Before reverse transcription, the RNA samples were treated with recombinant DNase I (Takara). The cDNA was amplified using Premix Ex Taq (Probe qPCR; Takara) in a CFX96 Touch Real-Time PCR Detection System (Bio-Rad, Hercules, CA, USA). The EnvV-Fca gene was amplified using Fe-gvm2Env-F and Fe-gvm2Env-R primers and detected using probe Fe-gvm2Env-P (containing 6-carboxy-fluorescein; FAM) (Takara). The internal control, feline peptidyl prolyl isomerase A (PPIA), was amplified with Fe-227S and Fe-204R primers using SYBR Premix Ex Taq II (Tli RNaseH Plus; Takara) (Table 2.2). Thermal cycling was performed according to the manufacturer’s instructions.

2.3.9. In situ hybridization analysis of placental sections

Fresh placental samples were fixed in situ, extracted, and dried on microscope slides in preparation for RNA-in situ hybridization (ISH) analysis. Fixed tissues were embedded in paraffin on CT-Pro20 (Genostaff, Tokyo, Japan) using G-Nox (Genostaff) as a less toxic organic solvent and sectioned into 6-μm thick sections. ISH analysis was performed with an ISH Reagent Kit (Genostaff) according to the manufacturer’s instructions. Tissue sections were deparaffinized with G-Nox and rehydrated in ethanol and PBS. The sections were then fixed with 10% neutral buffered formalin for 30 min at 37 °C, washed in distilled water, placed in 0.2% HCl for 10 min at 37 °C, and washed in PBS. The sections were then treated with 4

μg/mL Proteinase K in PBS for 10 min at 37 °C, washed in PBS, and placed within a Coplin jar containing 1× G-Wash (Genostaff) equal to 1× saline-sodium citrate. Hybridization was performed with probes (250 ng/mL) in G-Hybo-L (Genostaff) for 16 h at 60 °C. After hybridization, the sections were washed thrice with 50% formamide in 2× G-Wash for 30 min at 50 °C and five times in 0.1% Tween20 in Tris-buffered saline (TBST) at room temperature (20–25 °C). After treatment with 1× G-Block (Genostaff) for 15 min at room temperature, the sections were incubated with anti-DIG AP conjugate (Roche, Basel, Switzerland; 1:2000) with G-block (diluted 1/50) in TBST for 1 h at room temperature. The sections were washed twice with TBST and incubated in 100 mM NaCl, 50 mM MgCl2, 0.1% Tween20, and 100 mM Tris-HCl (pH 9.5). Coloring reactions were performed with nitro blue tetrazolium/5-bromo-4-chloro-3-indolyl phosphate solution (Sigma-Aldrich, St. Louis, MO, USA), and the sections were washed with PBS. Sections were counterstained with Kernechtrot Stain Solution (Muto) and mounted with G-Mount (Genostaff) and malinol (MUTO PURE CHEMICALS, Tokyo, Japan). Images were obtained using a NanoZoomer S210 digital slide Scanner: C13239-01 (Hamamatsu Photonics, Shizuoka, Japan) and NDP.view2 Plus Viewing Software: U12388-02 (Hamamatsu Photonics).

2.3.10. Functional assay of EnvV-Fca and EnvV2-Mac into cells

HEK293T cells were transfected with the expression vectors of EnvV-Fca and EnvV2-Mac using TransIT®-293 Transfection Reagent according to the manufacturer's instructions. HEK293T cells transfected with a pFUΔss empty vector were used as a negative control. The cells were cultured for 2 days, and the culture supernatant was removed and stained with a Diff-Quick staining solution according to the manufacturer’s instructions. Cell morphology was observed using an optical microscope to evaluate morphological changes.

2.3.11. Phylogenetic and sequencing analysis

A phylogenetic tree was constructed using the sequences listed in the “Accession numbers” section. The MEGA11 software package was used for phylogenetic analysis, and amino acid sequences were aligned using MUSCLE (88). A phylogenetic tree was constructed using the neighbor-joining method (34) and the amino acid substitutions JTT model (123), and robustness was evaluated through bootstrapping (1,000 times) (124). All bioinformatics analyses were conducted using MEGA11 (52).

2.3.12. Evolutionary analysis of EnvV2 among carnivores

Publicly available genome data was searched using the BLAST method to conduct evolutionary analyses of EnvV2. The vertebrate genome database was searched using the env ORF of EnvV-Fca (Carnivora), EnvV2-Mac (primate), and Bos indicus (even-toed ungulate) nucleotide sequences as references. EnvV2 sequences were obtained from carnivores and aligned using MUSCLE (88). The pairwise p-distance values of the amino acids, which represent the proportion of amino acid sites at which the two sequences differ, were then calculated. The number of non-synonymous substitutions (dN) and synonymous substitutions (dS) per site were calculated using the Nei–Gojobori method (38). The bioinformatics analyses were conducted using MEGA11 (52). To analyze amino acid similarity, the amino acids of EnvV2 Carnivores were aligned using MUSCLE, and the amino acid similarity (%) of all carnivore representatives was calculated using Genetyx 16 (Genetyx Corporation, Tokyo, Japan).

2.3.13. Ethical approval

All animal experiments were conducted in accordance with the Guidelines for the Care and Use of Laboratory Animals, provided by the Ministry of Education, Culture, Sports, Science

and Technology, Japan. The Genetic Modification Safety Committee of Yamaguchi University approved all experiments.

2.3.14. Accession numbers

The accession numbers obtained from publicly available data are as follows: Human (NM_001191055), Macaque (NM_001348393), Chimpanzee (NM_001307974), *Felis catus* (XM_019831672), *Ursus arctos* (XM_057304973), *Panthera pardus* (XM_019425134), *Miniopterus natalensis* (XM_016197129), *Myotis daubentonii* (XM_059699531), *Myotis lucifugus* (XM_023753138), *Phyllostomus discolor* (XM_036014176), *Pipistrellus pipistrellus* (LR862361), *Anas platyrhynchos* (XM_038171956), *Aquila chrysaetos chrysaetos* (XM_041121140, XM_030010836), *Cygnus atratus* (XM_050710036), *Grus americana* (XM_054826583), *Indicator indicator* (XM_054389296), *Opisthocomus hoazin* (XM_009944966), *Castor canadensis* (XM_020155210), *Ictidomys tridecemlineatus* (XM_040273522), *Marmota monax* (XM_046457090), *Rattus norvegicus* (NM_001408907), *Sciurus carolinensis* (XM_047551960, XM_047551962), *Bos indicus* (XM_019957350), *Bubalus bubalis* (XM_025288582), *Alligator mississippiensis* (XM_059724950), *Gopherus evgoodei* (XM_030542918, XM_030542367), *Oncorhynchus mykiss* (XM_036942505), *Syngnathus scovelli* (XM_049756540), *Elephas maximus indicus* (XM_049877704), *Rana temporaria* (XM_040342020). The sequences from the isolate described in this paper have been deposited in DDBJ/EMBL/GenBank under accession number LC794385.

2.4. RESULTS

2.4.1. EnvV-Fca is a retroviral-defected env gene in domestic cats

RNA-seq analysis was performed using RNA from the ovarian tissue of a domestic cat to identify a candidate for the retroviral env gene. Env gene fragments were identified and classified as EnvV2 by focusing on genes with high expression levels. EnvV2-Fca was isolated from various domestic cat samples (spleen and small intestine) using RT-PCR. A positive band of approximately 2.2 kb was identified in the spleen and small intestine. Molecular cloning of these PCR-positive samples was then conducted to obtain the EnvV2-Fca ORF sequence. EnvV2-Fca has a nucleotide sequence of 1317 bp, encodes 439 amino acids, and contains a putative signal peptide (SP), putative SU subunit, putative furin cleavage site, putative fusion peptide, putative immunosuppressive domain (ISD), and putative TM subunit (Figure 2.1A). EnvV2-Fca is an Env protein that differs from retroviral envelope-derived proteins due to its truncated TM subunit structure. Furthermore, several mutations were observed compared to the reference data (predicted EnvV2-Fca) in the NCBI database (accession number XM_019831672). Figure 2.1B displays the changes in the amino acid positions. Phenylalanine at position 13 was replaced with leucine (F13L), methionine at position 41 with valine (M41V), threonine at position 139 with alanine (T139A), and glutamine at position 321 with arginine (Q321R). According to the phylogenetic analysis, “EnvV2-Fca” was changed to “EnvV-Fca” and could be indistinguishable between EnvV1 and EnvV2 in humans and primates, respectively (Figure 2.2).

2.4.2. EnvV-Fca is expressed as a soluble protein

The EnvV-Fca ORF was cloned into the pFUΔss expression vector (49) to determine whether the protein of the EnvV-Fca gene can be expressed. EnvV-Fca expression was detected in the cell lysates at a molecular mass of 55 kDa (Figure 2.3A). However, the size of EnvV-Fca in the

cell supernatants was unexpectedly large, ranging from 60–70 kDa. This size difference may be due to various forms of protein modification. Based on the amino acid sequence, EnvV-Fca was expected to contain a furin cleavage site (R-R-K-R) (Figure 1.1B); however, cleavage of the EnvV-Fca protein was not observed when expressed in transfected HEK293T cells. Only a single band representing the protein expression of EnvV-Fca was observed in the cell lysates and supernatant (Figure 2.3A). These results indicate that EnvV-Fca was secreted from the cells as a soluble protein because these proteins were detected in the cell supernatants.

2.4.3. Expression analysis of EnvV-Fca in feline tissues and cell lines

Quantitative RT-PCR was performed to analyze the expression levels of EnvV-Fca and determine the tissue-specific EnvV-Fca expression. EnvV-Fca expression was quantified in normal feline tissues (SPF cats) and cell lines. EnvV-Fca was broadly expressed in various tissues, with the highest expression levels in the placental tissue (Figure 2.3B). EnvV-Fca was detected in all feline cell lines (Figure 2.3C). These findings suggest that EnvV-Fca is widely expressed in feline tissues and cell lines, with particularly high expression levels in the placenta. Our finding suggests that EnvV-Fca was expressed in a placenta-preferential manner.

2.4.4. ISH analysis of EnvV-Fca in the placenta

ISH was performed on paraffin-sectioned placental tissue to investigate the possible importance of specific EnvV-Fca expression in the placenta (Figure 2.3B). Specific digoxigenin-labeled anti-sense probes were developed, and sense probes were used as negative controls to detect EnvV-Fca transcripts. Specific labeling was observed only with anti-sense probes and not with the control probes (Figure 2.4). The specific labeling of EnvV-Fca was broadly distributed in the placenta, including the connective tissue, with a particularly

substantial signal in the trophoblast syncytiotrophobic layer (Figure 2.4, right). This finding indicates that EnvV-Fca is expressed in the placental tissue and is specific to the placenta.

2.4.5. EnvV-Fca exhibits non-fusogenic activity

EnvV2-Mac has fusogenic activity and plays a fundamental role in syncytiotrophoblast cell–cell fusion (20). However, a comparison of the structure schematic (Figure 2.1A) and ORF amino acids (Figure 2.1B) of EnvV-Fca, EnvV2-Hum, and EnvV2-Mac revealed that EnvV-Fca has a truncated TM subunit. Although EnvV-Fca has a different structure, it was specifically expressed in the placenta (Figure 2.3 and 2.4). Therefore, whether EnvV-Fca has cell fusion activity, which is the canonical function of retroviral env genes specifically expressed in the placenta, was investigated. A functional assay was performed by transfecting cell lines in culture with the abovementioned env-expression vectors, as previously described (114), and following up on syncytium formation two days post-transfection. EnvV-Fca exhibited non-fusogenic activity compared to the positive control, whereas EnvV2-Mac exhibited fusion activity (115) (Figure 2.5). This finding suggests that despite EnvV-Fca being expressed specifically in the placenta, it does not exhibit fusogenic activity.

Conservation and evolution of EnvV2 genes among mammals and non-mammalian vertebrates

We hypothesized that the evolution of EnvV2 is not limited to humans, primates, carnivores, and even-toed ungulates. EnvV2 was further investigated by analyzing publicly available sequence data using the env ORF of EnvV-Fca (carnivora), EnvV2-Mac (primate), and Bos indicus (even-toed ungulate) as search references. In the NCBI database, an EnvV2 prediction labeled as “endogenous retrovirus group V member 2 Env polyprotein-like” was identified and referred to as EnvV2. Therefore, all data labeled with EnvV2 from the NCBI database was analyzed. Several additional mammals, including bats, rodents, and elephants, also contain

EnvV2 (Figure 2.6A and 2.6B). The amino acid similarity of these mammals was compared to EnvV-Fca; bats, rodents, and elephants share amino acid similarities of 60–68%, 47–71%, and 57% with EnvV-Fca, respectively. Furthermore, publicly available data was searched by performing a BLAST search on vertebrates to determine whether EnvV2 is conserved only in mammals; EnvV2 also appears in several non-mammalian species, including birds, turtles, amphibians, fish, and reptiles (Figure 2.6).

A phylogenetic tree was constructed using the amino acid sequence of EnvV2 ORFs (Figure 2.6A). The currently identified genes are distinct from previously identified EnvV2 genes, especially between mammalian and non-mammalian vertebrates, which are located separately. Notably, EnvV2 in bats, rodents, and ungulates belong to the same lineage (Figure 2.6A). Additionally, EnvV-Fca, a carnivorous order, is located in the same clade as that of humans and primates. Therefore, further analyses were conducted on the identified sequences. The results revealed a characteristic structure of the retroviral protein (125-127) with a putative furin cleavage site and a consensus of R/K-X-R/K-R representing the SU and TM subunits. However, several of the identified EnvV2 proteins had a modified furin cleavage site. Additionally, a CX2C motif corresponding to the binding domain was observed between the two subunits, and a CX6CC motif was observed as an envelope glycoprotein predicted to facilitate fusion (126). Using Phobius (https://phobius.sbc.su.se/) (126), a signal peptide at the N-terminal of the sequences was identified. Based on sequence-structure analysis, we classified complete EnvV2 (containing a signal peptide, SU, furin cleavage site, and TM subunits) as present in humans, primates, elephants, birds (*Aquila chrysaetos chrysaetos* and *Grus americana*), rodents (*Castor canadensis, Sciurus carolinensis*), and reptiles. However, two defective EnvV2s were identified in two groups: one EnvV2 with a truncated TM subunit present in carnivores, even-toed ungulates, rodents (*Marmota monax, Ictidomys tridecemlineatus, Sciurus carolinensis,*

and *Rattus norvegicus*), birds (*Aquila chrysaetos chrysaetos*), and reptiles (*Gopherus evgoodei*), and the other lacked a signal peptide or partial deletion of the SU subunit in birds (*Cygnus atratus, Indicator indicator*, and *Opisthocomus hoazin*), fishes, and amphibia. Interestingly, some species (*Sciurus carolinensis, Aquila chrysaetos chrysaetos*, and *Gopherus evgoodei*) had two forms of EnvV2. The alignment of the amino acid sequence of the SU subunit of EnvV2 was constructed for all species (Figure 2.7). These identified EnvV2 sequences conserved the ISD, with the exception of one rodent species (*Rattus norvegicus*).

The evolution of EnvV2 was then analyzed. The evolution of EnvV2 can be investigated by comparing the rates of dN and dS changes in similar or related sequences (128). ERV genes, such as host genes, can be conserved in two ways: (a) when the dN/dS rate is < 1, the genes are under purifying selection and retain a beneficial function, or (b) if the dN/dS rate is > 1, the genes are classified under positive selection. The domestic cat (Felis catus), belonging to the order Carnivora, was used to study the conservation and evolution of EnvV-Fca in Carnivora species. The ratio of dN to dS mutation (dN/dS) was calculated as previously described (38). The dN/dS ratios of EnvV2 among carnivores ranged from 0.08–0.81 (Figure 2.8). These findings suggest that EnvV2 genes are subject to purifying selection in all Carnivora species.

The evolutionary relationships of the EnvV2-like sequences were determined through a genomic synteny comparison of the locus. Separate orthologs were identified in each group, with humans and primates located between the ZNF160 and ZNF816 genes, even-toed ungulates between the CCNY and CREM genes, carnivores between the BTN2A1 and BTN1A1 genes, and bats between the KPNA7 and ADAMTS19 genes. However, rodents, birds, reptiles, and fishes were non-orthologous within their respective groups. These results suggest that EnvV2 is non-orthologous among the groups (Figure 2.9).

Because the newly identified EnvV2 in these species did not provide a complete long terminal repeat (LTR) sequence, we were unable to investigate the integration time into the host genome completely. Therefore, we constructed a TimeTree of mammalian vertebrates, as modified from a previous report that demonstrated EnvV2 in Carnivora and ungulates were integrated at least 60 million years ago (116, 129) with additional data on newly identified EnvV2 from others. Based on the TimeTree analysis, it was estimated that the integration time for newly identified EnvV2 during mammalian evolution, particularly in rodents, elephants, and bats, was similar to that of EnvV2 in Carnivora and ungulates (Figure 2.10) (116). However, owing to limited information on non-mammalian vertebrates, such as birds, reptiles, fishes, and amphibians, we were unable to confirm an integration time of EnvV2 in non-mammalian vertebrates in this study.

2.5. DISCUSSION

In this study, while investigating the expression of ERV *env* genes in domestic cats, we discovered that EnvV-Fca is closely related to the EnvV2-Hum gene (114). EnvV-Fca comprises 439 amino acids, including a signal peptide, SU subunit, fusion peptide, and an ISD; however, the TM subunit was partially deleted. In contrast, human and macaque monkey EnvV2 genes exhibited no structural defects. EnvV-Fca is released from cells as a soluble protein, whereas the human and macaque monkey EnvV2 proteins are membrane-bound (115). This solubility may be due to the partial deletion of the TM subunit in the Env protein, which is not anchored to the cell membrane and can be efficiently released from cells (58).

EnvV-Fca is present in various feline tissues and cell lines. EnvV-Fca expression was observed at a similar level in tumor cell lines, specifically lymphoma and mammary carcinoma; however, cell type-specific expression was not observed in the cell lines used in this study. EnvV-Fca

expression in normal cells is currently unknown. In feline tissues, the highest level of EnvV-Fca expression was detected in the placenta and was specifically observed in the placental trophoblast syncytiotrophobic layer. These findings are similar to those of EnvV2-Mac, which is expressed in trophoblasts (115). When comparing EnvV2-Mac to EnvV-Fca, EnvV2-Mac retained cell fusion activity (115), whereas EnvV-Fca did not. The structural deletion in the TM subunit of the gene, resulting in EnvV-Fca secretion, may be the reason for the lack of fusion activity. However, EnvV2-Hum also lacks fusion activity (130), and because EnvV2-Hum exhibits no structural defects compared to EnvV-Fca and Env-Mac (Figure 2.1), the fusion ability of EnvV-Fca could have been lost due to a genetic mutation, although the exact cause is unknown. Instead, Syncytin-Car1 may be the primary mediator of this biological process in domestic cats (128).

As EnvV2 did not possess a complete LTR in newly identified species, the integration time into the host genome, as determined using the LTR-based method (91), could not be evaluated. Based on the TimeTree analysis by referring to a previous report (116), the integration time for additional EnvV2 during mammalian evolution in rodents, elephants, and bats was calculated to be at least 60 million years ago, around the Cretaceous–Paleogene boundary, which is similar to the findings of another study on carnivores and even-toed ungulates (116). However, we were unable to identify an integration time for non-mammalian vertebrates in this study due to limited information.

EnvV2 is identified in mammals and non-mammals as non-orthologous among the groups and can be classified into two groups: one contains a complete EnvV2, structurally similar to EnvV2-Hum and EnvV2-Mac, and the other is a defective EnvV2, similar to EnvV-Fca. These structural features are consistent in each species. However, determining the presence or absence

of fusion activity based on structural features is challenging, as in EnvV2-Hum, EnvV2-Mac, and EnvV-Fca. Notably, all identified EnvV2 proteins contained the ISD, except for Rattus norvegicus. The ISD may have a suppressive effect on the immune response in cellular and humoral responses (131). Therefore, EnvV2 may be involved in host immune tolerance. Currently, evidence is lacking to suggests that EnvV2 has a specific function. EnvV-Fca is specifically expressed in the placenta, suggesting that it may has a similar to the effect of suppresyn (111). Comparing the structure of the defective EnvV2 group with Refrex-1 and suppressyn (14, 15) indicated that the defective EnvV2 group may be an antiviral factor against retroviral infections. Alternatively, the role of EnvV2 may be altered and play a different role in each species.

ERVs can be transmitted between species (116, 132). Bats harbor several retroviruses, such as *Hervey pteropid gammaretrovirus* (30). Bats have unique ecological characteristics, such as flight, hibernation, a relatively long lifespan, and colonial roosting behavior, which make them ideal vectors for maintaining viral infections (133). Furthermore, rodents and birds are also involved in the transmission of retroviruses (134-136), which are directly derived from mammalian retroviruses (137). The identification of EnvV2 in birds, bats, and rodents indicates the potential for the transmission of EnvV2 through these intermediate vectors.

In conclusion, EnvV2 evolution is not limited to mammals but extends to several non-mammalian vertebrates. Furthermore, EnvV-Fca is a secreted protein and does not exhibit fusion activity, suggesting that EnvV-Fca is not directly involved in syncytiotrophoblast formation during pregnancy. Notably, EnvV2 may have possible implications in immunotolerance during pregnancy or may be a restrictive factor for exogenous retroviral infection. This study presents a scenario of retroviral transmission among species, which may

have significant implications for elucidating retroviral transmission and ERV evolution. Furthermore, the present study provides a comprehensive characterization of EnvV-Fca, detailing the identification of the EnvV gene, the investigation of its expression and possible function, and an evolutionary analysis of EnvV2 in mammalian and non-mammalian vertebrate hosts. However, further studies are needed to clarify the receptor and specific roles of the EnvV-Fca protein.

2.6. TABLES, FIGURES, SUPPLEMENTARY DATA IN CHAPTER TWO

Tables

Table 2.1 Primer information used for cloning EnvV-Fca (domestic cat)

Name	Sequence (5′ -3′)
Fe-669S	CAAGGGCGTTCCGTCTTTCC
Fe-649R	TGTAGCTCTCAGCCCTTTCTC
Fe-670S	CGCTGGTGCCGGAGGATAAG
Fe-650R	CATTGTGGTTAGGGTGGGGA

Table 2.2 Primer and probe information used for quantitative RT-PCR

Gene	Primer	Sequence (5′ -3′)
EnvV-Fca	Fe-gvm2Env-F	AGACCAACACCTGCCTGACC
EnvV-Fca	Fe-gvm2Env-R	GGGACACACGAAGAGCTTGC
EnvV-Fca	Fe-gvm2Env-P	[6FAM]CAGTTCGCCCTCCATTTATCCCATGTCC[TAM]
PPIA	Fe-227S	GTCAACCCCATCGTGTTTTT
PPIA	Fe-204R	CTGCTGTCTTGGGAACTTTGTC

Figures

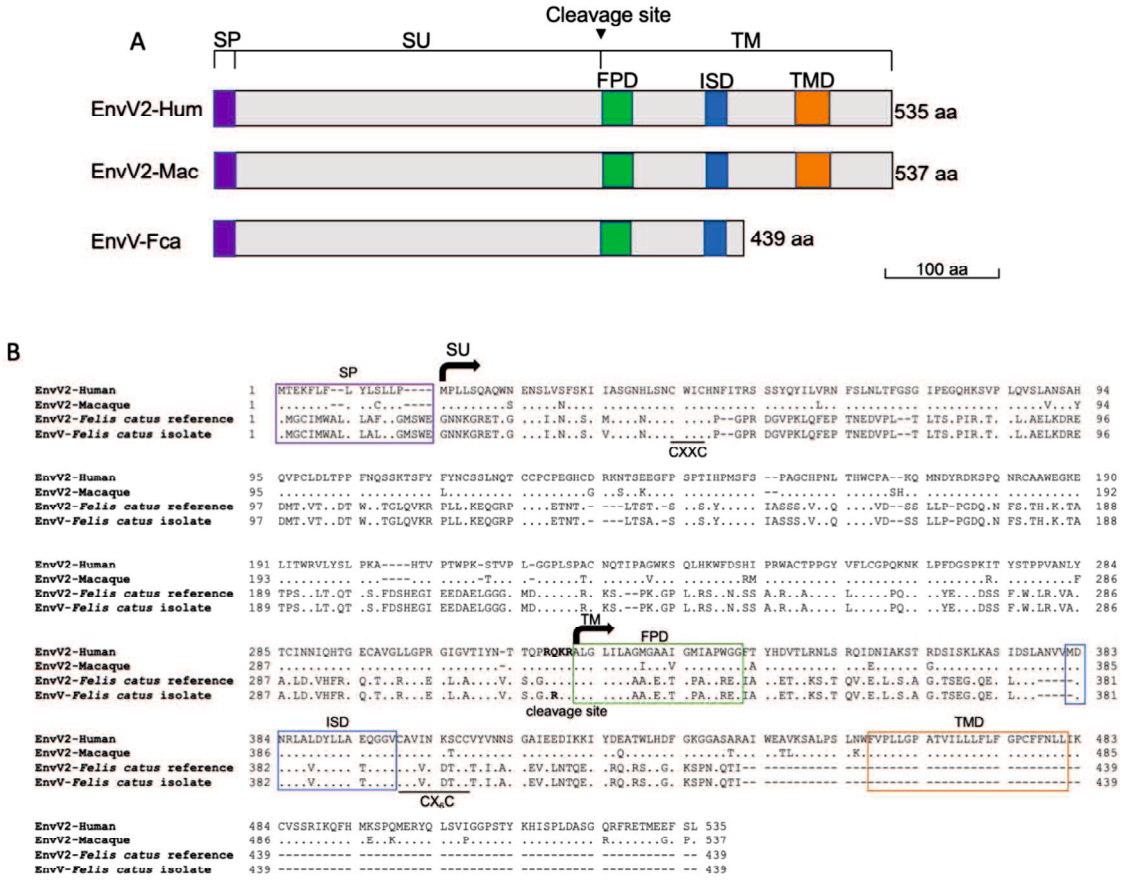

Figure 2.1 Structure schematic and amino acid alignment of EnvV-Fca.

(A) The schematic representation of the structure of EnvV-Fca, EnvV2-Hum, and EnvV2-Mac. The number of amino acids is indicated on the right. (B) Amino acid sequence alignment of the Env proteins of EnvV2-Hum, EnvV-Fca from the NCBI database (reference), and the isolate. SP, signal peptide; SU, surface unit; TM, transmembrane subunit; FPD, fusion peptide domain; ISD, immunosuppressive domain; TMD, trans-membrane domain; R-X-R/K-R is the cleavage motif; CXXC and CX6CC are sites of covalent interaction; EnvV-Fca, ERV group V member Env (EnvV) in *Felis catus*; EnvV2-Hum, EnvV2 in humans; EnvV2-Mac, EnvV2 in macaques

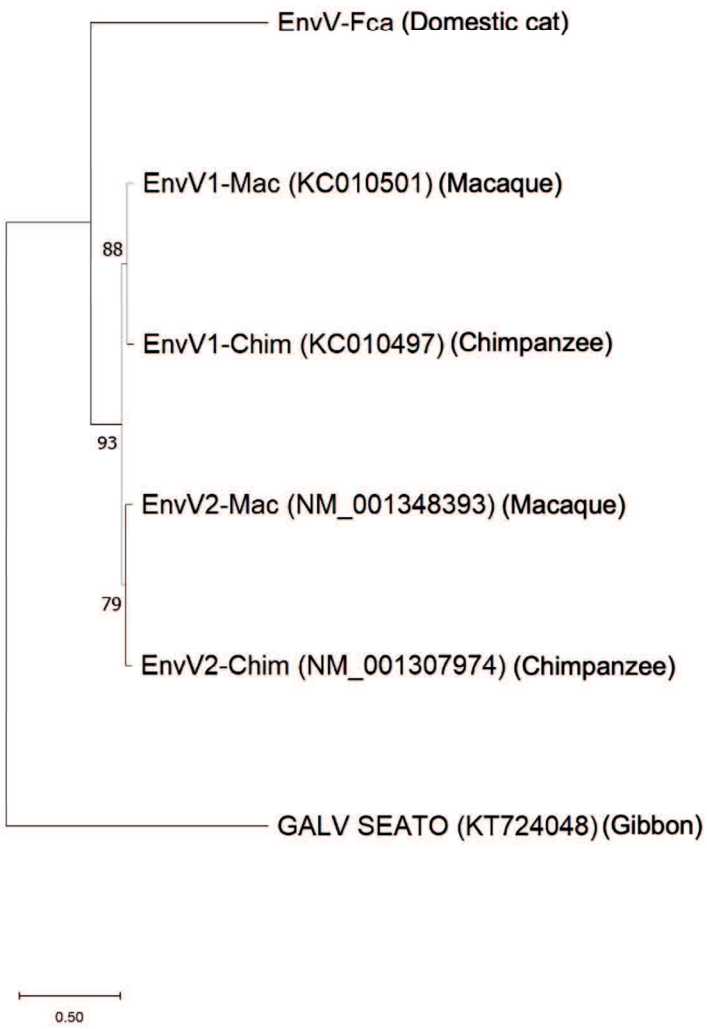

Figure 2.2 Phylogenetic tree EnvV-Fca comparing EnvV1 and EnvV2 of humans and primates. (A) The phylogenetic tree was constructed using the neighbor-joining method based on EnvV amino acid sequences. The length of the horizontal branches is the percentage of amino acid substitutions from the node (left scale bar), and the percentage bootstrap values from 1,000 replicates are indicated at the nodes.

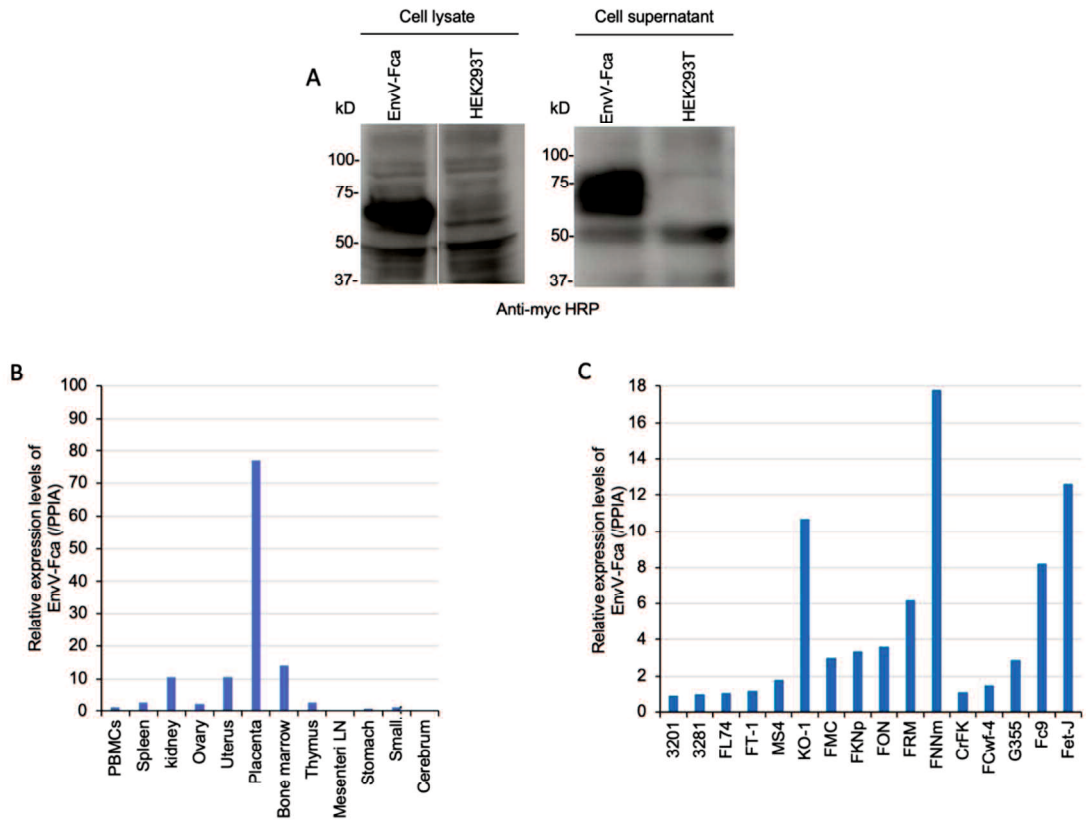

Figure 2.3 Expression of EnvV-Fca.

The presence of the EnvV-Fca protein was detected in the cell lysates (left) and supernatants (right) of HEK293T cells transfected with the indicated plasmids. (A) Detection of EnvV-Fca in cell lysate (left) and cell culture supernatant (right) by using an anti-Myc antibody. (B, C) EnvV-Fca expression was analyzed in feline tissues and cell lines. The EnvV-Fca transcripts were quantified using quantitative RT-PCR in feline tissues and cell lines. The x-axis represents the analyzed samples. The expression level on the y-axis is normalized to the expression of peptidylprolyl isomerase A (PPIA). The normalized expression in feline tissues and cell lines is shown as 1 in peripheral blood mononuclear cells (PBMCs). LN, lymph node

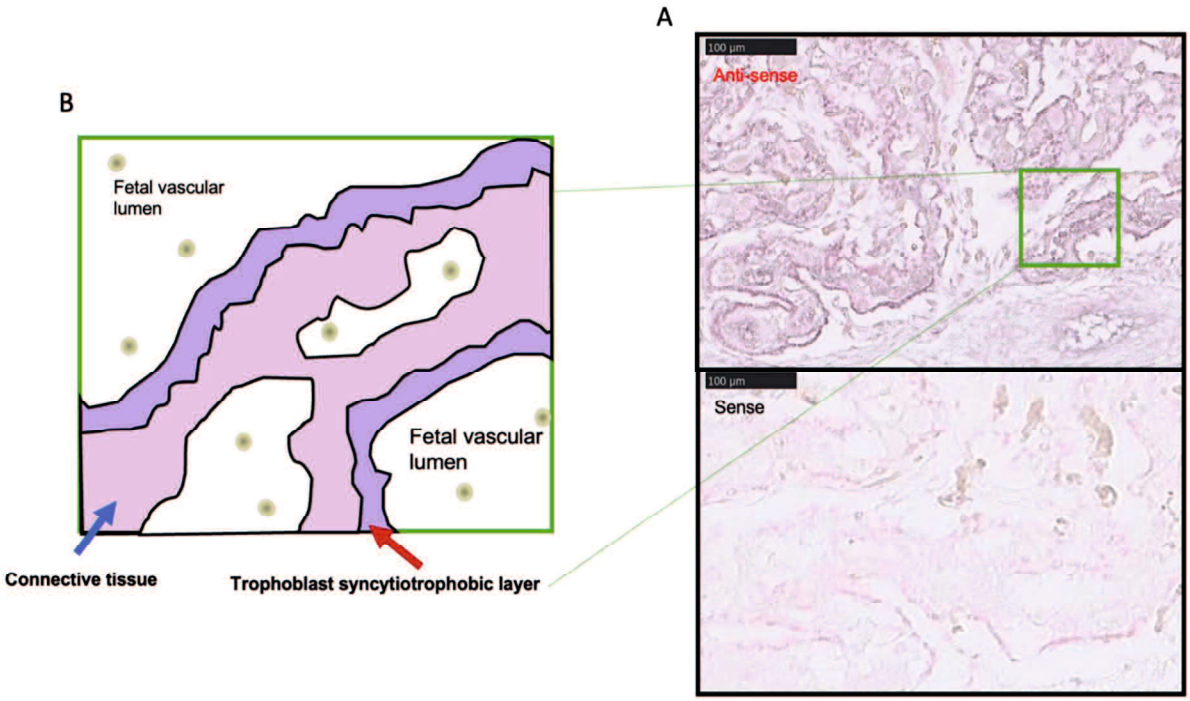

Figure 2.4 In situ hybridization analysis of EnvV-Fca in the placenta.

(A) Illustration of the cat placenta, which contains connective tissue, a fetal vascular lumen, and a trophoblast syncytiotropobic layer. (B) In situ hybridization was performed on placental sections using a digoxigenin-labeled anti-sense (upper) or sense probe (negative control; lower). The labeled syncytiotrophoblast was observed at a higher magnification. (Scale bars = 100 μm).

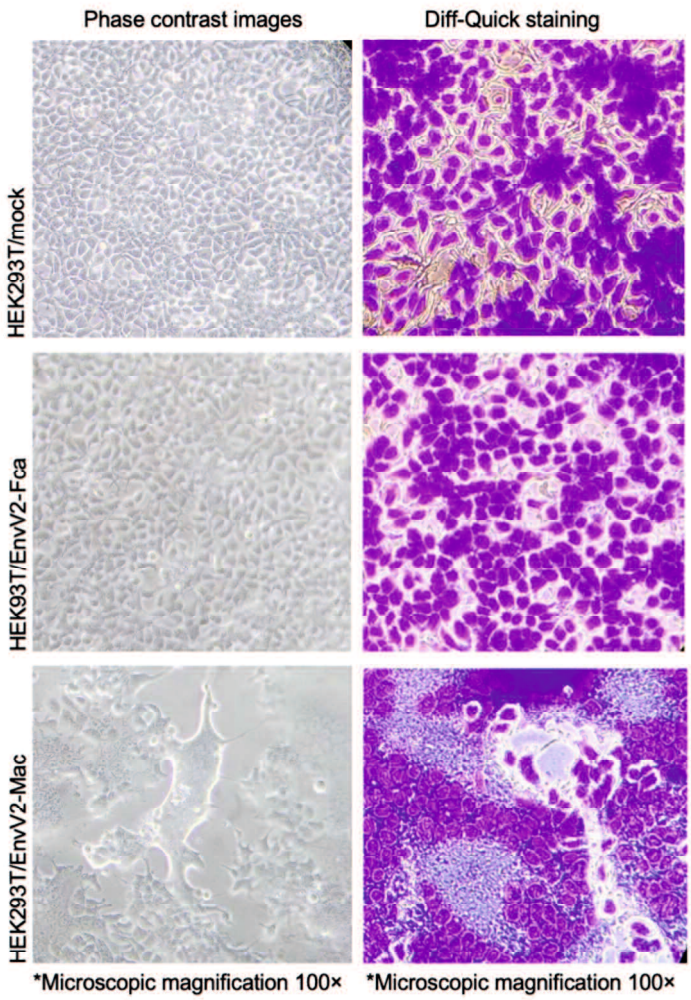

Figure 2.5. Functional assay of EnvV-Fca and EnvV2-Mac.

Morphology of HEK293T cells transfected with EnvV-Fca, EnvV2-Mac, and mock (empty vector). Images were obtained using optical microscopy, without staining (left) and after Diff-Quik staining (right) 24 h after transfection (microscopic magnification 10×)

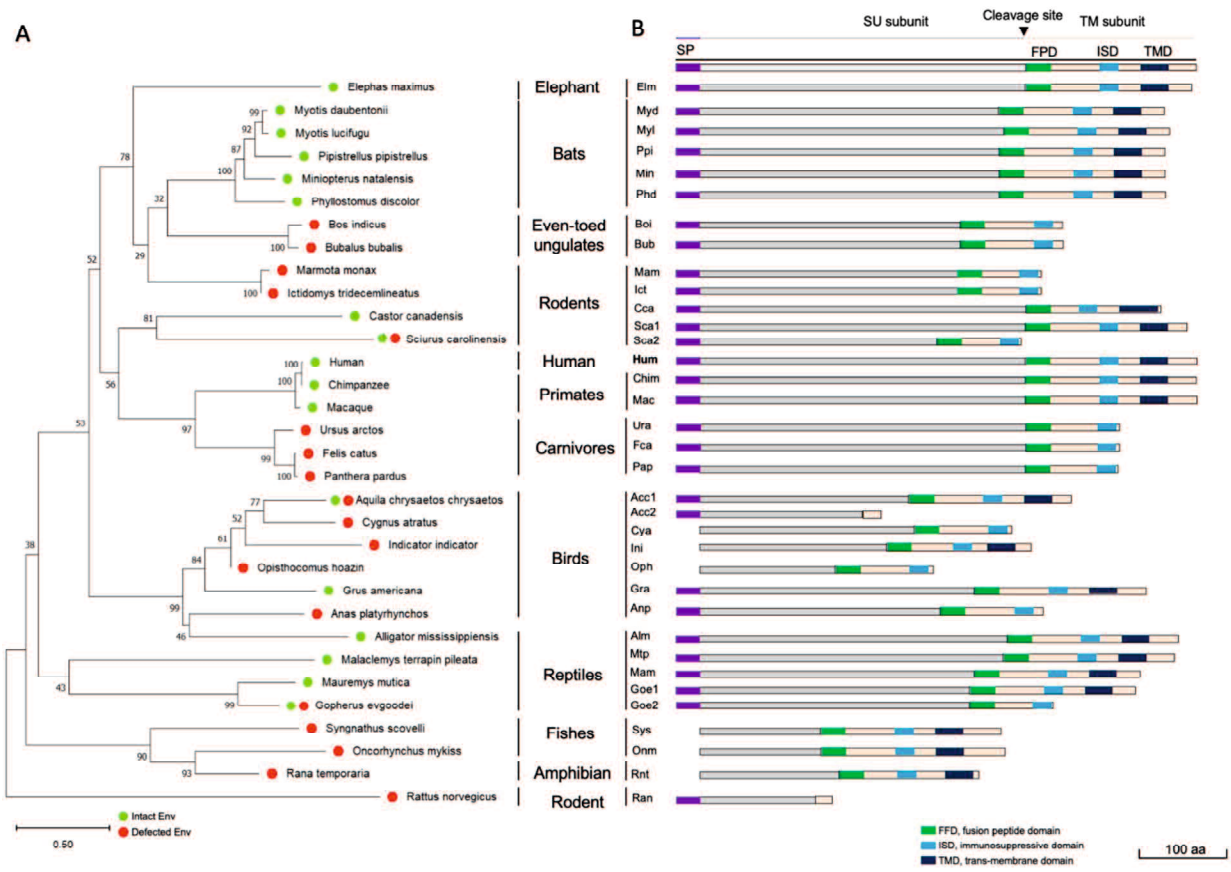

Figure 2.6. Phylogenetic tree and schematic of EnvV2 based on amino acids from mammalian and non-mammalian vertebrates.

(A) The phylogenetic tree was constructed using the neighbor-joining method based on EnvV2 amino acid sequences. The length of the horizontal branches is the percentage of amino acid substitutions from the node (left scale bar), and the percentage bootstrap values from 1,000 replicates are indicated at the nodes. (B) A schematic of EnvV2, which was classified based on amino acids from mammalian and non-mammalian vertebrates.

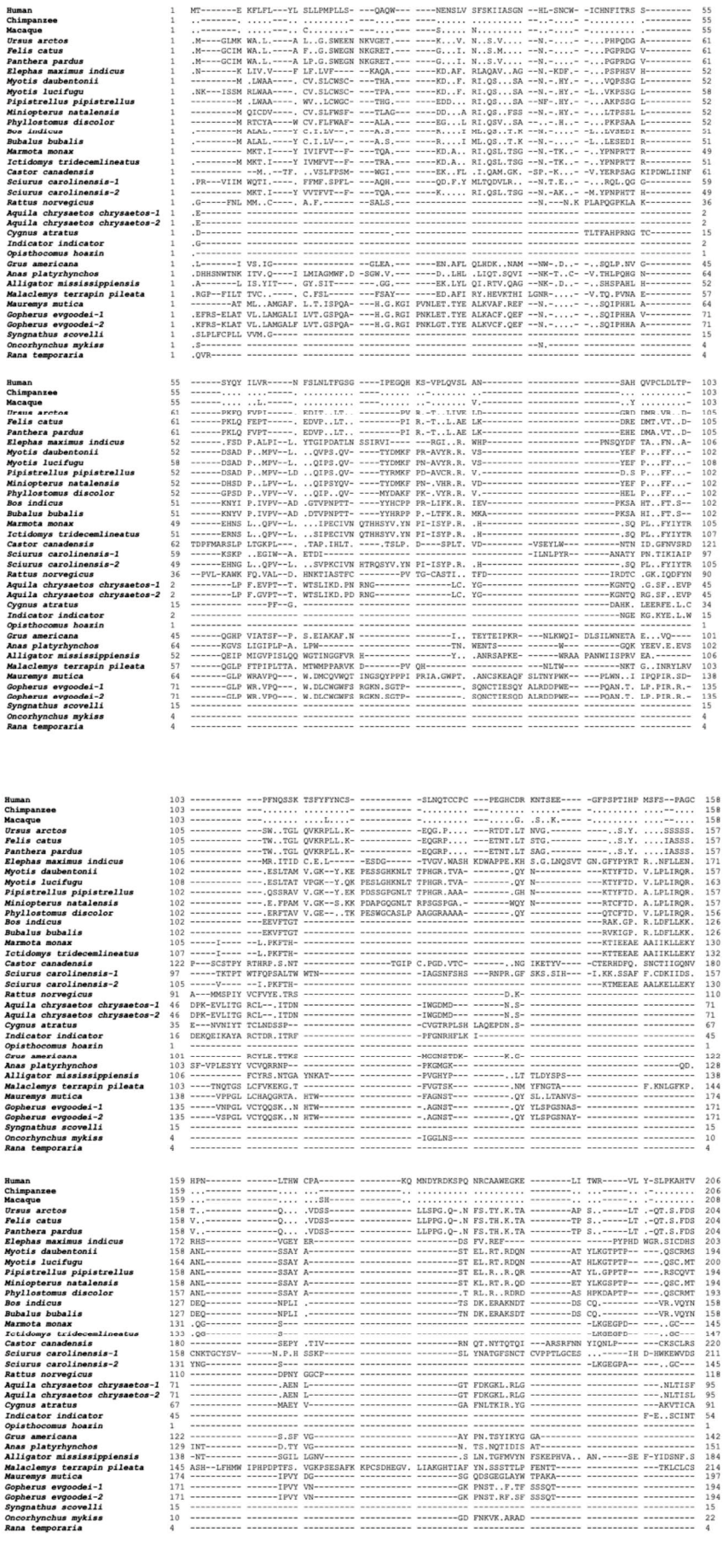

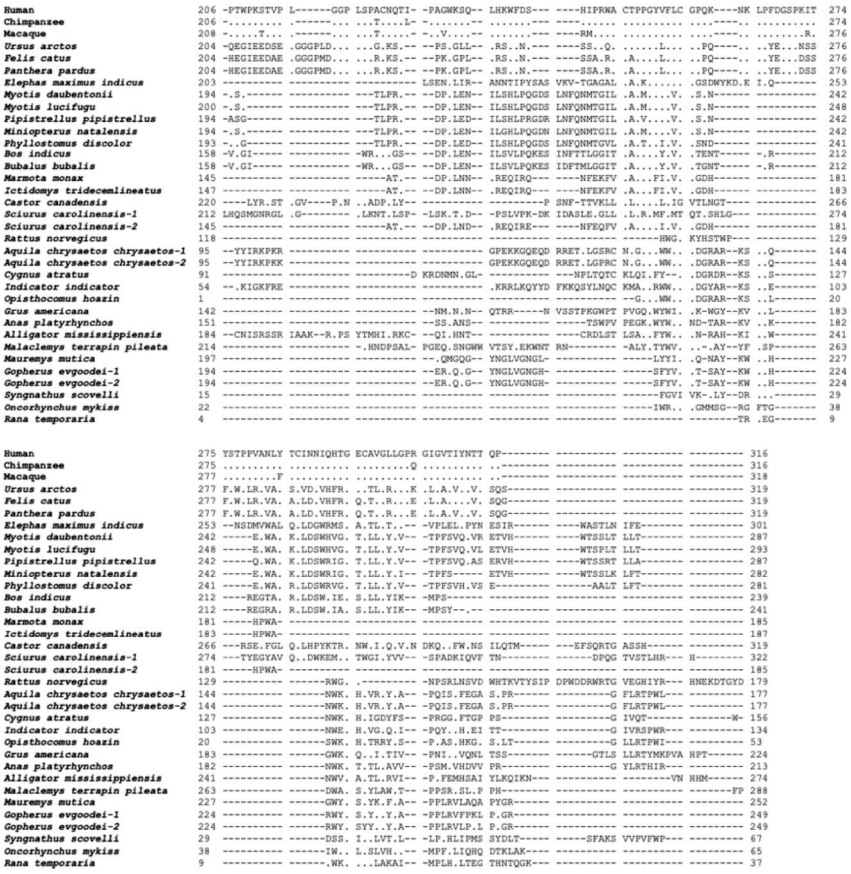

Figure 2.7 Alignment of SU subunit of EnvV2 among mammalian and non-mammalian

Alignment of the SU subunit of EnvV2 was constructed using MAFFT (33). SU, surface subunit

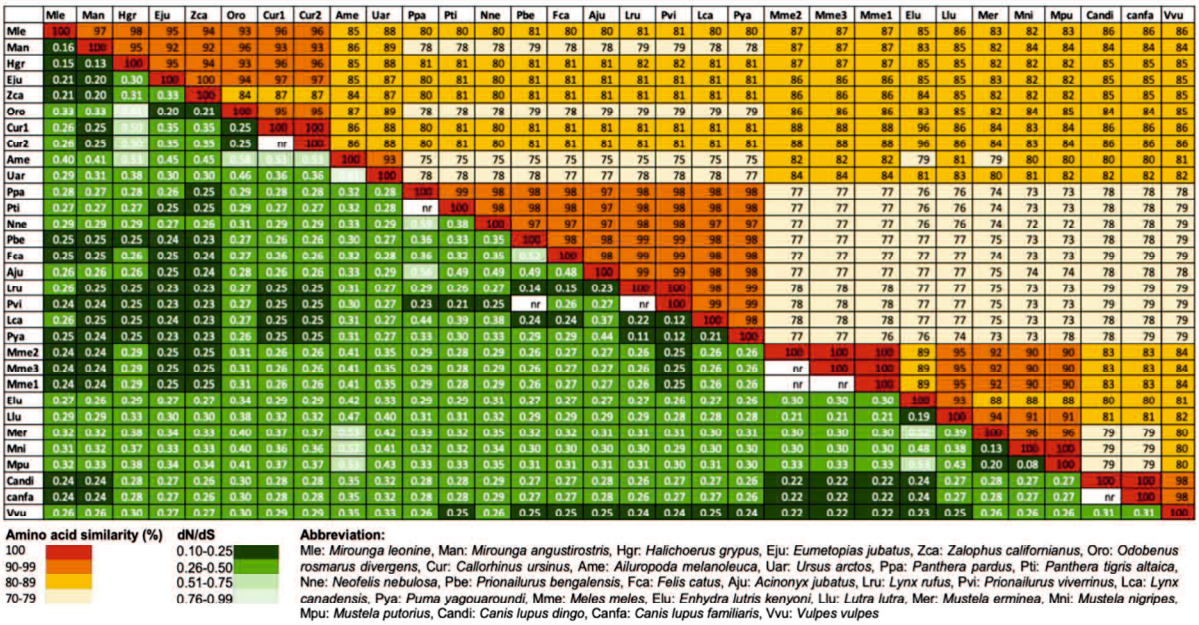

Figure 2.8 Sequence conservation and evidence for purifying selection of EnvV2 in Carnivora .

The table shows the pairwise percentages of amino acid sequence identity between EnvV2 and the indicated species in the upper triangular area, along with the non-synonymous/synonymous (dN/dS) rate. The pairwise Nei–Gojobori method (38) was used to construct the table. The n.r. code is due to the presence of only one or fewer dN and dS between species; n.r., relevant. Color codes are provided below the table for both series of values.

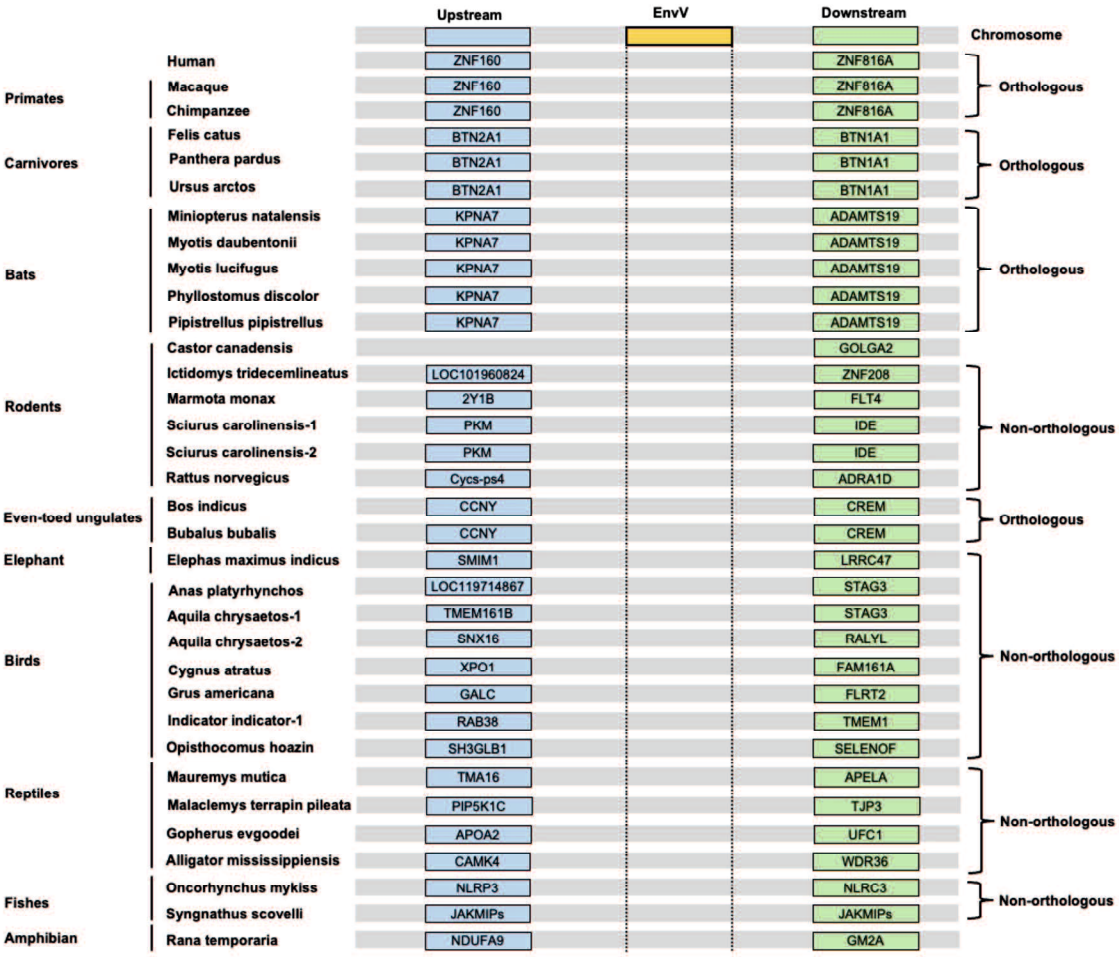

Figure 2.9 Schematic of location and conservation of EnvV2 in mammalian and non-mammalian genomes**.**

The figure illustrates the conservation of EnvV2 synteny in mammalian and non-mammalian genomes. The grey box represents the chromosome, the yellow box represents EnvV2, the light blue box represents the upstream gene, and the light green box represents the downstream gene. The conserved genes are shown inside the box.

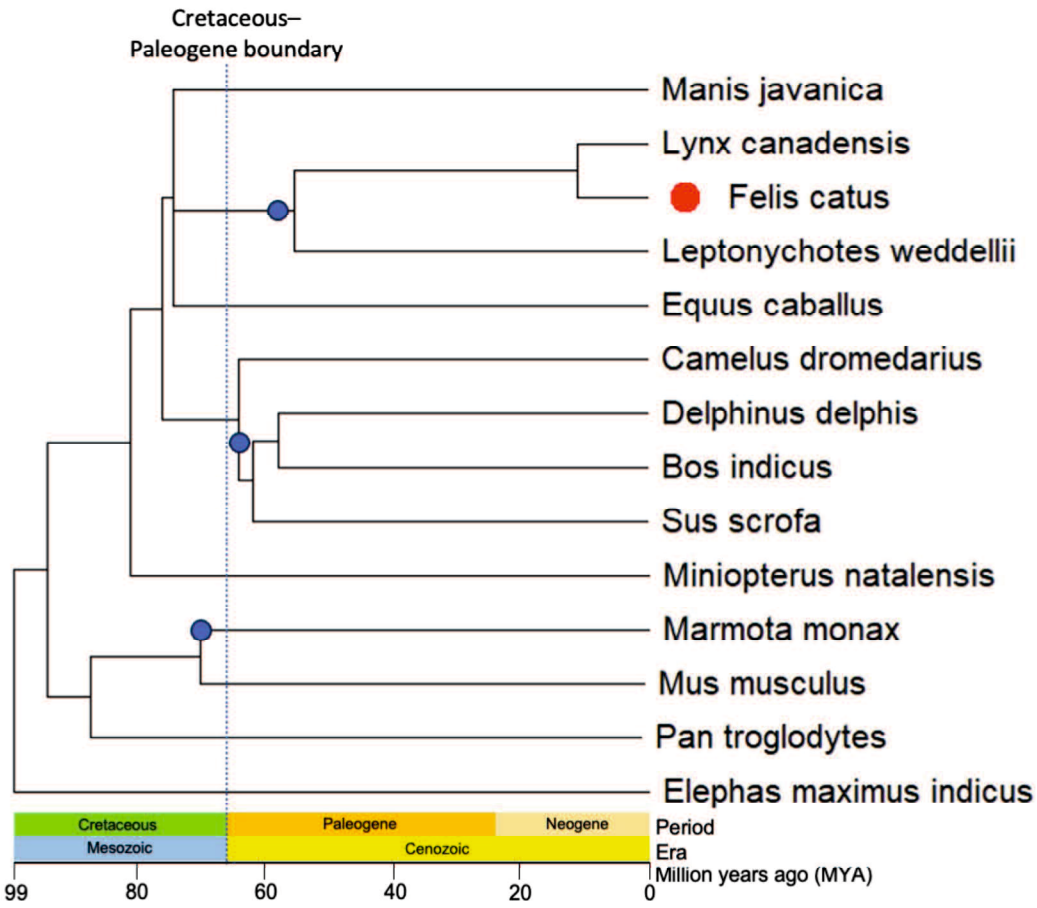

Figure 2.10 Evolution of ancient EnvV2 around the Cretaceous–Paleogene period in mammalian vertebrates.

(A) The cladogram illustrates the phylogenetic relationships among the indicated species belonging to mammalian vertebrates. The trees and divergence times were generated using TimeTree (44). Blue dots indicate the possible insertion of EnvV2 into the host genome. The bar scale indicates a million years ago (MYA).

3. CHAPTER THREE

Antiviral machinery evolution of the truncated envelope of koala retrovirus during endogenization.

This work will be published as follows:

Pramono D, Sakurai H, Miyake A, Kawasaki J, Nishigaki K.

3.1. ABSTRACT

Information on how koalas, gibbons, woolly monkeys, bats, and cats are infected with certain viruses is limited. We investigated the receptor usage of KoRV-A, KoRV-related retroviruses, and FeLV-B. Koala phosphate transporter (Pit) genes, Pit1 and Pit2, were transfected into Mus dunni fibroblast tail (MDTF) cells to establish cell lines expressing koala Pit1 (MDTF-koPit1) and koala Pit2 (MDTF-koPit2). koPit1, but not koPit2, was permissive to KoRV-A, woolly monkey virus, and FeLV-B infections. The Pit1 receptor may facilitate interspecies transmission of KoRV-related retroviruses. A KoRV-related search in public databases revealed the presence of endogenous KoRV (enKoRV) truncated envelope (env) genes, which were found to be expressed. KoRV truncated Env proteins inhibited the infection of KoRV-related viruses, including FeLV-B infection. Our findings imply that the evolutionary arms race between virus and koala has led to the emergence of viral resistance factors.

3.2. INTRODUCTION

Endogenous retroviruses (ERVs) are retroviral sequences that are transmitted to mammalian offspring and account for approximately 4–10% of their genome (4, 43-45) through repeated germline infections (46). Most ERVs are inactivated by mutations and produce non-infectious forms, with the resulting broken viral elements remaining in the host genome (47). Replication-competent ERVs are rare to find (49). However, the koala (*Phascolarctos cinereus*) and its retrovirus (KoRV) present a unique situation. KoRV is present in koala populations as both an exogenous and endogenous virus (31). It can be transmitted both vertically (from parent to offspring) and horizontally (from one animal to another) (32-34). Forms of horizontal transmission are poorly defined but likely require close contact (34). Eleven subtypes of KoRV (A–K) have been isolated and classified based on sequence variations in the receptor-binding

domain of the envelope gene, specifically in the hypervariable region (35). KoRV is a major infectious agent that affects the health of koala populations in both natural and captive environments (36, 37). It has also been associated with neoplastic diseases, including lymphoma and leukemia, leading to high mortality rates (37-39). Evidence of its immunosuppressive potential has been observed *in vitro* (40) but it is limited *in vivo*. KoRV provirus has been reported to circulate in 100% of koala populations in northern Australia, while koala populations in southern Australia are only partially infected. Some rare populations appear to be free of KoRV (35, 42). Based on the analysis of its LTRs, the koala was probably infected with KoRV approximately 22,20049,900 years ago. However, infection dates may go back to a much earlier period, highlighting the ongoing endogenization that is occurring in the Australian koala population(138). However, it is unknown whether endogenous KoRV serves as a functional molecule for the host.

KoRV and gibbon ape leukemia virus (GALV) are closely related *Gammaretroviruses* (139). There is limited information on how koalas, gibbons, woolly monkeys, bats, and cats are infected with these viruses as the habitats of the viral hosts, koalas in Australia and gibbons in Southeast Asia, do not overlap and are physically separated by an oceanic faunal boundary known as the Wallace line. However, the viruses likely originated from cross-species transmission of an ancestral retrovirus into koalas and gibbons via intermediate hosts, possibly rodents, based on the identification of a fragment of *Melomys burtoni* retrovirus in rats (140). Recently, bats have also been suggested as possible intermediate hosts after a novel reproduction-competent bat retrovirus, the Hervey pteropid gammaretrovirus (HPG), was identified and characterized in bats, *Pteropus alecto*. Several locations across northeastern Australia have been found to contain HPG- and KoRV-related sequences (30). Previous studies have demonstrated that KoRV uses the phosphate transporter 1 (Pit1) ortholog in rats (141), humans (139), felines (142), hamsters, bovines (29), and minks (143), which can be infected

in vitro, although mice cannot (143). KoRV-A is closely associated with GaLV, HPG, and woolly monkey virus (WMV) (30, 144), which belong to the same interference group and infect cells via the same receptors (30, 37). Additionally, WMV has been reported to use Pit1, possibly because of the horizontal transmission of GaLV from a gibbon (144). In addition, Feline leukemia virus subgroup B (FeLV-B) use both Pit1 and Pit2 as receptors for infection (10, 27) and can infect domestic and wild cats (Florida panthers) (96). Interference assays are based on the principle that when a virus is productively infected, it blocks access to all viruses that use the same receptor to enter cells (145). Retroviruses have traditionally been classified into same or different receptor classes based on their super-infection capabilities (146). However, the identification of Pit1 molecules in koalas as KoRV-A receptors is yet to be established.

Recently, the env gene derived from ERVs (env-ERV), has attracted considerable attention with respect to its potential role in ERV function. The presence of some ERV Envelope (Env) proteins may be indicative of an evolutionary role in the immunological response, specifically in the restriction of exogenous retroviruses (8, 59). Previous investigations have identified an env-ERV gene that is known to exhibit restrictive activity against retroviruses in mice (Fv4, Rmcf, and Rmcf2), sheep (enjS56A1), cats (Refrex-1 and FeLIX), and humans (Suppressyn) (8, 58-61, 147). In general, exogenous retrovirus infection uses envelope protein to bind to the receptors on the host cell surface and mediate virus–cell fusion and entry (148). In line with this, the antiviral mechanism of env-ERV genes is predicted to be their ability to block the entry of exogenous retroviruses into host cells, which has been proposed to be restricted by receptor interference. Env-ERV proteins compete with exogenous retroviral Env proteins for binding to these receptors, thus blocking viral entry and infection (8, 58, 59, 62, 147). We hypothesized that the restriction phenomenon may include env-ERV in the koala genome, which can protect against modern viruses, including KoRV-related viruses. Nevertheless, the interaction between enKoRV Env and KoRV-A infection remains largely unknown. Therefore, this study aimed to

explore the evolutionary arms race between the virus and koala, focusing on the emergence of viral resistance factors. In addition, we also investigated whether koala Pit1 (koPit1) and koPit2 are the KoRV-A receptors for infection.

3.3. MATERIALS AND METHODS

3.3.1. Koala samples

A female koala (*Phascolarctos cinereus*), aged approximately 8 years—born on November 19, 2014, and died on October 14, 2022 was obtained from Hirakawa Zoo in Kagoshima, Japan, and an autopsy was performed. The tissues of the koalas were stored at -80 °C until the extraction of DNA or RNA for further analysis.

3.3.2. Isolation of koPit1 and koPit2 and construction of the expression vector

Total RNA was isolated from the koala spleen and liver using the RNeasy kit (Qiagen, Hilden, Germany), and the extracted RNA was treated with recombinant DNase I (RNase-free; Takara, Shiga, Japan). Complementary DNA (cDNA) was synthesized using the PrimeScript II First-Strand cDNA Synthesis Kit (TaKaRa, Shiga, Japan) with oligo(dT) primers. The koPit1 cDNA was amplified (based on the predicted DNA sequences of koPit1 and koPit2) by nested PCR using the first primer pair, Fe-817S and Fe-839R, and the second primer pair, Fe-815S and Fe-837R. The koPit2 cDNA was amplified by nested PCR using the first primer pair, Fe-818S and Fe-840R, and the second primer pair, Fe-816S and Fe-838R (Table 3.1). PCR products were digested with BamH1 for koPit1 and with *Eco*R1 and *Bgl*II for koPit2, and each fragment was inserted into the pMSCVneo retroviral vector (TaKaRa). KOD-ONE Blue (Toyobo, Osaka, Japan) polymerase was used for the various PCRs according to the manufacturer's instructions. The resulting plasmids were confirmed by sequencing (Fasmac Corporation, Atsugi, Japan).

3.3.3. Cell lines

Cells were cultured in Dulbecco's modified Eagle's medium (FUJIFILM Wako Pure Chemical Corporation, Osaka, Japan) supplemented with 10% fetal calf serum and 1X penicillin-streptomycin. They were incubated in a CO_2 incubator at 37 °C. In this study, we used the following cell lines: *Mus dunni* fibroblast tail (MDTF) cells (74) and GPLac (an *env*-negative packaging cell line containing the murine leukemia virus (MuLV) *gag-pol* gene and beta-galactosidase (LacZ)-coding pMXs retroviral vector) (49). MDTF cells expressing koPit1 (MDTF-koPit1) and koPit2 (MDTF-koPit2) were established.

3.3.4. Establishment of cell lines expressing koPit1, and koPit2

PLAT-A (amphotropic MuLV) packaging cells were transfected with expression vectors (pMSCVneo-koPit1, pMSCVneo-koPit2, or pMSCVneo empty vector) using the TransIT®-293 reagent (Takara). Two days later, the supernatants were collected, filtered through a 0.22-μm filter, and then used to inoculate MDTF cells in the presence of polybrene (10 μg/mL; Nakarai). The cells were cultured in a medium containing 600 μg/mL neomycin (G418) for 2 weeks. These cells were termed MDTF-koPit1, MDTF-koPit2, and MDTF-empty for further analyses.

3.3.5. Env-pseudotyped virus preparation

The method for preparing Env-pseudotyped viruses carrying LacZ as a marker has been previously described (49). Briefly, GPLac cells were seeded at a concentration of approximately 1×10^6 cells in a six-well plate one day prior to transfection. The Env expression plasmids used for viral preparation were pFUΔss GaLV Env (147), pFUΔss KoRV Env (opt-KoRV-A2), pFUΔss HPG Env (opt-HPG) (147), pFUΔss FeLV-B/GA, pFUΔss FeLV-B/ON-T, pFUΔss FeLV-B/MZ40-5B, pFUΔss FeLV-B/KG20-5B, pFUΔss FeLV-B/FO36-5B (49), and

pFUΔss FeLV-A/clone33 (80). The *env* genes of opt-KoRV-A2 env, opt-HPG, and opt-WMV env were synthesized by Eurofins Genomics (Tokyo, Japan) (147). The KoRV Env, HPG Env, and WMV env genes were myc-tagged at the C-terminus and inserted into the pFUΔss vector. The original WMV Env sequence without valine (V; accession number: AF055064) did not indicate infection. WMV V655 was reconstructed by inserting a valine (V) amino acid at position 655 (Table 3.2). The GaLV Env was PCR-amplified from PG13 cells (44) and cloned into the pFUΔss vector. The culture supernatants were collected 48 h after transfection using TransIT-293 transfection reagent, then filtered through a 0.22-μm filter or centrifuged at 15,400 ×*g* for 2 min at 4 °C and stored at -80 °C as virus stock for further experiments.

3.3.6. Infection assay

Target cells were seeded at a concentration of 1–3 × 10^4 cells in 24-well plates one day prior to infection. The cells were infected with 250 μL of Env-pseudotyped virus each, in the presence of 10 μg/mL of Polybrene (Nacalai Tesque, Kyoto, Japan) for 2 h. After the addition of fresh medium, the cells were cultured for 2 days post-infection. After incubation for 48 h, the supernatants were removed, and the cells were fixed with 250 μL of 2% glutaraldehyde for 15 min at room temperature (20–25 °C). The cells were then stained with 5-bromo-4-chloro-3-indolyl-β-D-galactopyranoside and those with blue-stained nuclei were counted under a microscope. Viral titers were presented as infectious units (IU) per milliliter with standard deviations. MDTF cells expressing only the vector were used as a negative control.

3.3.7. Quantification of expression levels and retrieval of candidate truncated Env KoRV from public database

To identify enKoRV-related sequences in the koala, we conducted RNA-seq analysis using publicly available RNA-seq data from the National Center for Biotechnology Information (GSM3665253, GSM3665254, GSM3665255, GSM3665256, GSM3665257, GSM3665258,

GSM3665259, and GSM3665260). The RNA-seq data were downloaded from the NCBI Sequence Read Archive (SRA) database (149) using fasterq-dump (version 2.10.0; https://github.com/ncbi/sra-tools) and preprocessed with fastp (version 0.20.1) (150) using the options "-w 4," "-y -3," and "-x." The expression levels were calculated as transcripts per million (TPM) using the formula: $TPM = RPKM / \sum(RPKM) \times 10^6$. Reads per kilobase of exon per million mapped reads (RPKM) were calculated using featureCounts (version 2.0.1) (151). Mapped patterns of RNA-seq reads were visualized using IGV (version 2.9.4) (152). Due to the limited availability of RNA-seq data, we only investigated expression levels in the following tissues: testis, brain, and liver from two individual koalas. For further experiments, we selected suitable truncated Env candidates with amino acid sizes between 200 and 400 and high expression levels.

3.3.8. Construction of truncated Env expression vectors

The expression vector pFUΔss was utilized for the construction of truncated Env KoRV expression plasmids. The truncated *env* gene was constructed based on pFUΔss KoRV-A1 via single or multiple site-directed mutagenesis, owing to its high similarity with KoRV-A (LC033970) (58). Trunc-ko1 used first, the primer Fe-802S and Fe-820R; second, Fe-803S and Fe-821R. Trunc-ko2 used first, Fe-802S and Fe-820R; second, Fe-804S and Fe-822R; third, Fe-805S and Fe-823R; fourth Fe-814S and Fe-832R. Trunc-ko3 used first, Fe-802S and Fe-820R; second, Fe-805S and Fe-823R; third, Fe-814S and Fe-833R. Trunc-ko4 used first, Fe-802S and Fe-820R; second, Fe-804S and Fe-822R; third, Fe-814S and Fe-833R. Trunc-ko5 used first, Fe-802S and Fe-820R; second, Fe-806S and Fe-824R; third, Fe-814S and Fe-834R (Table 3.1). Next, positive control for this experiment were constructed by having a minimal structure containing receptor-binding domain (RBD). We constructed 3 series truncated Envs of KoRV-A which has lengths 251, 279, and 303 aa and term as RBD-1, RBD-2, and RBD-3,

respectively. RBD-1 was constructed by using primer pair, Fe-814S and Fe-851R. RBD-2 used Fe-814S and Fe-852R and RBD-3 used Fe-814S and Fe-853R. Following the completion of the multiple site-directed mutagenesis and construction, each plasmid was digested using the appropriate restriction enzymes (BamH1 and EcoR1) and cloned into the pFUΔss expression plasmid. The resulting plasmids were confirmed using sequencing (Fasmac Corporation).

3.3.9. Viral inhibition assay in the presence of truncated Env proteins

MDTF-koPit1 cells were seeded at a concentration of approximately 1×10^6 cells in a six-well plate 1 day prior to transfection with truncated Env expression plasmids. The supernatants of HEK293T cells transfected with pFUΔss truncated Env proteins (Trunc-ko1, Trunc-ko2, Trunc-ko3, Trunc-ko4, and Trunc-ko5) and pFUΔss empty vector (negative control) for approximately 48 h were used as the source of truncated Env proteins. The inhibition assay was conducted as previously described in the "infection assay section" with modifications. In 24-well plates, target cells were treated with 250 µL of cell supernatant (source of truncated Env protein) for 2 h. Subsequently, 250 µL of Env-pseudotyped viruses were inoculated into the target cells with 10 µg/mL polybrene for 2 h, after which 250 µL of fresh medium was added. Two days post infection, the cells were stained with X-Gal. Single-cycle infectivity was determined by counting blue-stained nuclei under a microscope. IU per milliliter and standard deviations were used to represent the viral titers.

3.3.10. Immunoprecipitation and immunoblotting

Plasmids were introduced into HEK293T cells in six-well plates using the TransIT®-293 reagent (Takara). Two days after transfection, cell pellets were collected by washing with phosphate-buffered saline three times. Cells were resuspended in lysis buffer (20 mM Tris-HCl [pH 7.5], 150 mM NaCl, 10% glycerol, 1% Triton X-100, 2 mM EDTA, 1 mM Na_3VO_4, and

1 μg/mL each of aprotinin and leupeptin) to prepare cell lysates, which were then incubated for 20 min on ice. Top-speed centrifugation (15,400 ×*g*) for 20 min at 4 °C was used to remove the insoluble components, and a protein assay kit (Bio-Rad Laboratories, Carlsbad, CA, USA) was used to determine the protein concentrations.

Cell supernatants were filtered through a 0.22 μm filter and incubated overnight at 4 °C with the desired antibody. The purified protein (cell lysate and supernatant) was mixed with sample buffer solution (Nacalai Tesque) and heated at 95–100 °C for 5 min. Sodium dodecyl sulfate-polyacrylamide gel electrophoresis was conducted using 4–20% gels (Invitrogen, Carlsbad, CA, USA) at 100 V for 2 h, and the sample was then transferred to nitrocellulose filters for western blotting. The following primary antibodies were used in the assays: anti-Myc monoclonal antibody conjugated with horseradish peroxidase (FUJIFILM Wako Pure Chemical Corporation; dilution 1:1,000). The substrate used was LumiGLO® Reagent (20×) and 20X peroxide (Cell Signaling Technology). For imaging, the blots were developed using Amersham ImageQuant 800 (Cytiva, Shinjuku, Japan).

3.3.11. Phylogenetic and sequencing analysis

A tree was constructed using the sequences listed in the accession numbers section. MUSCLE was used to align the amino acid sequences for phylogenetic analysis (88). All other procedures were performed using the MEGA11 software package (52). For the phylogenetic analysis of Pit1, Pit2, and related proteins of *Gammaretrovirus* receptors, the neighbor-joining method (153) was employed to construct a phylogenetic tree with amino acid substitutions in the JTT model (123). The Maximum Likelihood method with the LG+G model based on the lowest Bayesian Information Criterion score was used for the phylogenetic analysis of KoRV-related viruses (89). The robustness of the trees was evaluated by bootstrapping 1,000 times (124).

3.3.12. Accession numbers

The accession numbers for publicly available data used in this study are as follows: *Felis catus* ASCT1 (NM_001278844), human ASCT1 (NM_001193493), *Felis catus* ASCT2 (XM_045045413), human ASCT2 (NM_001145144), *Felis catus* FLVCR1 (NM_001009302), human FLVCR1 (NM_014053), *Felis catus* FLVCR2 (XM_045060279), human FLVCR2 (NM_001195283), *Felis catus* RFC (XM_023238625), human RFC (NM_001205206), *Felis catus* THTR1 (NM_001039956), human THTR1 (NM_001319667), *Felis catus* THTR2 (NM_001278820), human THTR2 (NM_001371411), mouse CAT (NM_001301424), human CAT (NM_003045), human CTR1 (NM_001859), feline CTR1 (LC705724), koala Pit1 (XM_020963641), gibbon Pit1 (XM_032176718), rat Pit1 (NM_031148), mouse Pit1 (NM_015747), human Pit1 (NM_005415), *Gracilinanus agilis* Pit1 (XM_044663086), *Monodelphis domestica* Pit1 (XM_007477569), *Vombatus ursinus* Pit1(XM_027861243), koala Pit2 (XM_020969564), gibbon Pit2 (XM_032143780), rat Pit2 (NM_017223), mouse Pit2 (NM_001424901), human Pit2 (NM_001257180), *Gracilinanus agilis* Pit2 (XM_044663538), *Monodelphis domestica* Pit2 (XM_007476407), and *Vombatus ursinus* Pit2 (XM_027865172). The sequences from the isolated sample described in this paper have been deposited in DDBJ/EMBL/GenBank under the accession number LC817414 and LC817415.

3.4. RESULTS

3.4.1. Isolation and characterization of koPit1 and koPit2

Pit1 and Pit2 are members of the solute carrier protein family SLC20A1 and SLC20A2, respectively. The koPit1 and koPit2 have not been previously isolated. Therefore, we first searched for predictions of koPit1 and koPit2 in the NCBI koala genome database (GCF_002099425.1). Next, we isolated koala cDNA from koala spleen using RT-PCR. Molecular cloning of the PCR-positive samples was carried out to obtain koPit1 and koPit2

open reading frames. There were no differences between our isolates (spleen) and the predictions for koPit1 and koPit2 in the database; koPit1 and koPit2 were predicted to encode proteins with 683 and 654 amino acids, respectively, and the amino acid sequences of their respective proteins were found to have approximately 89.1% similarity. Alignments of the amino acid sequences of the proteins encoded by the isolated koPit1 and koPit2 with several mammalian Pit1 and Pit2 sequences are shown in Figures 3.1 and 3.2, respectively. Next, we conducted phylogenetic analysis of the koPit1 and koPit2 sequences. Our koPit1 and koPit2 clones were compared to related sequences, such as those of *Gammaretrovirus* group receptors, and found that koPit1 and koPit2 receptors are distinguishable from other previously identified receptors (Figure 3.3A).

3.4.2. Functional evaluation of koPit1 and koPit2 in retroviral infection

To evaluate the functions of koPit1 and koPit2 in retroviral infection, MDTF cells that were not susceptible to KoRV infection were transfected with pMSCVneo/koPit1 and pMSCVneo/koPit2 to establish MDTF-koPit1 and MDTF-koPit2 cells, respectively. Subsequently, MDTF-koPit1 and MDTF-koPit2 cells were tested for infection with KoRV-A, and the analysis was extended to several mammalian retroviruses, including GaLV, HPG, WMV, and FeLV-B (GA, MZ-40, KG20, FO36, and ON-T strains, respectively) Env-pseudotyped viruses. This was due to their genetic similarity (Figure 3.3B) and receptor usage, as reported previously (22, 27). The results showed that MDTF-koPit1 cells were permissive to all these viruses. Notably, the original WMV Env strain did not confer any infection. Analysis of the amino acid sequence revealed a valine (V) deletion at position 655; therefore, we constructed WMV V655 and confirmed the infection. The viral titers for KoRV-related viruses were mostly similar, ranging from 5,000 to 10,000 IU/mL. Notably, KoRV-A showed higher viral titers compared with those of GaLV, HPG, and WMV V655. Cells with koPit1 were highly

permissive for the FeLV-B Env-pseudotyped viruses. Notably, MDTF-koPit2 cells were only permissive to GaLV and HPG but showed lower titers compared to MDTF-koPit1 cells. In contrast, MDTF-koPit2 cells were not infected with KoRV-A, WMV V655, or FeLV-B Env-pseudotyped viruses. MDTF cells expressing only the vector as a negative control were not infected with any of the Env-pseudotyped viruses (Figure 3.4). Taken together, our results suggest that KoRV-A, WMV V655, and FeLV-B use only koPit1, whereas GaLV and HPG can use both koPit1 and koPit2 for infection.

3.4.3. Expression of koPit1 and koPit2

The koPit1 and koPit2 levels were also investigated using publicly available RNA-sequencing (RNA-seq) data collected from koala. The expression was detected in the testis, brain, and liver. As the RNA-seq data was incomplete, the expression levels in other tissues could not be evaluated. These results suggest that koPit1 and koPit2 are expressed in koalas.

3.4.4. enKoRV-derived truncated Env proteins

The interaction between KoRV infection and enKoRV Env remains poorly understood, and the functional analysis of enKoRV truncated Env has not been conducted. Therefore, in this study, we searched for candidates of enKoRV-derived truncated Env proteins in publicly available data. Sequence analysis revealed the existence of five truncated Env proteins, namely Trunc-ko1 through Trunc-ko5, with lengths ranging from 200 to 400 amino acids (aa; Figure 3.5A). All five truncated Env proteins contain a putative signal peptide, a defective surface subunit (SU), and lack a transmembrane subunit (TM). In detail, Trunc-ko1 has 289 aa with 9 aa mutations compared with KoRV-A (LC033970) as a reference. Trunc-ko2 has 294 aa with 14 aa mutations. Trunc-ko3 has 316 aa with 24 aa mutations. Trunc-ko4 has 316 aa with 36 aa mutations. Trunc-ko5 has 376 aa with 40 aa mutations (Figure 3.5A).

3.4.5. Truncated Envs derived from enKoRV expressions

During the analysis of the candidate truncated Env, we also investigated the expression levels using publicly available RNA-seq data collected from koalas. Truncated Env expression was detected in the testis, brain, and liver. However, we could not evaluate the expression levels in other tissues due to the unavailability of RNA-seq data. Next, we determined the expression of truncated Env proteins as soluble proteins from cells. The supernatants of HEK293T cells transfected with truncated Env protein expression plasmids were immunoprecipitated using an anti-Myc antibody, and western blot analysis was conducted using the same antibody (Figure 3.5B and 3.5C). Overall, the results showed that these proteins were present in the cell supernatants, suggesting that Trunc-ko1, Trunc-ko2, Trunc-ko3, Trunc-ko4, and Trunc-ko5 are secreted from cells as soluble proteins.

3.4.6. enKoRV-derived truncated Env proteins blocked KoRV-related viral infection

Next, we investigated whether truncated Env proteins derived from enKoRV exhibited antiviral activity, which benefits the host. HEK293T cells were transfected with each expression plasmid, and the supernatants were collected as sources of truncated Env proteins. Truncated Env proteins (Trunc-ko1, Trunc-ko2, Trunc-ko3, Trunc-ko4, and Trunc-ko5) were assessed for their inhibitory effects on KoRV-related Env-pseudotyped viruses (KoRV-A, GaLV, HPG, and WMV V665) in MDTF-koPit1 cells. The target cells were treated with the truncated Env proteins for 2 h. Subsequently, pseudotyped viruses were infected into target cells for infection analysis 2 days later. Trunc-ko1, Trunc-ko3, and Trunc-ko4 significantly ($p < 0.05$) inhibited infection by all KoRV-related Env-pseudotyped viruses (Figure 3.5D). Trunc-ko2 inhibited KoRV-A, HPG, and WMV ($p < 0.05$) but not GaLV infection. Trunc-ko5 did not show any inhibition against any KoRV-related viruses. Notably, the inhibitory effect of all truncated Env

proteins was more sensitive to WMV infections, whereas no such effect was observed in the mock control. Collectively, truncated Env proteins blocked the infection of KoRV-related viruses via koPit1 but not koPit2, although the inhibition was partial.

Next, we investigated the reason why the aforementioned inhibitory effect does not completely block infections. Existing studies have revealed that truncated Env could inhibit infection by having a minimal structure containing RBD and a length ranging from 250 to 279 aa (35, 38). To test this, we constructed three series of truncated Env proteins from KoRV-A, with lengths of 251, 279, and 303 aa, and named them RBD-1, RBD-2, and RBD-3, respectively. Subsequently, we evaluated the inhibitory effect of RBD-1, RBD-2, and RBD-3 on KoRV-A infection in MDTF-koPit1 cells. The results showed that RBD-1, RBD-2, and RBD-3 significantly inhibited KoRV-A infections ($p < 0.05$; Figure 3.5E). Notably, RBD-1 (the shortest form) exhibited a more potent inhibitory effect against KoRV-A compared to RBD-2, RBD-3, and truncated Env proteins (Trunc-ko1, Trunc-ko2, Trunc-ko3, Trunc-ko4, and Trunc-ko5). Taking together, our findings suggest that the frameshift mutation and length of truncated Env may influence the inhibitory effect functions.

3.4.7. Inhibitory effect of truncated Env on feline retroviruses, FeLV-B

The entry receptors of feline retroviruses, FeLV-B, have been reported (10, 27) and in this study, we found koPit1 but not koPit2 as the FeLV-B receptor. Next, we tested the inhibitory effects of truncated Env proteins (Trunc-ko1, Trunc-ko2, Trunc-ko3, Trunc-ko4, and Trunc-ko5) on FeLV-B strains (GA, ON-T, MZ40-5B, KG20-5B, and FO36-5B) in MDTF-koPit1 as target cells. The results showed that all truncated Env proteins exhibited marked inhibitory effects, while the control did not. However, the inhibitory effects varied in intensity. Trunc-ko1, Trunc-ko2, Trunc-ko4, and Trunc-ko5 exhibited inhibitory effects against all FeLV-B infections. In contrast, Trunc-ko3 exhibited only partial inhibitory effects (Figure 3.5F). Overall, these results

indicate that truncated Env proteins of KoRV could also confer resistance against feline retroviral infections, specifically FeLV-B via koPit1.

3.5. DISCUSSION

KoRV infects several hosts *in vitro*, as shown in previous studies (29, 37, 143). According to interference assay methods, Pit1 and Pit2 are potential receptors for KoRV (140). Furthermore, previous reports have demonstrated that KoRV can also use human Pit1 (37) and feline Pit1 (147) as receptors to infect MDTF-expressing cells. In this study, we aimed to evaluate the potential of koPit1 and koPit2 as KoRV receptors. We found that the enKoRV-derived truncated Env proteins expressed as soluble proteins could inhibit KoRV-related viral infections, including FeLV-B infections.

Our phylogenetic analysis revealed that koPit1 and koPit2 were distinguishable from other receptors identified in retroviral infections, such as RFC, THTR1, THTR2, CAT, FLVCR1, FLVCR2, ASCT1, and ASCT2. Additionally, Pit1 is broadly expressed in mammalian vertebrates (154). KoPit1 is highly similar to Pit1 in several hosts including humans, gibbons, felines, mice, and rats. Thus, Pit1 may serve as a suitable receptor for infection in different animal hosts. Our findings show that koPit1, but not koPit2, is the receptor for KoRV-A infection. Comparison of our findings with those of other studies confirms that Pit1 is the receptor for KoRV infection (29). Although KoRV, GaLV, HPG, WMV, and FeLV-B can infect human cells in culture, they have different host ranges *in vivo*. For example, although GaLV cannot be transmitted to rats, KoRV can be (141). *In vitro* studies have shown that infection in rats is affected by the lysine (K) residue at position 550 of Pit1 (140). Alignment of the binding motif within mammalian *Pit1* genes (Figure 3.1) supports this result, as the binding sites within

koPit1 share permissive amino acid residues, which are distinct from the non-permissive motif within mouse Pit1 due to the presence of K at position 550.

Our analysis revealed that koPit2 does not conserve K at position 552, which is responsible for preventing GaLV infection (155), and probably GaLV cannot infect gibbons using Pit2 only due to the presence of K at position 552 in predicted gibbon Pit2 (Figure 3.2). Notably, KoRV, WMV V655, and FeLV-Bs did not use koPit2 for infection, even in the absence of K at position 552. This suggests that the amino acid at position 552 in koPit2 is not responsible for KoRV-A and WMV V655 infection but is essential for GaLV and HPG infection. We propose that KoRV-A receptor usage may depend on variations in the RBD, based on a comparison of 70.4% and 69.4% similarity of KoRV-A RBD with GaLV and HPG, respectively. During the investigation of the receptor, we also noted that WMV (WT) did not confer infection owing to the lack of valine (V) at position 655. In contrast, WMV V655 was able to cause infection. The absence of V results in the inactivation of cleavage activity and the production of a non-infectious virus (156). In addition, KoRV-A RBD is more likely to be similar to WMV V655 since both KoRV and WMV V655 did not exhibit infection through koPit2. According to previous reports, FeLV-Bs could use fePit1 and fePit2 (10, 27). However, our findings demonstrate that FeLV-Bs use only koPit1 for infection. This may be due to the sequence diversity of Pit2 among species.

Along with serving as receptors, Pit1 and Pit2 are widely expressed throughout the mammalian body as regulators of phosphate transport in the metabolic system (157). Additionally, KoRV, GaLV, HPG, WMV, and FeLV-B have been widely detected in host body fluids (19, 30, 37, 95, 138). Taken together, our findings support the possibility of cross-species transmission among these animals, which may occur through the sharing of the same receptors, interactions within

the food chain (predation), or sharing of terrestrial areas (contamination), especially through intermediate vectors such as bats and rodents.

In this study, we determined that truncated Env proteins derived from enKoRV act as a restriction factor for KoRV-related viruses, as well as for feline retroviruses, FeLV-B. The antiviral effect of enKoRV truncated Env proteins depends on koPit1. We analyzed the antiviral machinery driven by truncated Env proteins encoded by KoRV-A, which are secreted from the testis, brain, and liver, using RNA-seq analysis. Our findings demonstrate that enKoRV truncates Env as a soluble protein, conferring inhibitory effects. However, the extent of these effects varies and may be influenced by the length and similarity to KoRV-A. Additionally, a frameshift mutation of enKoRV truncates Env has affected the level of inhibitory effect. We speculate that this may be due to the fact that truncated Env enKoRV is not yet fixed in the koala population. Compared with previous reports, FeLIX (vs FeLV-B), Refex-1 (vs FeLV-D), and Suppresyn (vs type D retroviruses) have been found in a fixed form in the host genome and have been demonstrated to be fully functional *in vitro* (58, 59, 147). Furthermore, KoRV has been reported to undergo endogenization in the Australian koala population (138). Therefore, our present results support the idea that the evolutionary process of ERVs is consistent with the ongoing endogenization of KoRV in the koala population. However, enKoRV-derived restriction factors may exist in a fixed or temporary form (lost from the host genome) depending on many factors in natural selection (55, 158). Despite the antiviral effects of enKoRV Env proteins observed *in vitro* in this study, the specific functions of these soluble proteins *in vivo* are unknown. This is a limitation of the current study.

In conclusion, we isolated and identified koPit1 and determined its function as a receptor for KoRV infection, but not koPit2. Furthermore, we found that truncated Env proteins derived

from enKoRV, which are soluble proteins, could inhibit KoRV-related viruses and FeLV-B infections. This study highlights the role of soluble Env proteins as restriction factors in controlling retrovirus spread within and between species. This could potentially enhance host immunity and antiviral defense. Our findings could be valuable for further analyses to determine the host pathogenicity of KoRV in koalas and are applicable to related studies on KoRV for a more comprehensive understanding of retroviral cross-transmission.

3.6. TABLES, FIGURES, SUPPLEMENTARY DATA IN CHAPTER TWO

Tables

Table 3.1. Sequences of primers used in this study

Name	Sequence (5`-3`)*	Expression vector
Fe-817S	TCCTCATACCTCATTTACACAGC	1st PCR koPit1
Fe-839R	GAGCTTGATCCCGAATGGCT	
Fe-815S	ACCTGGATCCGCCACCATGGCCACCCCCCTGGGCTC	2nd PCR koPit1
Fe-837R	TGCAGGATCCTCACACTCTGAGAATGGCATACTTG	
Fe-818S	AGAAAAACTCCTGCGGTCCAC	1st PCR koPit2
Fe-840R	ACACACACTGGACTCTCCCT	
Fe-816S	ACCTGAATTCGCCACCATGGCTATGGAAGATTACTTG	2nd PCR koPit2
Fe-838R	TGCAAGATCTTCACACATATGGCAGGATGCCATAC	
Fe-802S	AGAACAAGGACCTCCCAGAAAAATTCCCTTCCTCCCC	
Fe-820R	GGGGAGGAAGGGAATTTTTCTGGGAGGTCCTTGTTCT	
Fe-803S	GCCGGTTCCTACCCTATCCCCCAGCGTCCCCTATC	
Fe-821R	GATAGGGGACGCTGGGGGATAGGGTAGGAACCGGC	
Fe-804S	GCCGGTTCCTACCCTATCACCCCAGCGTCCCCTATC	
Fe-822R	GATAGGGGACGCTGGGGTGATAGGGTAGGAACCGGC	
Fe-805S	ATCCCCACGGTACAGGCTAGCCCCCGGCCCCTAGTAC	
Fe-823R	GTACTAGGGGCCGGGGGCTAGCCTGTACCGTGGGGAT	
Fe-806S	GCTCTGTCTAGCCCTCGGCCCCCTTATTACGAAGGAA	
Fe-824R	TTCCTTCGTAATAAGGGGGCCGAGGGCTAGACAGAGC	
Fe-814S	ACCTGGATCCGCCGCCACCATGCTTCTCATCTCAAACCC	
Fe-831R	TGCAGAATTCTCACAGATCCTCCTCGGAGATCAGCTTCT GCTCGCCTGTACCGTGGGGATAGG	Trunc-ko1
Fe-832R	TGCAGAATTCTCACAGATCCTCCTCGGAGATCAGCTTCT GCTCGGGGCCGGGGGCTAGCCTGT	Trunc-ko2
Fe-833R	TGCAGAATTCTCACAGATCCTCCTCGGAGATCAGCTTCT GCTCAGGCCAGAAAGGCCCCTTGT	Trunc-ko3, Trunc-ko4
Fe-834R	TGCAGAATTCTCACAGATCCTCCTCGGAGATCAGCTTCT GCTCTACATAACCCGAGTCCAGAG	Trunc-ko5
Fe-851R	TGCAGAATTCTCACAGATCCTCCTCGGAGATCAGCTTCT GCTCTACTACCGGTGGGGGACTTG	RBD-1
Fe-851R	TGCAGAATTCTCACAGATCCTCCTCGGAGATCAGCTTCT GCTCTGATAGGGTAGGAACCGGCA	RBD-2
Fe-851R	TGCAGAATTCTCACAGATCCTCCTCGGAGATCAGCTTCT GCTCGCCCGTGGTGGGAGATGGAG	RBD-3

* Restriction enzymes are underlined. Expression vectors shown in Table 1 were constructed using the indicated enzyme sites.

Table 3.2. Amino acid sequence of WMV V655 constructed in this study

Name	**Sequence (**5`-3`)
WMV	MLLTSSLHHPRHQMSPGSWKRLIILLSCVFGGGGTSLQNKNPHQPMTLTW
V655	QVLSQTGDVVWVTEAVQPLWTWWPSLKPDVCALAAGLESWDIPESDVS
	ASKRIRPLDSNYNNANKQISWGAIGCSYPRARTRIANSPFYVCPRDGRTLS
	EARRCGELESLYCKEWGCETTGNVHWQPRSSWDLITVKWGRNRQWEQN
	MLSVCEQTGWCNPLKIDFTEKGKHSRDWIKGRTWGLRFNVAGHPGVQLT
	IRLKVTSMPAVAVGPDPVLAEQRPPSKPLPPPSREAPPTSLPPAASGQAPTVR
	ERTVTLSTPPPTTGDRLFGLVQGAFLALNATNPGATESCWLCLAMGPPYYE
	GIASLGEVAYTSDHTRCRWGTQGKLTLTEVSGHGLCIGKVPSTHQHLCNQT
	LPINSSKDHQYLLPFNYSWWACSTGLTPCLSTSVFNQSRDFCIQIQLIPRIYY
	HPEGTLLQAYDNSHPRLKREPVSLTLAVLLGLGIAAGIGTGSTALIKGPMDL
	QQGLTSLQIAMDADLRAIQDSISKLENSLTSLSEVALQNRRGLDLLFLKEGG
	LCAALKEECCFYVDHSGAVRDSMRKLKERLDKRQLERQKNQNWYEGWF
	NSSPWFTTLLSTIAGPLLLLLLLLILGPCIINRLVQFINDRVSAVKILVLRQKY
	QTLDNEDNL<u>EQKLISEEDL</u>

* The underlined text indicates the myc tag sequence. WMV, woolly monkey virus.

Figures

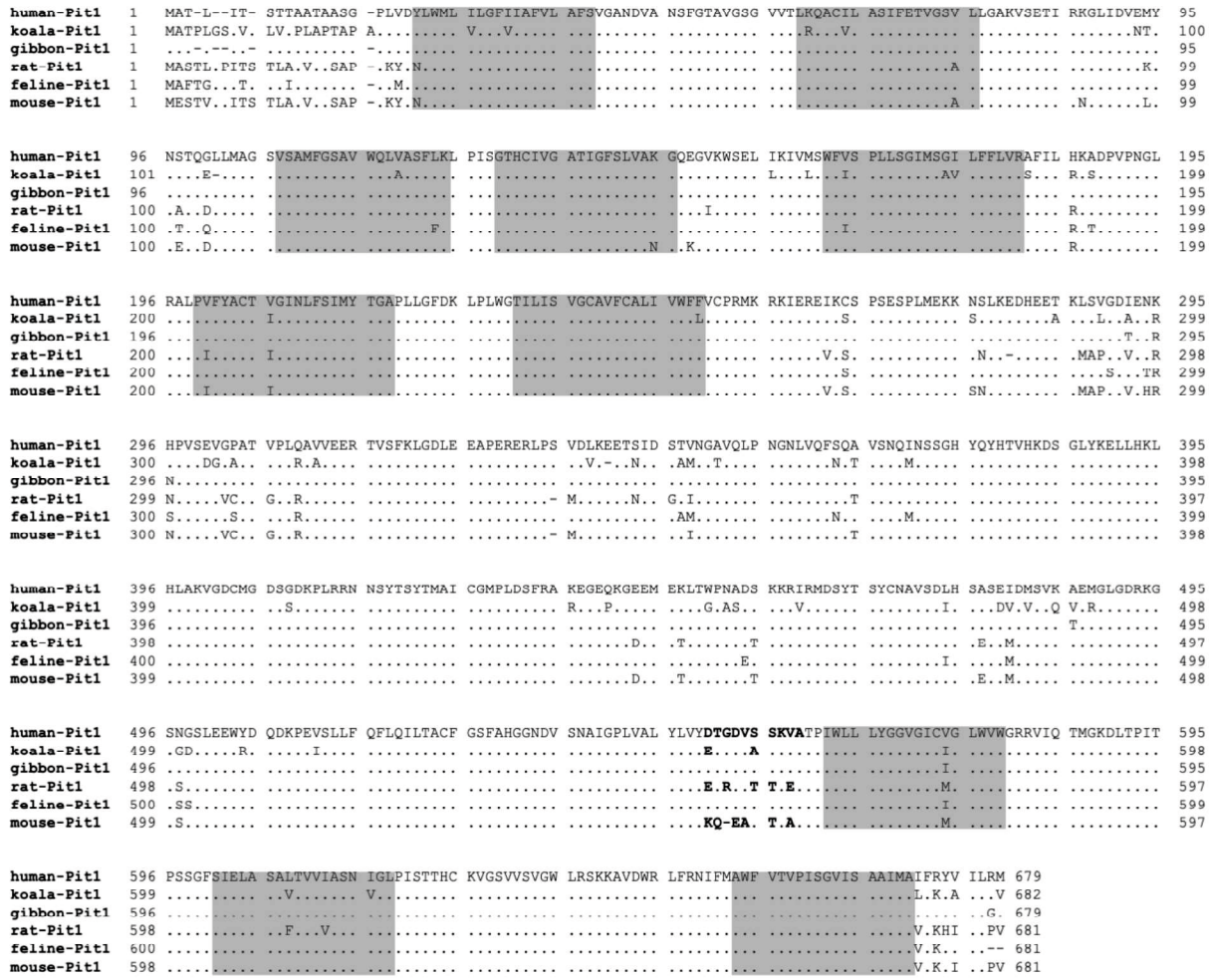

Figure 3.1 Alignment of amino acid sequences of human, koala, gibbon, rat, feline, and mouse Pit1. Conserved amino acid residues are indicated by dots, while positions with differences are shown as letters. Gaps in the amino acid sequence are indicated by hyphens. The putative transmembrane domains (boxes) were predicted based on human Pit1.

Figure 3.2 Alignment of amino acid sequences of human, koala, gibbon, rat, and feline Pit2. Conserved amino acid residues are indicated by dots, while positions with differences are shown as letters. Gaps in the amino acid sequence are indicated by hyphens. The putative transmembrane domains (boxes) were predicted based on human Pit2.

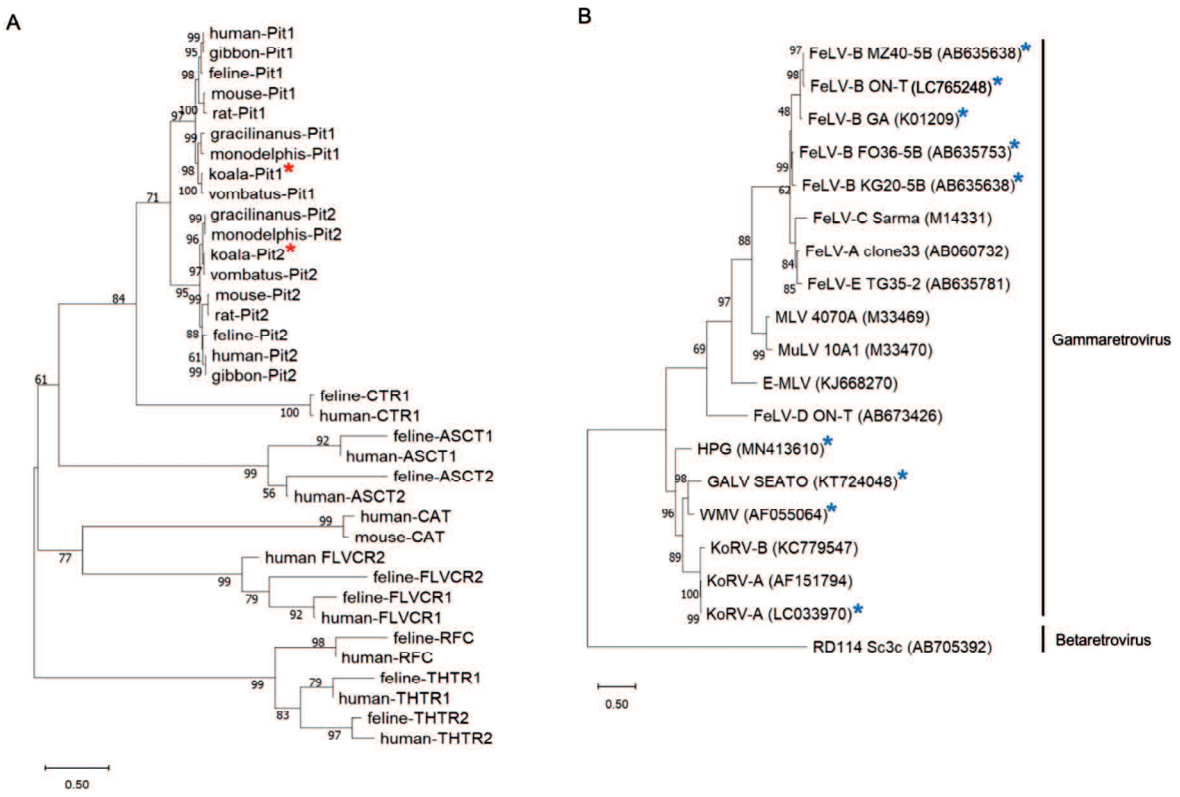

Figure 3.3 Phylogenetic analysis. (A) Phylogenetic tree of koala Pit1, koala Pit2, and related proteins with *Gammaretrovirus* receptors. The amino acid sequences of receptors were used to construct a neighbor-joining tree. The scale bar indicates the evolutionary distance in amino acid substitutions per site. (B) Phylogenetic tree of *Gammaretroviruses* based on SU subunit of *env* genes was constructed by using Maximum Likelihood method. The scale bar indicates the evolutionary distance substitutions per site. The samples in this study are indicated by red and blue asterisks.

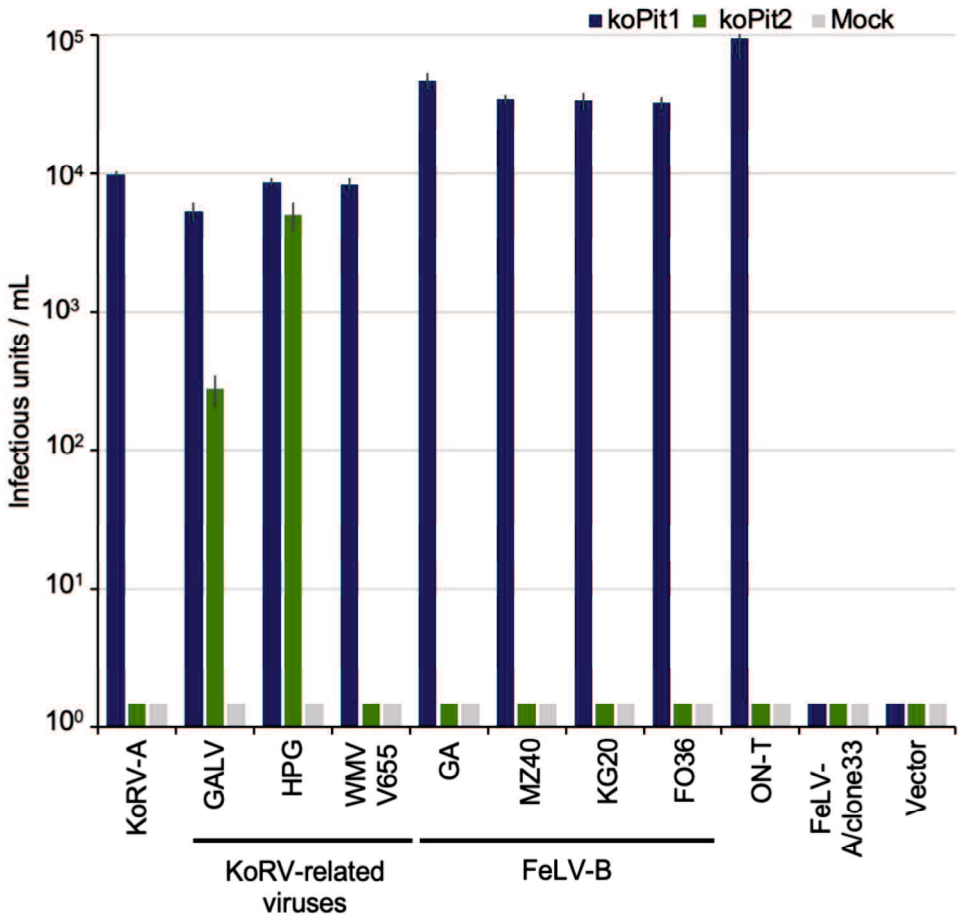

Figure 3.4 Receptor usage of KoRV, GALV, HPG, WMV V655 and FeLV-B Env-pseudotyped viruses. The indicated Env-pseudotyped viruses were used to infect MDTF-koPit1, MDTF-koPit2, and MDTF-empty target cells to determine their receptor usage. The x-axis indicates viral titers, while the y-axis shows the number of $\log_{10}$-galactosidase (LacZ)-positive cells per mL of virus, measured in infectious units (IU). The virus infection titers, along with their standard deviations, were averaged from three independent experiments. The negative control (MDTF cells expressing only the vector) is indicated as "Mock."

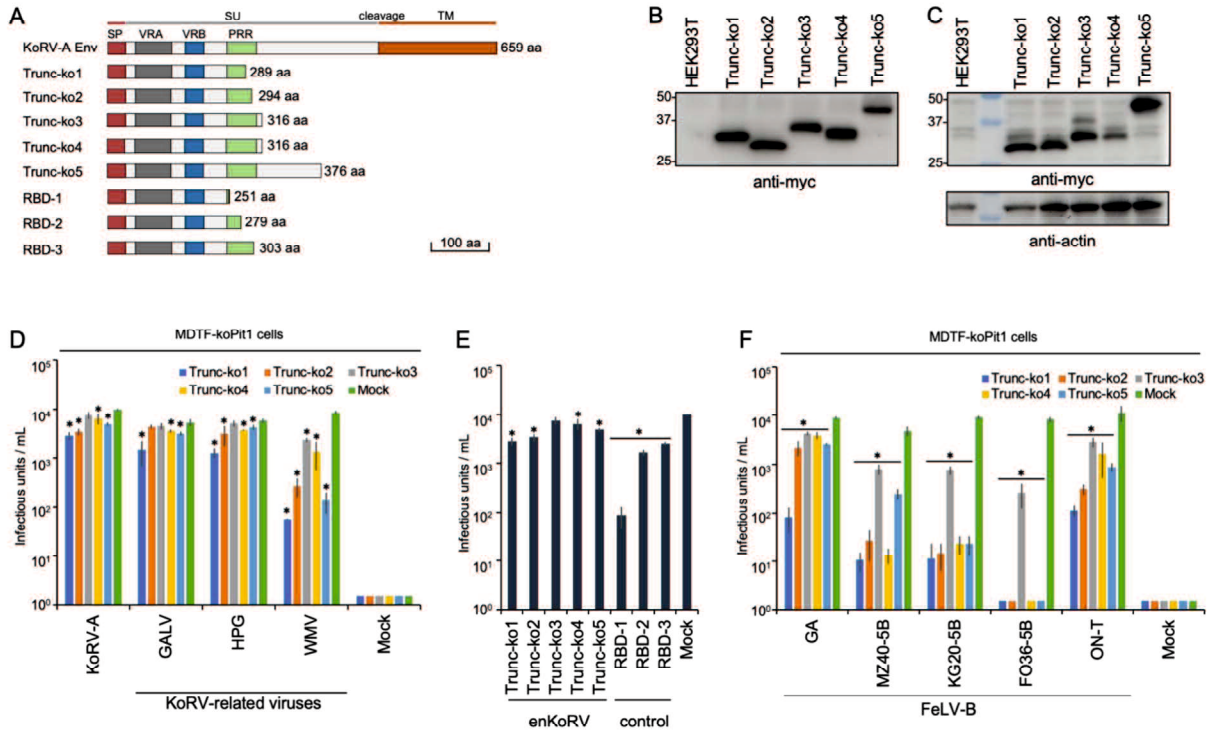

Figure 3.5. Structural schematic, expression, and inhibitory effect of the truncated Env proteins derived from enKoRV for KoRV-related viruses and FeLV-B infections. (A) Schematic representation of the structure of truncated Env enKoRV and series deletion of RBD. All proteins contain a myc-tag in the C-terminal region. SP, signal peptide; SU, surface unit; TM, transmembrane unit; VRA, variable region A; VRB, variable region B; PRR, proline-rich region. The number of amino acids is indicated on the right side. (B) Detection of truncated Env proteins enKoRV in cell culture supernatants and (C) in cell lysates from HEK293T cells transfected with indicated plasmids. The samples were analyzed via immunoprecipitation (IP) and western blotting (WB) using a goat anti -Myc antibody. (D) Inhibition assay using truncated Env proteins enKoRV to evaluate the infection of Env-pseudotyped viruses of KoRV-A and KoRV-related viruses. (E) Inhibition assay using series deletion of KoRV-A-derived RBD as control. (F) Truncated Env proteins enKoRV on FeLV-B (GA, MZ40-5B, KG20-5B, FO36-5B, and ON-T) infections. The infectious units (IU) shown on the x-axis were determined by counting the number of $\log_{10}$-galactosidase (LacZ)-positive cells per milliliter

(mL) of virus indicated on the y-axis. Virus infection titers with standard deviations represent the means of three independent infection experiments. Comparisons were performed using Student's *t*-test (*$p < 0.05$).

GENERAL DISCUSSIONS AND CONCLUSIONS

Retroviruses are unique because they use reverse transcriptase to convert their RNA genome into DNA, which can then be integrated into the host genome (4). ERVs infect germ cells, integrate into the host genome, and are vertically transmitted to offspring (43-45). This study highlights that the presence of defective Env is beneficial to the host, and that Env, which is scattered throughout the mammalian genome, functions as an antiviral molecule. Notably, the presence of antiviral mechanisms highlights the possibility of cross-species utilization. The objectives of this study were as follows: First, the functions of defective env-ERVs were characterized and investigated. Next, I determined the biological functions of ERVs and elucidated their evolution. Finally, I intended to investigate the evolution of animal genomes and their relationship with ERV evolution.

In Chapter One, I demonstrated that FeLIX derived from enFeLV can act as a restriction factor for mammalian retroviruses. FeLV-B transmission in domestic cats does not occur naturally. Furthermore, *in vivo* infection models demonstrated resistance to FeLV-B infections (64). FeLIX is a restrictive factor for the feline retroviruses FeLV-B and enFeLV, as well as for the mammalian retroviruses KoRV, GaLV, and HPG. The antiviral machinery is driven by truncated Env proteins encoded by enFeLVs secreted from feline cells. The antiviral effect of FeLIX is dependent on fePit1. These results implied that receptor interference was the mechanism of action underlying FeLIX activity. FeLIX is broadly expressed in tissues, with the highest levels identified in immune system tissues (spleen, bone marrow, and lymph nodes) and PBMCs. Therefore, FeLIX may function as a barrier to the intraspecies and interspecies transmission of retroviruses. These results suggested that truncated Env may constitute an antiviral system in cats. This is consistent with the results of previous studies, suggesting that the non-coding RNA of enFeLV-LTRs also tend to control FeLV replication via an RNA interference mechanism

(70). Additionally, another study suggested that FeLV-B Env confers strong resistance against feline SERINC5, which depends on glycoGag to develop this resistance (106). These results explain a possible synergistic antiviral phenomenon in cats regarding the role of ERVs in the protection against FeLV infection. These findings provide insight into the co-evolutionary history of retroviruses and their hosts. In particular, we focused on retroviruses that infect cells in a pit-dependent manner and spread infections.

In Chapter Two, I characterized other defective env-ERVs, called EnvV-Fca, which is an ERV-derived placenta-specific soluble protein from domestic cats. EnvV-Fca is closely related to the EnvV2-Hum gene, which contains 439 amino acids, including a signal peptide, SU subunit, fusion peptide, and interferon stimulatory DNA (ISD); however, the TM subunit is partially deleted. EnvV-Fca is expressed in various feline tissues and cell lines. In feline tissues, the highest expression levels of EnvV-Fca was detected in the placenta and was specifically observed in the placental trophoblast syncytiotrophobic layer using *in situ* hybridization . These findings are similar to those for EnvV2-Mac, which is expressed in trophoblasts (115). Furthermore, through genetic analysis, I found that EnvV2 is non-orthologous in mammals and non-mammals, and can be classified into two groups: complete EnvV2 and defective EnvV2. Notably, all the identified EnvV2 proteins contained ISD, except for *Rattus norvegicus*. ISD may suppress the cellular and humoral immune responses. Therefore, EnvV2 may be involved in the host immune tolerance. However, the role of EnvV2 may vary in different species. The integration time for additional EnvV2 during mammalian evolution in rodents, elephants, and bats was calculated to be at least 60 million years ago, around the Cretaceous–Paleogene boundary, which is similar to the findings of another study on carnivores and even-toed ungulates (116). However, we were unable to determine the integration time for non-mammalian vertebrates in this study because of limited information. Additionally, EnvV2 has

been identified in birds, bats, and rodents (134-136). Bats have unique ecological characteristics, such as flight, hibernation, a relatively long lifespan, and colonial roosting behavior, which make them ideal vectors for maintaining viral infections (133) and indicate the potential for cross-transmission of EnvV2.

In Chapter Three, I demonstrated that koPit1 as KoRV receptors, but not koPit2. A comparison of our findings with those of other studies confirms that Pit1 is the receptor for KoRV infection (29). We propose that KoRV-A receptor usage depends on variations in its receptor-binding domain (RBD). In addition, KoRV-A RBD is more likely to be similar to that of WMV V655 because neither KoRV nor WMV V655 exhibited infection through koPit2. These findings demonstrate that FeLV-B uses only koPit1 for infection. This may be due to the sequence diversity of Pit2 among the species. Taken together, our findings support the possibility of cross-species transmission among these animals, which may occur through sharing of the same receptors, interactions within the food chain (predation), or sharing of terrestrial areas (contamination), especially through intermediate vectors such as bats and rodents. Furthermore, I determined that truncated Env enKoRV, expressed as a soluble protein, could inhibit KoRV-related viruses and extend to FeLV-B infections. The antiviral effects of enKoRV-truncated Env is dependent on koPit1. According to RNA-seq analysis, truncated Env proteins encoded by KoRV-A are secreted from the testis, brain, and liver. Our findings demonstrated that enKoRV truncates Env into a soluble protein and confers inhibitory effects, although the extent of these effects varies. This may be due to the truncation of Env enKoRV is not fixed yet in the koala population. Compared to previous reports, FeLIX (vs. FeLV-B), Refex-1 (vs. FeLV-D), and Suppresyn (vs. type D retroviruses) were found in a fixed form in the host genome and had full function, as demonstrated *in vitro* (58, 59, 147). In addition, KoRV has been reported to undergo endogenization in an Australian koala population (138). Regardless, enKoRV derived

as a restriction factor may assume a fixed or temporary form (lost from the host genome), depending on many factors in natural selection (55, 158). Taken together, our results support the idea that the evolutionary process of ERVs is consistent with the ongoing endogenization of KoRV in the koala population.

In conclusion, the truncated Env of ERV exists and has a biological function in the mammalian genome. Truncated Env may facilitate host antiviral defense, particularly during the early stages of virus-cell interactions, thus preventing infection. These findings provide a better understanding of how soluble Env proteins restrict retroviruses from diverse host species by sharing receptor usage. This study also captured an evolutionary scenario of host-pathogen interactions and may contribute to the development of infectious disease treatments.

REFERENCES

1. Greenwood AD, Ishida Y, O'Brien SP, Roca AL, Eiden MV. Transmission, Evolution, and Endogenization: Lessons Learned from Recent Retroviral Invasions. Microbiol Mol Biol Rev. 2018;82(1).
2. Coffin J. Structure and classification of retroviruses. The Retroviridae. Plenum Press, NY; 1992.
3. Murphy FA, Fauquet CM, Bishop DH, Ghabrial SA, Jarvis AW, Martelli GP, et al. Virus taxonomy: classification and nomenclature of viruses: Springer Science & Business Media; 2012.
4. Coffin JM, Hughes SH, Varmus HE. Retroviruses. Cold Spring Harbor (NY): Cold Spring Harbor Laboratory Press. 1997.
5. Jarrett O, Hardy WD, Jr., Golder MC, Hay D. The frequency of occurrence of feline leukaemia virus subgroups in cats. Int J Cancer. 1978;21(3):334-7.
6. Hisasue M, Nagashima N, Nishigaki K, Fukuzawa I, Ura S, Katae H, et al. Myelodysplastic syndromes and acute myeloid leukemia in cats infected with feline leukemia virus clone33 containing a unique long terminal repeat. Int J Cancer. 2009;124(5):1133-41.
7. Hartmann K, Hofmann-Lehmann R. What's new in feline leukemia virus infection. Vet Clin North Am Small Anim Pract. 2020;50(5):1013-36.
8. Miyake A, Ngo MH, Wulandari S, Shimojima M, Nakagawa S, Kawasaki J, et al. Convergent evolution of antiviral machinery derived from endogenous retrovirus truncated envelope genes in multiple species. Proc Natl Acad Sci U S A. 2022;119(26):e2114441119.
9. Sarma PS, Log T. Viral interference in feline leukemia-sarcoma complex. Virology. 1971;44(2):352-8.

10. Anderson MM, Lauring AS, Robertson S, Dirks C, Overbaugh J. Feline Pit2 functions as a receptor for subgroup B feline leukemia viruses. J Virol. 2001;75(22):10563-72.

11. Anderson MM, Lauring AS, Burns CC, Overbaugh J. Identification of a cellular cofactor required for infection by feline leukemia virus. Science. 2000;287(5459):1828-30.

12. Mendoza R, Anderson MM, Overbaugh J. A putative thiamine transport protein is a receptor for feline leukemia virus subgroup A. J Virol. 2006;80(7):3378-85.

13. Miyake A, Kawasaki J, Ngo H, Makundi I, Muto Y, Khan AH, et al. Reduced folate carrier: an entry receptor for a novel feline leukemia virus variant. J Virol. 2019;93(13).

14. Quigley JG, Burns CC, Anderson MM, Lynch ED, Sabo KM, Overbaugh J, et al. Cloning of the cellular receptor for feline leukemia virus subgroup C (FeLV-C), a retrovirus that induces red cell aplasia. Blood. 2000;95(3):1093-9.

15. Sarma PS, Log T. Subgroup classification of feline leukemia and sarcoma viruses by viral interference and neutralization tests. Virology. 1973;54(1):160-9.

16. Shalev Z, Duffy SP, Adema KW, Prasad R, Hussain N, Willett BJ, et al. Identification of a feline leukemia virus variant that can use THTR1, FLVCR1, and FLVCR2 for infection. J Virol. 2009;83(13):6706-16.

17. Tailor CS, Willett BJ, Kabat D. A putative cell surface receptor for anemia-inducing feline leukemia virus subgroup C is a member of a transporter superfamily. J Virol. 1999;73(8):6500-5.

18. Takeuchi Y, Vile RG, Simpson G, O'Hara B, Collins MK, Weiss RA. Feline leukemia virus subgroup B uses the same cell surface receptor as gibbon ape leukemia virus. J Virol. 1992;66(2):1219-22.

19. Watanabe S, Kawamura M, Odahara Y, Anai Y, Ochi H, Nakagawa S, et al. Phylogenetic and structural diversity in the feline leukemia virus env gene. PLoS One. 2013;8(4):e61009.

20. Petch RJ, Gagne RB, Chiu E, Mankowski C, Rudd J, Roelke-Parker M, et al. Feline Leukemia Virus Frequently Spills Over from Domestic Cats to North American Pumas. J Virol. 2022;96(23):e0120122.

21. Ortega C, Valencia AC, Duque-Valencia J, Ruiz-Saenz J. Prevalence and Genomic Diversity of Feline Leukemia Virus in Privately Owned and Shelter Cats in Aburrá Valley, Colombia. Viruses. 2020;12(4):464.

22. Westman M, Norris J, Malik R, Hofmann-Lehmann R, Harvey A, McLuckie A, et al. The diagnosis of feline leukaemia virus (FeLV) Infection in owned and group-housed rescue cats in Australia. Viruses. 2019;11(6).

23. Stavisky J, Dean RS, Molloy MH. Prevalence of and risk factors for FIV and FeLV infection in two shelters in the United Kingdom (2011-2012). Vet Rec. 2017;181(17):451.

24. Novacco M, Kohan NR, Stirn M, Meli ML, Díaz-Sánchez AA, Boretti FS, et al. Prevalence, geographic distribution, risk factors and co-infections of feline gammaherpesvirus infections in domestic cats in Switzerland. Viruses. 2019;11(8).

25. Overbaugh J, Riedel N, Hoover EA, Mullins JI. Transduction of endogenous envelope genes by feline leukaemia virus in vitro. Nature. 1988;332(6166):731-4.

26. Erbeck K, Gagne RB, Kraberger S, Chiu ES, Roelke-Parker M, VandeWoude S. Feline leukemia virus (FeLV) Endogenous and exogenous recombination events result in multiple FeLV-B subtypes during natural infection. J Virol. 2021;95(18):e0035321.

27. Boomer S, Eiden M, Burns CC, Overbaugh J. Three distinct envelope domains, variably present in subgroup B feline leukemia virus recombinants, mediate Pit1 and Pit2 receptor recognition. J Virol. 1997;71(11):8116-23.

28. O'Hara B, Johann SV, Klinger HP, Blair DG, Rubinson H, Dunn KJ, et al. Characterization of a human gene conferring sensitivity to infection by gibbon ape leukemia virus. Cell Growth Differ. 1990;1(3):119-27.

29. Oliveira NM, Farrell KB, Eiden MV. In vitro characterization of a koala retrovirus. J Virol. 2006;80(6):3104-7.

30. Hayward JA, Tachedjian M, Kohl C, Johnson A, Dearnley M, Jesaveluk B, et al. Infectious KoRV-related retroviruses circulating in Australian bats. Proc Natl Acad Sci U S A. 2020;117(17):9529-36.

31. Kayesh MEH, Hashem MA, Tsukiyama-Kohara K. Koala retrovirus epidemiology, transmission mode, pathogenesis, and host immune response in koalas (*Phascolarctos cinereus*): a review. Arch Virol. 2020;165(11):2409-17.

32. Olagoke O, Quigley BL, Eiden MV, Timms P. Antibody response against koala retrovirus (KoRV) in koalas harboring KoRV-A in the presence or absence of KoRV-B. Sci Rep. 2019;9(1):12416.

33. Tarlinton RE, Meers J, Young PR. Retroviral invasion of the koala genome. Nature. 2006;442(7098):79-81.

34. Hashem MA, Maetani F, Kayesh MEH, Eiei T, Mochizuki K, Ito A, et al. Transmission of koala retrovirus from parent koalas to a Joey in a Japanese zoo. J Virol. 2020;94(11).

35. Joyce BA, Blyton MDJ, Johnston SD, Young PR, Chappell KJ. Koala retrovirus genetic diversity and transmission dynamics within captive koala populations. Proc Natl Acad Sci U S A. 2021;118(38).

36. Quigley BL, Ong VA, Hanger J, Timms P. Molecular dynamics and mode of transmission of koala retrovirus as it invades and spreads through a wild queensland koala population. J Virol. 2018;92(5).

37. Xu W, Stadler CK, Gorman K, Jensen N, Kim D, Zheng H, et al. An exogenous retrovirus isolated from koalas with malignant neoplasias in a US zoo. Proc Natl Acad Sci U S A. 2013;110(28):11547-52.

38. Tarlinton R, Meers J, Hanger J, Young P. Real-time reverse transcriptase PCR for the endogenous koala retrovirus reveals an association between plasma viral load and neoplastic disease in koalas. J Gen Virol. 2005;86(Pt 3):783-7.

39. Fabijan J, Sarker N, Speight N, Owen H, Meers J, Simmons G, et al. Pathological Findings in Koala Retrovirus-positive Koalas (Phascolarctos cinereus) from Northern and Southern Australia. J Comp Pathol. 2020;176:50-66.

40. Waugh CA, Hanger J, Loader J, King A, Hobbs M, Johnson R, et al. Infection with koala retrovirus subgroup B (KoRV-B), but not KoRV-A, is associated with chlamydial disease in free-ranging koalas (Phascolarctos cinereus). Sci Rep. 2017;7(1):134.

41. Hanger JJ, Bromham LD, McKee JJ, O'Brien TM, Robinson WF. The nucleotide sequence of koala (*Phascolarctos cinereus*) retrovirus: a novel type C endogenous virus related to Gibbon ape leukemia virus. J Virol. 2000;74(9):4264-72.

42. Simmons GS, Young PR, Hanger JJ, Jones K, Clarke D, McKee JJ, et al. Prevalence of koala retrovirus in geographically diverse populations in Australia. Aust Vet J. 2012;90(10):404-9.

43. Waterston RH, Lindblad-Toh K, Birney E, Rogers J, Abril JF, Agarwal P, et al. Initial sequencing and comparative analysis of the mouse genome. Nature. 2002;420(6915):520-62.

44. Pontius JU, Mullikin JC, Smith DR, Lindblad-Toh K, Gnerre S, Clamp M, et al. Initial sequence and comparative analysis of the cat genome. Genome Res. 2007;17(11):1675-89.

45. Lander ES, Linton LM, Birren B, Nusbaum C, Zody MC, Baldwin J, et al. Initial sequencing and analysis of the human genome. Nature. 2001;409(6822):860-921.

46. Belshaw R, Katzourakis A, Paces J, Burt A, Tristem M. High copy number in human endogenous retrovirus families is associated with copying mechanisms in addition to reinfection. Mol Biol Evol. 2005;22(4):814-7.

47. Slotkin RK, Martienssen R. Transposable elements and the epigenetic regulation of the genome. Nat Rev Genet. 2007;8(4):272-85.

48. Johnson WE. Origins and evolutionary consequences of ancient endogenous retroviruses. Nat Rev Microbiol. 2019;17(6):355-70.

49. Anai Y, Ochi H, Watanabe S, Nakagawa S, Kawamura M, Gojobori T, et al. Infectious endogenous retroviruses in cats and emergence of recombinant viruses. J Virol. 2012;86(16):8634-44.

50. McAllister RM, Nicolson M, Gardner MB, Rongey RW, Rasheed S, Sarma PS, et al. C-type virus released from cultured human rhabdomyosarcoma cells. Nat New Biol. 1972;235(53):3-6.

51. Treger RS, Pope SD, Kong Y, Tokuyama M, Taura M, Iwasaki A. The lupus susceptibility locus sgp3 encodes the suppressor of endogenous retrovirus expression SNERV. Immunity. 2019;50(2):334-47.e9.

52. Tamura K, Stecher G, Kumar S. MEGA11: Molecular evolutionary genetics analysis version 11. Mol Biol Evol. 2021;38(7):3022-7.

53. Oliveira NM, Satija H, Kouwenhoven IA, Eiden MV. Changes in viral protein function that accompany retroviral endogenization. Proc Natl Acad Sci U S A. 2007;104(44):17506-11.

54. Votteler J, Schubert U. Human immunodeficiency viruses: molecular biology. *Encyclopedia of Virology*, 3rd edn. 2008. pp. 517–525. Elsevier

55. Malfavon-Borja R, Feschotte C. Fighting fire with fire: endogenous retrovirus envelopes as restriction factors. J Virol. 2015;89(8):4047-50.

56. Tury S, Chauveau L, Lecante A, Courgnaud V, Battini JL. A co-opted endogenous retroviral envelope promotes cell survival by controlling CTR1-mediated copper transport and homeostasis. Cell Rep. 2023;42(9):113065.

57. Sugimoto J, Schust DJ, Kinjo T, Aoki Y, Jinno Y, Kudo Y. Suppressyn localization and dynamic expression patterns in primary human tissues support a physiologic role in human placentation. Sci Rep. 2019;9(1):19502.

58. Ito J, Watanabe S, Hiratsuka T, Kuse K, Odahara Y, Ochi H, et al. Refrex-1, a soluble restriction factor against feline endogenous and exogenous retroviruses. J Virol. 2013;87(22):12029-40.

59. Frank JA, Singh M, Cullen HB, Kirou RA, Benkaddour-Boumzaouad M, Cortes JL, et al. Evolution and antiviral activity of a human protein of retroviral origin. Science. 2022;378(6618):422-8.

60. Ikeda H, Laigret F, Martin MA, Repaske R. Characterization of a molecularly cloned retroviral sequence associated with Fv-4 resistance. J Virol. 1985;55(3):768-77.

61. Kozak CA. Origins of the endogenous and infectious laboratory mouse gammaretroviruses. Viruses. 2014;7(1):1-26.

62. Varela M, Spencer TE, Palmarini M, Arnaud F. Friendly viruses: the special relationship between endogenous retroviruses and their host. Ann N Y Acad Sci. 2009;1178:157-72.

63. Gardner MB, Kozak CA, O'Brien SJ. The Lake Casitas wild mouse: evolving genetic resistance to retroviral disease. Trends Genet. 1991;7(1):22-7.

64. Phipps AJ, Hayes KA, Al-dubaib M, Roy-Burman P, Mathes LE. Inhibition of feline leukemia virus subgroup A infection by coinoculation with subgroup B. Virology. 2000;277(1):40-7.

65. Lauring AS, Anderson MM, Overbaugh J. Specificity in receptor usage by T-cell-tropic feline leukemia viruses: implications for the in vivo tropism of immunodeficiency-inducing variants. J Virol. 2001;75(19):8888-98.

66. Cheng HH, Anderson MM, Overbaugh J. Feline leukemia virus T entry is dependent on both expression levels and specific interactions between cofactor and receptor. Virology. 2007;359(1):170-8.

67. Sakaguchi S, Shojima T, Fukui D, Miyazawa T. A soluble envelope protein of endogenous retrovirus (FeLIX) present in serum of domestic cats mediates infection of a pathogenic variant of feline leukemia virus. J Gen Virol. 2015;96(Pt 3):681-7.

68. Rohn JL, Moser MS, Gwynn SR, Baldwin DN, Overbaugh J. In vivo evolution of a novel, syncytium-inducing and cytopathic feline leukemia virus variant. J Virol. 1998;72(4):2686-96.

69. Overbaugh J, Donahue PR, Quackenbush SL, Hoover EA, Mullins JI. Molecular cloning of a feline leukemia virus that induces fatal immunodeficiency disease in cats. Science. 1988;239(4842):906-10.

70. Chiu ES, McDonald CA, VandeWoude S. Endogenous Feline Leukemia Virus (FeLV) siRNA Transcription May Interfere with Exogenous FeLV Infection. J Virol. 2021;95(23):e0007021.

71. McDougall AS, Terry A, Tzavaras T, Cheney C, Rojko J, Neil JC. Defective endogenous proviruses are expressed in feline lymphoid cells: evidence for a role in natural resistance to subgroup B feline leukemia viruses. J Virol. 1994;68(4):2151-60.

72. Ngo MH, Arnal M, Sumi R, Kawasaki J, Miyake A, Grant CK, et al. Tracking the Fate of Endogenous Retrovirus Segregation in Wild and Domestic Cats. J Virol. 2019;93(24): :e01324-19.

73. Graham FL, Smiley J, Russell WC, Nairn R. Characteristics of a human cell line transformed by DNA from human adenovirus type 5. J Gen Virol. 1977;36(1):59-74.

74. Lander MR, Chattopadhyay SK. A *Mus dunni* cell line that lacks sequences closely related to endogenous murine leukemia viruses and can be infected by ectropic, amphotropic, xenotropic, and mink cell focus-forming viruses. J Virol. 1984;52(2):695-8.

75. Puck TT, Cieciura SJ, Robinson A. Genetics of somatic mammalian cells. III. Long-term cultivation of euploid cells from human and animal subjects. J Exp Med. 1958;108(6):945-56.

76. Rasheed S, Gardner M. Characterization of cat cell cultures for expression of retrovirus, FOCMA and endogenous sarc genes. In Proceedings of the third international feline leukemia virus meeting 1980 (pp. 393-400).

77. Crandell RA, Fabricant CG, Nelson-Rees WA. Development, characterization, and viral susceptibility of a feline (Felis catus) renal cell line (CRFK). In Vitro. 1973;9(3):176-85.

78. Snyder HW, Jr., Hardy WD, Jr., Zuckerman EE, Fleissner E. Characterisation of a tumour-specific antigen on the surface of feline lymphosarcoma cells. Nature. 1978;275(5681):656-8.

79. Kuse K, Ito J, Miyake A, Kawasaki J, Watanabe S, Makundi I, et al. Existence of two distinct infectious endogenous retroviruses in domestic cats and their different strategies for adaptation to transcriptional regulation. J Virol. 2016;90(20):9029-45.

80. Nishigaki K, Hanson C, Thompson D, Yugawa T, Hisasue M, Tsujimoto H, et al. Analysis of the disease potential of a recombinant retrovirus containing Friend murine leukemia virus sequences and a unique long terminal repeat from feline leukemia virus. J Virol. 2002;76(3):1527-32.

81. Riedel N, Hoover EA, Gasper PW, Nicolson MO, Mullins JI. Molecular analysis and pathogenesis of the feline aplastic anemia retrovirus, feline leukemia virus C-Sarma. J Virol. 1986;60(1):242-50.

82. Miyake A, Watanabe S, Hiratsuka T, Ito J, Ngo MH, Makundi I, et al. Novel Feline Leukemia Virus Interference Group Based on the env Gene. J Virol. 2016;90(9):4832-7.

83. Miller AD, Garcia JV, von Suhr N, Lynch CM, Wilson C, Eiden MV. Construction and properties of retrovirus packaging cells based on gibbon ape leukemia virus. J Virol. 1991;65(5):2220-4.

84. Cheney CM, Rojko JL, Kociba GJ, Wellman ML, Di Bartola SP, Rezanka LJ, et al. A feline large granular lymphoma and its derived cell line. In Vitro Cell Dev Biol. 1990;26(5):455-63.

85. Mochizuki H, Takahashi M, Nishigaki K, Ide T, Goto-Koshino Y, Watanabe S, et al. Establishment of a novel feline leukemia virus (FeLV)-negative B-cell cell line from a cat with B-cell lymphoma. Vet Immunol Immunopathol. 2011;140(3-4):307-11.

86. Galtier N, Gouy M, Gautier C. SEAVIEW and PHYLO_WIN: two graphic tools for sequence alignment and molecular phylogeny. Comput Appl Biosci. 1996;12(6):543-8.

87. Hall TA, editor BioEdit: a user-friendly biological sequence alignment editor and analysis program for Windows 95/98/NT. Nucleic acids symposium series; 1999: Oxford.

88. Edgar RC. MUSCLE: multiple sequence alignment with high accuracy and high throughput. Nucleic Acids Res. 2004;32(5):1792-7.

89. Nei M, Kumar S. Molecular evolution and phylogenetics: Oxford University Press, USA; 2000.

90. Lopez JV, Culver M, Stephens JC, Johnson WE, O'Brien SJ. Rates of nuclear and cytoplasmic mitochondrial DNA sequence divergence in mammals. Mol Biol Evol. 1997;14(3):277-86.

91. Kimura M. A simple method for estimating evolutionary rates of base substitutions through comparative studies of nucleotide sequences. J Mol Evol. 1980;16(2):111-20.

92. Kumar DV, Berry BT, Roy-Burman P. Nucleotide sequence and distinctive characteristics of the env gene of endogenous feline leukemia provirus. J Virol. 1989;63(5):2379-84.

93. Rudra-Ganguly N, Ghosh AK, Roy-Burman P. Retrovirus receptor PiT-1 of the Felis catus. Biochim Biophys Acta. 1998;1443(3):407-13.

94. Barnett AL, Wensel DL, Li W, Fass D, Cunningham JM. Structure and mechanism of a coreceptor for infection by a pathogenic feline retrovirus. J Virol. 2003;77(4):2717-29.

95. Kawakami TG, Huff SD, Buckley PM, Dungworth DL, Synder SP, Gilden RV. C-type virus associated with gibbon lymphosarcoma. Nat New Biol. 1972;235(58):170-1.

96. Chiu ES, Kraberger S, Cunningham M, Cusack L, Roelke M, VandeWoude S. Multiple introductions of domestic cat feline leukemia virus in endangered florida panthers. Emerg Infect Dis. 2019;25(1):92-101.

97. Elder JH, McGee JS, Munson M, Houghten RA, Kloetzer W, Bittle JL, et al. Localization of neutralizing regions of the envelope gene of feline leukemia virus by using anti-synthetic peptide antibodies. J Virol. 1987;61(1):8-15.

98. Pandey R, Bechtel MK, Su Y, Ghosh AK, Hayes KA, Mathes LE, et al. Feline leukemia virus variants in experimentally induced thymic lymphosarcomas. Virology. 1995;214(2):584-92.

99. Faix PH, Feldman SA, Overbaugh J, Eiden MV. Host range and receptor binding properties of vectors bearing feline leukemia virus subgroup B envelopes can be modulated by

envelope sequences outside of the receptor binding domain. J Virol. 2002;76(23):12369-75.

100. Barnett AL, Davey RA, Cunningham JM. Modular organization of the Friend murine leukemia virus envelope protein underlies the mechanism of infection. Proc Natl Acad Sci U S A. 2001;98(7):4113-8.

101. Soltis RD, Hasz D, Morris MJ, Wilson ID. The effect of heat inactivation of serum on aggregation of immunoglobulins. Immunology. 1979;36(1):37-45.

102. Beyer W, Möhring R, Drescher B, Nötzel U, Rosenthal S. Molecular cloning of an endogenous cat retroviral element (ECE 1)--a recombinant between RD-114 and FeLV-related sequences. Brief report. Arch Virol. 1987;96(3-4):297-301.

103. Shimode S, Nakagawa S, Miyazawa T. Multiple invasions of an infectious retrovirus in cat genomes. Sci Rep. 2015;5:8164.

104. van der Kuyl AC, Dekker JT, Goudsmit J. Discovery of a new endogenous type C retrovirus (FcEV) in cats: evidence for RD-114 being an FcEV(Gag-Pol)/baboon endogenous virus BaEV(Env) recombinant. J Virol. 1999;73(10):7994-8002.

105. Best S, Le Tissier P, Towers G, Stoye JP. Positional cloning of the mouse retrovirus restriction gene Fv1. Nature. 1996;382(6594):826-9.

106. Cano-Ortiz L, Gu Q, de Sousa-Pereira P, Zhang Z, Chiapella C, Twizerimana AP, et al. Feline leukemia virus-B envelope together with its GlycoGag and human immunodeficiency virus-1 Nef mediate resistance to feline SERINC5. J Mol Biol. 2022;434(6):167421.

107. Blyton MDJ, Young PR, Moore BD, Chappell KJ. Geographic patterns of koala retrovirus genetic diversity, endogenization, and subtype distributions. Proc Natl Acad Sci U S A. 2022;119(33):e2122680119.

108. Monteil V, Kwon H, Prado P, Hagelkrüys A, Wimmer RA, Stahl M, et al. Inhibition of SARS-CoV-2 infections in engineered human tissues using clinical-grade soluble human ACE2. Cell. 2020;181(4):905-13.e7.

109. Llewellyn GN, Chen HY, Rogers GL, Huang X, Sell PJ, Henley JE, et al. Comparison of SARS-CoV-2 entry inhibitors based on ACE2 receptor or engineered Spike-binding peptides. J Virol. 2023; 31;97(8):e0068423

110. Spodick DA, Ghosh AK, Parimoo S, Roy-Burman P. The long terminal repeat of feline endogenous RD-114 retroviral DNAs: analysis of transcription regulatory activity and nucleotide sequence. Virus Res. 1988;9(2-3):263-83.

111. Sugimoto J, Sugimoto M, Bernstein H, Jinno Y, Schust D. A novel human endogenous retroviral protein inhibits cell-cell fusion. Sci Rep. 2013;3:1462.

112. Mi S, Lee X, Li X, Veldman GM, Finnerty H, Racie L, et al. Syncytin is a captive retroviral envelope protein involved in human placental morphogenesis. Nature. 2000;403(6771):785-9.

113. Kjeldbjerg AL, Villesen P, Aagaard L, Pedersen FS. Gene conversion and purifying selection of a placenta-specific ERV-V envelope gene during simian evolution. BMC Evol Biol. 2008;8:266.

114. Blaise S, de Parseval N, Heidmann T. Functional characterization of two newly identified Human Endogenous Retrovirus coding envelope genes. Retrovirology. 2005;2:19.

115. Esnault C, Cornelis G, Heidmann O, Heidmann T. Differential evolutionary fate of an ancestral primate endogenous retrovirus envelope gene, the EnvV syncytin, captured for a function in placentation. PLoS Genet. 2013;9(3):e1003400.

116. Simpson J, Kozak CA, Boso G. Cross-species transmission of an ancient endogenous retrovirus and convergent co-option of its envelope gene in two mammalian orders. PLoS Genet. 2022;18(10):e1010458.

117. Beltz GA, Marciani DJ, Hung C-H, Kensil CA. Vaccine comprising recombinant feline leukemia antigen and saponin adjuvant. Google Patents; 1994.

118. Pedersen NC, Theilen GH, Werner LL. Safety and efficacy studies of live- and killed-feline leukemia virus vaccines. Am J Vet Res. 1979;40(8):1120-6.

119. Kano R, Sato E, Okamura T, Watanabe S, Hasegawa A. Expression of Bcl-2 in feline lymphoma cell lines. Vet Clin Pathol. 2008;37(1):57-60.

120. Uyama R, Hong SH, Nakagawa T, Yazawa M, Kadosawa T, Mochizuki M, et al. Establishment and characterization of eight feline mammary adenocarcinoma cell lines. J Vet Med Sci. 2005;67(12):1273-6.

121. Pedersen NC, Boyle JF, Floyd K. Infection studies in kittens, using feline infectious peritonitis virus propagated in cell culture. Am J Vet Res. 1981;42(3):363-7.

122. Haapala DK, Robey WG, Oroszlan SD, Tsai WP. Isolation from cats of an endogenous type C virus with a novel envelope glycoprotein. J Virol. 1985;53(3):827-33.

123. Jones DT, Taylor WR, Thornton JM. The rapid generation of mutation data matrices from protein sequences. Comput Appl Biosci. 1992;8(3):275-82.

124. Felsenstein J. Confidence limits on phylogenies: an approach using the bootstrap. Evolution. 1985;39(4):783-91.

125. Vogt V. Retroviral virions and genomes. In``Retroviruses"(JM Coffin, SH Hughes, and HE Varmus, Eds.). Cold Spring Harbor Laboratory Press, Cold Spring Harbor, NY; 1997.

126. Cornelis G, Heidmann O, Bernard-Stoecklin S, Reynaud K, Véron G, Mulot B, et al. Ancestral capture of syncytin-Car1, a fusogenic endogenous retroviral envelope gene involved in placentation and conserved in Carnivora. Proc Natl Acad Sci U S A. 2012;109(7):E432-41.

127. Swanstrom R, Wills J. Synthesis, assembly, and processing of viral proteins. Coffin JM, Hughes SH, Varmus HE (Eds.), Retroviruses, Cold Spring Harbor Laboratory Press, Cold Spring Harbor, NY. 1997.

128. Choudhuri S. Fundamentals of molecular evolution. Bioinformatics for beginners: genes, genomes, molecular evolution, databases and analytical tools. New York, NY: Academic Press. 2014:27-53.

129. Kumar S, Suleski M, Craig JM, Kasprowicz AE, Sanderford M, Li M, et al. TimeTree 5: an expanded resource for species divergence times. Mol Biol Evol. 2022;39(8).

130. Vargas A, Thiery M, Lafond J, Barbeau B. Transcriptional and functional studies of human endogenous retrovirus envelope EnvP(b) and EnvV genes in human trophoblasts. Virology. 2012;425(1):1-10.

131. Dupressoir A, Lavialle C, Heidmann T. From ancestral infectious retroviruses to bona fide cellular genes: role of the captured syncytins in placentation. Placenta. 2012;33(9):663-71.

132. Zhuo X, Feschotte C. Cross-Species Transmission and differential fate of an endogenous retrovirus in three mammal lineages. PLoS Pathog. 2015;11(11):e1005279.

133. Calisher CH, Childs JE, Field HE, Holmes KV, Schountz T. Bats: important reservoir hosts of emerging viruses. Clin Microbiol Rev. 2006;19(3):531-45.

134. Cui J, Tachedjian G, Wang LF. Bats and rodents shape mammalian retroviral phylogeny. Sci Rep. 2015;5:16561.

135. Hayward JA, Tachedjian G. Retroviruses of Bats: a Threat Waiting in the Wings? mBio. 2021;12(5):e0194121.

136. Woźniakowski G, Frant M, Mamczur A. Avian Reticuloendotheliosis in Chickens - An Update on Disease Occurrence and Clinical Course. J Vet Res. 2018;62(3):257-60.

137. Niewiadomska AM, Gifford RJ. The extraordinary evolutionary history of the reticuloendotheliosis viruses. PLoS Biol. 2013;11(8):e1001642.

138. Ishida Y, Zhao K, Greenwood AD, Roca AL. Proliferation of endogenous retroviruses in the early stages of a host germ line invasion. Mol Biol Evol. 2015;32(1):109-20.

139. Denner J, Young PR. Koala retroviruses: characterization and impact on the life of koalas. Retrovirology. 2013;10:108.

140. Alfano N, Michaux J, Morand S, Aplin K, Tsangaras K, Löber U, et al. Endogenous gibbon ape leukemia virus identified in a rodent (*Melomys burtoni* subsp.) from Wallacea (Indonesia). J Virol. 2016;90(18):8169-80.

141. Fiebig U, Hartmann MG, Bannert N, Kurth R, Denner J. Transspecies transmission of the endogenous koala retrovirus. J Virol. 2006;80(11):5651-4.

142. Shojima T, Yoshikawa R, Hoshino S, Shimode S, Nakagawa S, Ohata T, et al. Identification of a novel subgroup of koala retrovirus from koalas in Japanese zoos. J Virol. 2013;87(17):9943-8.

143. Shojima T, Hoshino S, Abe M, Yasuda J, Shogen H, Kobayashi T, et al. Construction and characterization of an infectious molecular clone of koala retrovirus. J Virol. 2013;87(9):5081-8.

144. Ting YT, Wilson CA, Farrell KB, Chaudry GJ, Eiden MV. Simian sarcoma-associated virus fails to infect Chinese hamster cells despite the presence of functional gibbon ape leukemia virus receptors. J Virol. 1998;72(12):9453-8.

145. Marcus PI, Carver DH. Intrinsic interference: a new type of viral interference. J Virol. 1967;1(2):334-43.

146. Overbaugh J, Miller AD, Eiden MV. Receptors and entry cofactors for retroviruses include single and multiple transmembrane-spanning proteins as well as newly described

glycophosphatidylinositol-anchored and secreted proteins. Microbiol Mol Biol Rev. 2001;65(3):371-89.

147. Pramono D, Takeuchi D, Katsuki M, AbuEed L, Abdillah D, Kimura T, et al. FeLIX is a restriction factor for mammalian retrovirus infection. J Virol. 2024;98(4):e0177123.

148. Ross SR. Cellular immune responses to retroviruses. Retrovirus-cell interactions: Elsevier; 2018. p. 401-20.

149. Leinonen R, Sugawara H, Shumway M. The sequence read archive. Nucleic Acids Res. 2011;39(Database issue):D19-21.

150. Chen S, Zhou Y, Chen Y, Gu J. fastp: an ultra-fast all-in-one FASTQ preprocessor. Bioinformatics. 2018;34(17):i884-i90.

151. Liao Y, Smyth GK, Shi W. featureCounts: an efficient general purpose program for assigning sequence reads to genomic features. Bioinformatics. 2014;30(7):923-30.

152. Robinson JT, Thorvaldsdóttir H, Wenger AM, Zehir A, Mesirov JP. Variant review with the integrative genomics viewer. Cancer Res. 2017;77(21):e31-e4.

153. Saitou N, Nei M. The neighbor-joining method: a new method for reconstructing phylogenetic trees. Mol Biol Evol. 1987;4(4):406-25.

154. Bøttger P, Pedersen L. Evolutionary and experimental analyses of inorganic phosphate transporter PiT family reveals two related signature sequences harboring highly conserved aspartic acids critical for sodium-dependent phosphate transport function of human PiT2. Febs j. 2005;272(12):3060-74.

155. Johann SV, van Zeijl M, Cekleniak J, O'Hara B. Definition of a domain of GLVR1 which is necessary for infection by gibbon ape leukemia virus and which is highly polymorphic between species. J Virol. 1993;67(11):6733-6.

156. Rein A, Mirro J, Haynes JG, Ernst SM, Nagashima K. Function of the cytoplasmic domain of a retroviral transmembrane protein: p15E-p2E cleavage activates the membrane

fusion capability of the murine leukemia virus Env protein. J Virol. 1994;68(3):1773-81.

157. Chande S, Caballero D, Ho BB, Fetene J, Serna J, Pesta D, et al. Slc20a1/Pit1 and Slc20a2/Pit2 are essential for normal skeletal myofiber function and survival. Sci Rep. 2020;10(1):3069.

158. Aswad A, Katzourakis A. Paleovirology and virally derived immunity. Trends Ecol Evol. 2012;27(11):627-36.